KINETIC STABILITY OF THE BENNETT EQUILIBRIUM

BY

USHA KRISHNAMURTHI

A THESIS

SUBMITTED FOR THE DEGREE OF

DOCTOR OF PHILOSOPHY

OF THE

GUJARAT UNIVERSITY

OCTOBER 1986

PHYSICAL RESEARCH LABORATORY
AHMEDABAD 380 009
INDIA

TO MY SISTER

NIMMU

CERTIFICATE

I hereby declare that the work presented in this thesis is original and has not formed the basis for the award of any degree or diploma by any University or Institution.

Usha Krishnamurthi
Usha Krishnamurthi

Certified by:

Professor Abhijit Sen
Thesis Supervisor
Plasma Physics Programme
Physical Research Laboratory
Ahmedabad 380 009, India

Abstract

The present thesis is devoted to a detailed study of the linear stability properties of the Bennett equilibrium. The main emphasis is on the Kinetic aspects and non-local effects arising from the large excursion betatron orbits of the particles in the inhomogeneous magnetic field. An appropriate non-local theory is developed within the framework of the Vlasov-Maxwell equations. A matrix dispersion relation is obtained whose solutions represent the eigenfrequencies of the system against electromagnetic perturbations. In general, the dispersion relation is difficult to solve analytically except in certain simple limits. The principal approach taken in this thesis is therefore a detailed numerical solution using a variety of methods (e.g. graphical scanning, Nyquist method, Muller's method etc.). Analytical solutions are also obtained in some limits to support the numerical results as well as to delineate the physical mechanisms.

The dispersion relation is used to study three important physical problems, which are related to experiments where the Bennett equilibrium provides a realistic representation of the plasma configuration. In the low frequency electrostatic

limit, an ion-acoustic type instability is studied. This mode is driven by the relative drift between electrons and ions in a two component plasma. The ion betatron motion is found to have a stabilizing influence on the mode by raising the instability threshold and by shifting the real frequency. These results are discussed in the context of microinstability observations of Z-pinch and plasma focus experiments. For the Z-pinch the m=1 kink instability is another very important mode, which has been studied extensively in the past, usually within the framework of MHD theory. This instability is quite sensitive to the plasma profile. A detailed study is therefore carried out for this mode both in the MHD and the kinetic limits, using the Bennett profile. Kinetic effects are again found to have an important influence. They stabilize the mode at large k - an effect not predicted by MHD theory. The third application of the dispersion relation is made to the resistive firehose instability which is studied in the context of a non-relativistic beam propagating in a resistive background plasma. This instability which arises due to the resistive phase-lag between the plasma and the magnetic field is found to be stable at very large and very small wavenumbers. Earlier theoretical models of this mode accounted

for the phase-mixing between the particle orbits arising from the radial dependence of the betatron frequency, but ignored the wave-particle effects as well as non-local effects arising from density inhomogeneities. These effects are included in our calculation, although, phase mixing is omitted. It is found that Kinetic damping effects are comparable to the damping effect due to the phase-mixing of orbits in realistic parameter regimes. Our calculation also predicts a lower cut-off in k which is not predicted by the earlier models.

ACKNOWLEDGEMENT

I wish to express my gratitude to my supervisor, Professor Abhijit Sen, whose tolerant attitude, inspiring nature and competent guidance have helped me immensely in this endeavour. I consider it a privilege to have been associated with him.

It is a great pleasure to thank Dr. A.S. Sharma for his valuable help and fruitful discussions throughout the course of this work. I also wish to thank him for the critical reading of the manuscript and for his valuable comments.

I wish to thank Drs. Mohan, Sitaram, Sheorey and Duttagupta for numerous helpful discussions I had with them.

I would like to thank my friends Chitra, Sheela, Anitha, Ammu, Subbaraman, Aparna, Rhama, Krishnakumar, Vinod, Sandhya, Veena and Sridhar for the friendly and warm atmosphere provided by them during the course of my research work.

I am grateful to Mr. Dholakia, Dr. Kulkarni and Dr. Ahalpara of the Computer Centre, for their help in the numerical problems, and to Mr. Bhoi and Mr. Patel of Plasma Physics Programme for their drafting services.

This manuscript was typed by Mr. V.T. Viswanathan on the DEC1091 System using the software program ECRITE developed by Dr. B.R. Sitaram and Mr. Amarendra Narayan. I am also indebted to them.

I wish to thank Mrs. Bharucha, Mrs. Ghiya and Mrs. Patil and the library staff for their valuable cooperation during this work.

Lastly, I would like to thank my husband, Nagesha, for helping me in a number of ways, and above all for his enormous understanding and infinite patience.

Usha Krishnamurthi

Table of Contents

Chapter 1

Introduction

1.1 Background

The confinement of plasmas by magnetic fields has been a major subject of study over the past several decades. The principal motivation has come from the field of controlled thermonuclear fusion - where the aim is to build a reactor capable of exploiting the energy released in the fusion reaction of light elements. For example, if a nucleus of Deuterium and a nucleus of Tritium are made to fuse they produce one nucleus of Helium and the reaction gives off a lot of energy in the form of a fast neutron. Several such reactions are possible (see Table 1, where some important ones are listed) and the energies released are quite large - of the order of several Mevs. This energy can be captured in a reactor by either slowing down the energetic neutron in appropriate blanket materials or in the case of charged particles by devising a direct means of converting it to electrical energy. However, in order to bring about

the fusion reactions, enormous amount of energy has to be initially supplied to the reacting nuclei so that they can overcome the strong electrostatic repulsion between them. The required temperature for D-D and D-T reactions is in the range of 10 KeV. At such high temperatures the reacting nuclei (the plasma) will tend to fly apart and one needs to devise a method of holding them together. In fact, to get a net gain in energy the reacting plasma must be dense enough and must be held long enough for a large number of nuclear reactions to happen so that they can compensate for the initial energy investment. A quantitative criterion to express this breakeven condition was first worked out by Lawson [1]. The Lawson condition states that the product of the plasma density (in particles per cubic centimetre) and confinement time (in seconds) should be greater than 10^{14}. Attainment of this condition has been the major goal of fusion research and several ideas and schemes have been developed over the years. They can be broadly classified into two categories - the magnetic confinement approach and the inertial confinement method.

Since charged particles remain tied to magnetic field lines due to the Lorentz force, the first approach is to create suitable magnetic traps that will hold a tenuous plasma (of density about 10^{14}) for about a second. Heating is primarily done by passing strong currents which lead to Joule dissipation on account of the plasma resistivity. Beyond a certain temperature, however, this heating method becomes ineffective as the plasma becomes less resistive.

Additional methods of heating rely on shining strong electromagnetic radiation that helps excite collective modes in the plasma (which are eventually damped by interaction with the particles) or injecting energetic neutral particles which get ionised and transfer energy through collisions. In the inertial approach there is no attempt to confine the plasma but solid fuel pellets are imploded and compressed by intense pulses of laser radiation or energetic particle beam.At such high densities Lawson criterion can be satisfied for times less than a nanosecond which is of the order of the time for free expansion of the plasma. The laser pulse also leads to heating the plasma.

Historically, the magnetic confinement approach developed earlier [2] and is today in a more advanced stage of achievement than the inertial approach. One of the earliest magnetic confinement devices (and conceptually one of the simplest) that was used in fusion research is the linear Z-pinch. In this, a strong current flows in the axial (z) direction of a cylindrical plasma inducing a magnetic field in the azimuthal ($\hat{\theta}$) direction (Fig.1.1).The self-induced magnetic field compresses (pinches) the plasma and confines it.The basic equilibrium is established by the balance between the magnetic and thermal forces.The early experiments showed that the linear Z-pinch was an unstable configuration and exhibited various growing oscillations. The prominent ones were identified as gross

and kink modes. In a sausage mode (Fig.1.2) the plasma column is constricted at some places and develops bulges in between two necks. The plasma current flowing through the necks produces a stronger azimuthal field in that region (due to the small cross section of the plasma in that region) and this stronger field tends to further constrict the plasma. This is thus an unstable situation which favours the growth of the sausage mode. Fig. (1.3) shows a plasma column subjected to a kink type perturbation - involving a gross motion of the plasma off the symmetry axis and a helical distortion.It is seen that as a result of the perturbation the magnetic field lines are compressed together on the concave side of the bend and separated out on the convex side. This creates an imbalance in the magnetic pressure on the two sides.Again the net magnetic force is such as to enhance the perturbation and further distort the plasma column and eventually break it up.These instabilities were predicted from fluid theory studies by Kruskal and Schwarzchild [3].Further work in this direction was done by Newcomb [4] who enunciated some general stability conditions for the hydromagnetic stability of a diffuse linear pinch.Growth rate calculations using normal mode analysis of the linear MHD equations were done using various current models -such as the skin current model [5] and various distributed current models [6, 7]. The experimental work of Carruthers and Davenport [8] first demonstrated the unstable wriggling of the discharge, which was probably dominated by the m=1 kink mode. Another MHD

instability, the m=0 Rayleigh-Taylor instability, was extensively studied by Curzon et al [9]. Uncontrolled contractions and expansions of the plasma column were also observed by Cousins and Ware [10] who took streak photographs of this motion.

Further theoretical studies and some experimental evidence indicated enhanced stability in the presence of a strong axial magnetic field. This brought about a major shift in the choice of magnetic configurations considered for plasma confinement. The preference was for configurations with strong axial fields (equal to or larger than the induced field) and toroidal geometries to eliminate the end losses endemic to linear devices. Examples of such devices are the tokamaks and reversed field pinches. With the remarkable success of tokamak experiments in achieving higher and higher $n\tau$ values and pushing up the ion temperature by means of various heating schemes, interest in linear pinches diminished considerably.

The largest operating fusion type experiments today are tokamaks and it is expected that some of them will demonstrate scientific breakeven in a very short time.

However, there is a resurgence of interest in the Z-pinch. There are several reasons for this surprising renewed interest. Despite their remarkable laboratory success, it is widely accepted that tokamaks are not ideally suited for a reactor configuration. The toroidal geometry puts severe engineering difficulties in the design of blankets and other operational aspects. The tokamak is

also limited to rather small β values because of ballooning instabilities[11-13] (where β is the ratio of the plasma pressure to the magnetic field pressure). Thus it is not a very efficient device in terms of utilising the magnetic energy invested to hold the hot plasma. For magnetic field values of 5 -10T and β of about 10% the plasma density is restricted to values of about 10^{14} cm^{-3}. To satisfy the Lawson criterion this requires energy containment time of the order of seconds which in turn requires plasma radii to be of the order of metres (from present thermal conduction values). As against this, devices such as linear Z-pinches can, in principle, offer a more compact and efficient alternative. Theoretical calculations show [14-16] that a Z-pinch of 0. 1m length and 20μm radius with a density of 10^{21} cm^{-3} and self magnetic field of 10^4 T from a current of 10^6A gives a confinement time of 100ns against end losses to satisfy the Lawson condition. These parameter values place the potential Z-pinch reactor somewhere between the tokamak approach and the inertial fusion schemes. A linear device has also a simpler geometry aiding accessibility and other design considerations for a reactor.

Interest in the Z-pinch has been further heightened by some recent experimental evidence which suggests improved stability of this configuration. In particular, a related configuration, the plasma focus has already demonstrated the achievment of plasma density of $10^{19}cm^{-3}$ and an electron temperature of several keV in a narrow pinch a few millimetres in diameter and about a centimetre in

length[17]. The plasma focus is created between two annular electrodes connected to a condenser bank (Fig.1.4). As the bank is fired across the gap between the electrodes, breakdown occurs along the insulator and the resulting current sheet is accelerated by a J X B force in the axial direction. As the plasma reaches the end of the inner electrode it undergoes rapid three dimensional compression and becomes a highly compressed cylindrical filament very much similar to a linear Z-pinch. Another recent experiment which has shown good promise is the Extrap Z-pinch [18,19] in which a high density pinch is embedded in an octopole field (Fig. 1. 5). Again the plasma is found to exhibit remarkably good stability. The FLR effects could be a stabilizing mechanism for linear Z-pinches, provided, the pinch is operated in a suitable regime. Such a prospect has spurred both theoretical [20,21] and experimental work [22, 23] in this direction. Fluid theory assumes smallness of the Larmor radius compared to plasma dimensions. Hence to properly account for FLR effects the attempts are to include them in a perturbative sense or resort to kinetic formulations. Experimental interest has shifted towards high density Z-pinch configurations aided to a great extent by the developments in high voltage, high current pulse technology.

1.2 Motivation

The present work is motivated by this renewed interest in linear pinches and the need for a detailed understanding of their stability properties from a microscopic point of view. For a proper theoretical treatment of particle orbit effects, a kinetic formulation is most appropriate. The Bennett equilibrium [24,25] is a particular case of a class of Vlasov equilibria characterised by a constant axial macroscopic velocity for the plasma species.It has several features which make it ideally suited to represent the linear pinch and other related configurations. We have therefore chosen to study the kinetic stability of this equilibrium. It is important to point out two significant features that have hitherto not received adequate attention with regard to this problem - inhomogeneity effects and betatron orbit effects. There are a variety of possible particle orbits in the inhomogeneous magnetic field of the Bennett profile. In addition to the usual Larmor orbits (near the plasma edge), there are large excursion betatron orbits close to the axis of the plasma where the magnetic field is nearly linear.In many situations these orbits can be the dominant ones and,as our work shows, they can have a significant influence on the stability properties of the plasma. Since their orbit radii are comparable to the spatial scale lengths of the plasma column, a non-local and kinetic approach is necessary to take account of

wave-particle resonances and the radial dependence of perturbations. In this thesis, such a non-local theory for general electromagnetic perturbations of the Bennett equilibrium has been developed within the framework of the Vlasov-Maxwell equations, taking into account betatron orbit effects. The theory is applicable to a variety of physical situations including the Z-pinch, plasma focus, Extrap and beamplasma propagation experiments and allows us to gain some insight into their macroscopic and microscopic behaviour.

1.3 Scope of the thesis

The thesis has been organised as follows. In chapter 2 we have carried out a systematic development of a non-local kinetic stability theory for the Bennett equilibrium taking into account its large excursion betatron orbits. Various non-local theories for the plasma stability analysis have been developed earlier [26-32]. Our formulation is closest to the one developed by Davidson [33] for the theta pinch and further adapted by Sharma [34] for the Z-pinch. It uses a Bessel function representation for the radial amplitudes of the perturbed quantities. Using the linearised Vlasov-Maxwell theory we obtain a set of integro-differential equations for the perturbed quantities - ϕ_1 the scalar potential and $\bar{A}_1$ the vector potential. These are converted to an infinite set of algebraic relations with the help of the basis function expansions. The solvability condition of these equations requires the vanishing of a determinant and leads to the dispersion relation for the linear modes of the system. The elements of the determinant are functions of ω, the frequency, k the wave number and the basic parameters of the plasma. In obtaining them we perform orbit integrations over the betatron orbits (analytically) and express the nonlocal contributions in terms of radial integrals which are to be evaluated numerically. This chapter also contains a general discussion on the Bennett equilibrium and the

betatron orbits. In deriving the dispersion relation we also make the assumption that the principal contribution to the perturbed currents are those arising from A_{1z} (the axial component of the wave vector) and neglect contributions from A_{1r} and $A_{1\theta}$. This assumption is valid for low frequency perturbations.

In general the dispersion relation is difficult to solve analytically except in certain simple limits. The principal approach taken in this thesis is therefore a detailed numerical solution of the dispersion relation using a variety of complex-root solving techniques. These results are supplemented wherever possible by limiting analytic expressions. The latter are very helpful in clarifying some of the underlying physics. The dispersion relation has been studied in detail for three distinct problems which are related to important physical situations.

In chapter 3, we have looked at the m=1(kink type) instability which is one of the most important modes for the Z-pinch configuration. For this electromagnetic mode the contribution from the scalar potential is negligible and putting $\phi_1=0$ we simplify the dispersion relation somewhat. However, the determinant is still of infinite order and we truncate it to appropriate dimensions (20x20) or (40x40) by checking the convergence of a given root. We have also been able to reduce the matrix dispersion relation to a simpler form by exploiting certain analytic relations between the coefficients. This reduced form is faster to solve numerically and yields limiting analytic

forms as well. Our results indicate that the current driven kink mode can be stabilised beyond a certain k value by virtue of the damping introduced by the betatron effects. At low k the behaviour of the growth rate is similar to that predicted by fluid theory treatments. Incidentally the earlier fluid calculations are based on simple current profile models. We also solve the linearized MHD equations with a Bennett profile for a more realistic comparison with our kinetic results.

There is also ample experimental evidence for a variety of microinstabilities in the pinch configuration, particularly in the later compression stages[35]. These have been discussed by various workers[36,37] and some of the possible modes suggested are the Buneman, the ion-acoustic and the lower hybrid drift instabilities. With a view to understanding some of this activity, we have next looked at the electrostatic limit of our generalized dispersion relation in Chapter 4. Numerical solutions reveal an unstable mode whose characteristics are very similar to those of an ion-acoustic mode in a two component plasma with a relative drift. The mode is stable for very large and very small values of the wave number. The range of unstable k increases with the increase in V_e, the electron drift. There is also a threshold V_e below which the mode is stable. The real part of the frequency at large k is close to $-kC_s$ where C_s is the ion-acoustic speed. But at small k there is a significant departure from

the ion-acoustic frequency which is a modification arising from the ion betatron motion. There is also a significant stabilization effect arising from the betatron motion which raises the threshold of instability much above the onset of the usual current driven ion-acoustic instability. The results of this calculation are applied to some recent experiments on the Extrap Z-pinch and the plasma focus.

In the next chapter, Chapter 5, we return to the m=1 kink mode but look at a resistive version of this instability. Better known as the resistive (fire)hose instability, it is a growing lateral distortion of an energetic self-pinched beam propagating in a dense resistive plasma. The instability is driven by a resistive lag of the magnetic field in responding to transverse displacements of the beam. The hose instability has been studied extensively [38-41], but most of the theoretical work is based on very simplified models of beam particle dynamics. There are two important physical effects that need to be taken into account properly. Since the pinch force is anharmonic whenever the radial profile of current density is rounded, particles have a spread of betatron frequencies that introduces phase mixing and tends to damp the mode. The other effect has to do with the betatron particle orbits and the localized wave-particle resonances they introduce. In some of the recent work [42-44] realistic estimates have been obtained for the phase mixing effect through improved beam modelling (e.g. "spread mass" model

etc.) However the wave -particle effect is still not treated very satisfactorily. Our present formulation is quite well suited for this purpose and we have applied it to this problem by including the resistive contribution from the background plasma. Our numerical results show that in some regimes the damping effects of the Landau type (due to wave particle resonances) are comparable to the phase mixing effects. We discuss the implications of these for experimental situations.

Our final chapter, Chapter 6, contains a short summary of the main results of the thesis. It also discusses some of the main assumptions made in our theoretical analyses and the consequent limitations of the present work. These also provide a clue to possible future extensions of this work and these are briefly stated.

References

1. Lawson, J.D., Proc. Phys. Soc. B70, 6 (1957).

2. See for example 'Project Sherwood' by Bishop, A.S., Addison-Wesley, Reading, Massachussetts (1958), for an early history of the fusion program.

3. Kruskal, M. & Schwarzchild, M., Proc. Roy. Soc. A223, 348 (1954).

4. Newcomb, W.A., Annals of Physics (N.Y.) 10, 232 (1960).

5. Kadomtsev, B. B., in Reviews of Plasma Physics, Ed. M.A. Leontovich (Consultants Bureau, N.Y.) II, 153 (1966).

6. Friedberg, J.P., Phys. Fluids 13, 1812 (1970).

7. Hain, K. & Lust, R., Z. Naturforsch. 13a, 936 (1958).

8. Carruthers, R. & Davenport, P.A., Proc. Phys. Soc. B70, 49 (1957).

9. Curzon, F. L., Folkierski, A., Lathem, R. & Nation, J.A., Proc. Roy. Soc. A257, 386 (1960).

10. Cousins, S. W. & Ware, A.A., Proc. Phys. Soc. B64, 159 (1951).

11. Mercier, C., Nucl. Fusion 1, 47 (1969).

12. Dobrott, D., Nelson, D.B., Greene, J.M., Glasser, A.H.,

Chance, M. S. & Frieman,E.A., Phys. Rev. Lett. 39, 943 (1977).

13. Coppi,B., Phys. Rev. Lett. 39, 938 (1977).

14. Haines,M.G., Phys. Scripta T2/2, 380 (1982).

15. Hartman, C. W. , Carlson, G., Hoffman,M., Werner,R. & cheng,D.Y.,Nucl. Fusion 17, 909 (1977).

16. Hagenson, R.L., Tai,A.S. & Krakowski,R.A., Nucl. Fusion 21, 1351 (1981).

17. Bernard, A. , Coudeville,A., Garconnet,J.P., Genta,P., Jolas,A., Landure,Y., deMascureau,J., Nazet,C. & Vezin, R. , Plasma Physics and Controlled Nuclear Fusion,IAEA, III, 83 (1974).

18. Drake,J.R., Plasma Phys. 26, 387 (1984)

19. Drake, J. R. , Hellsten, T., Landberg,R., Lehnert,B., Wilner, B. , Plasma physics and controlled Nuclear fusion research,IAEA, II, 717 (1981).

20. Wright,R.J., Pott,D.F.R., Haines,M.G., Plasma Phys. 18, 1 (1976).

21. Akerstedt, H. O. , Ph. D. Thesis, Uppsala University, Sweden (1985).

22. Struve, K. W. , Ph. D. Thesis, Lawrence Livermore Laboratory (1980).

23. Choi, P., Dangor,A.E., Folkierski,A., Kahan,E., Potter, D. E., Slade, P. D., Webb,S.J.,Plasma Physics and Controlled Nuclear Fusion,IAEA, II, 69 (1978).

24. Bennett,W.H., Phys. Rev. 45, 980 (1934).

25. Bennett,W.H., Phys. Rev. 98, 1584 (1955).

26. Marchand, R., Zhang,C.F. & Lee,Y.C., Phys. Fluids 26, 194 (1983).

27. Myra, J. R., Catto,P.J., Aamodt,R.E., Phys. Fluids 24, 651 (1981).

28. Symon,K.R., Seyler,C.E., Lewis,H.R., J.Plasma Phys. 27, 13 (1982)

29. Lewis, H. R. & Seyler, C. E., J. Plasma Phys. 27, 25 (1982).

30. Lewis, H. R. & Seyler, C. E., J. Plasma Phys. 27, 37 (1982).

31. Ferraro, R.D., Sanuki,H., Littlejohn,R.G. & Fried,B.D., Phys. Fluids. 28,2181 (1985).

32. Chen,J. & Lee,Y.C., Phys. Fluids. 28, 2137 (1985).

33. Davidson,R.C., Phys. Fluids 19, 1189 (1976).

34. Sharma,A.S., Nucl. Fusion 23, 1493 (1983).

35. Bernard, A., Coudeville,A., Jolas,A., Launspach,J. &

36. Liewer,P.C. & Krall,N.A., Phys. Fluids 16, 1953 (1973).

37. Vikhrev, V.V. & Korzhavin,V.M., Sov. J. Plasma Phys. 4, 411 (1978).

38. Rosenbluth,M.N., Phys. Fluids 3, 932 (1960).

39. Weinberg,S., J. Math. Phys. 8, 614 (1967).

40. Lee,E.P., Phys. Fluids 21, 1327 (1978).

41. Lauer, E.J., Briggs,R.J., Fessenden,T.J., Hester,R.E. & Lee,E.P.,Phys. Fluids 21, 1344 (1978).

42. Uhm,H.S. & Lampe,M., Phys. Fluids 23, 1574 (1980).

43. Sharp, W.M., Lampe,M. & Uhm,H.S., Phys. Fluids 25, 1456 (1982).

44. Lampe, M., Sharp,W., Hubbard,R.F., Lee,E.P. & Briggs,R. J., Phys. Fluids 27, 2921 (1984).

Table 1

$D + D \longrightarrow T\ (1\ Mev) + p(3\ Mev).$

$D + D \longrightarrow He^3(.8Mev) + n(2.5Mev).$

$D + T \longrightarrow He^4(3.5Mev) + n(14\ Mev).$

$D + He^3 \longrightarrow He^4(3.6\ Mev) + p(14.7\ Mev).$

$P + Li^6 \longrightarrow He^4 + He^3 + 4.0\ Mev$

$P + B^{11} \longrightarrow 3He^4 + 8.7\ Mev$

Figure captions for chapter 1

Fig. (1.1) The Z-pinch configuration.

Fig. (1.2) m = 0 Sausage Instability.

Fig. (1.3) m = 1 Kink Instability.

Fig. (1.4) Schematic view of the Plasma Focus.

Fig. (1.5) The Extrap configuration.

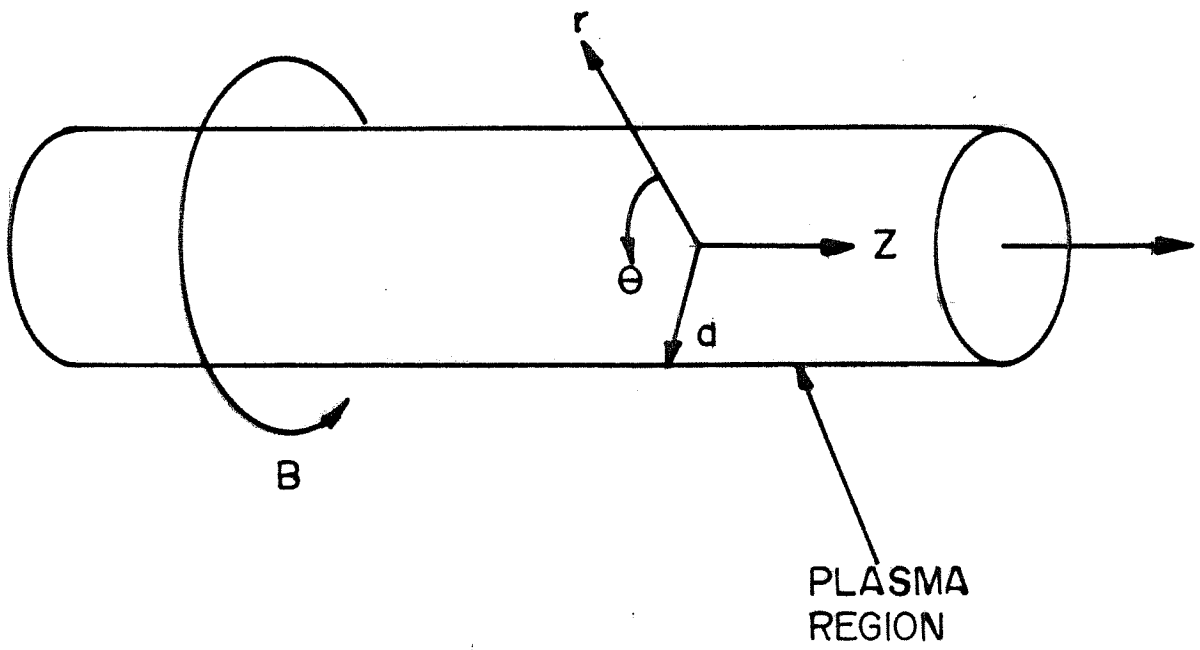

FIG. 1.1

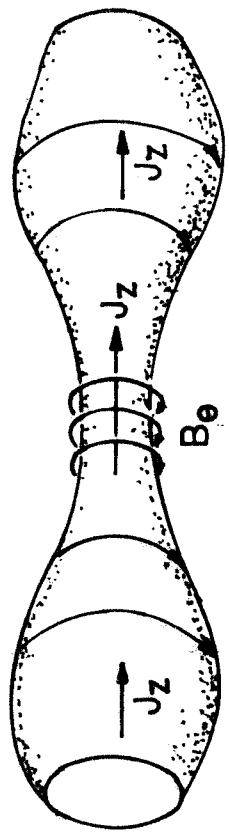

FIG. 1.2

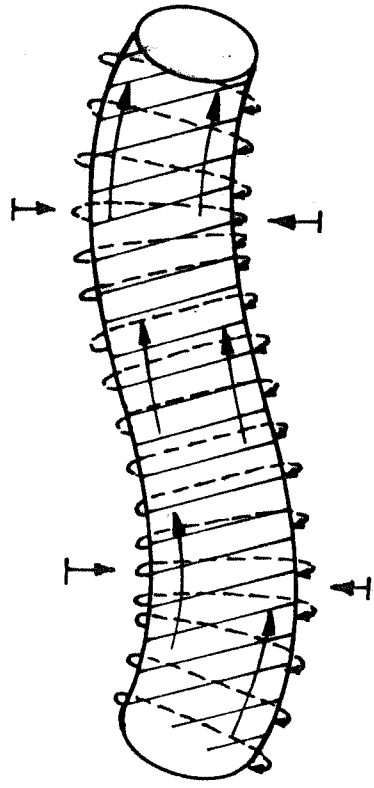

FIG. 1.3

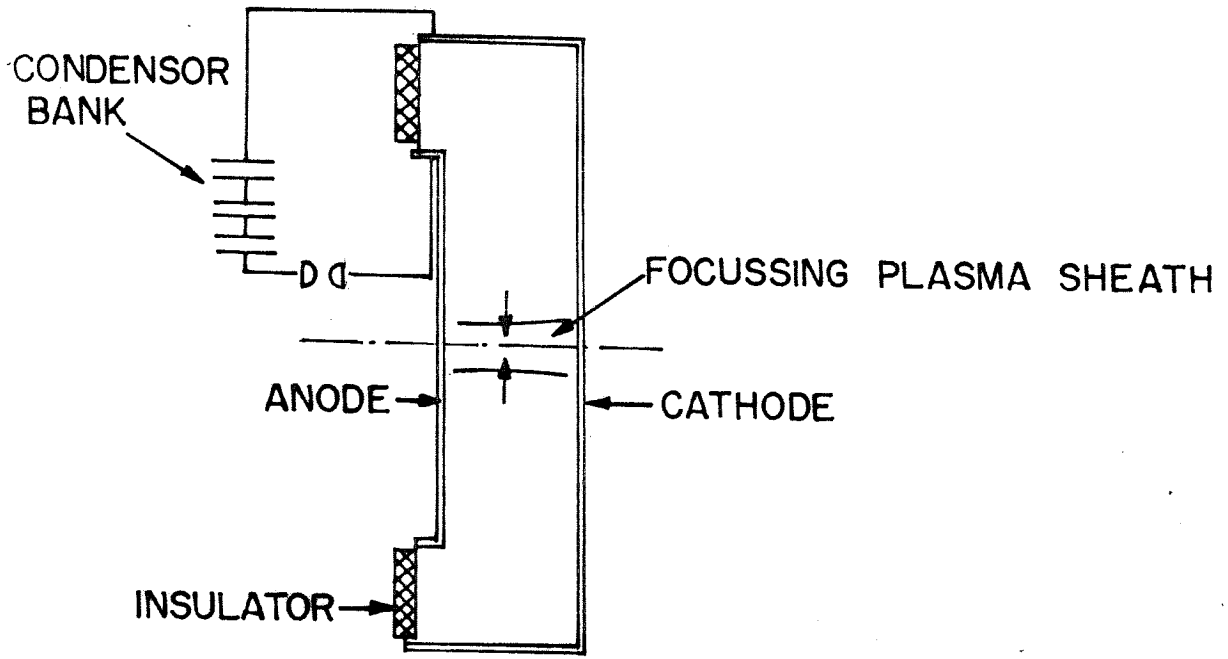
CONDENSOR
BANK
D
FOCUSSING PLASMA SHEATH
ANODE
CATHODE
INSULATOR

FIG. 1.4

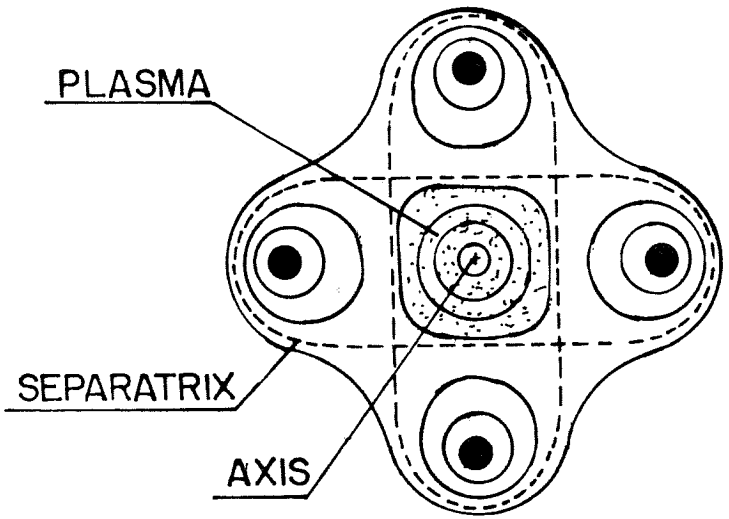

FIG. 1.5

Chapter 2

Non-local stability theory for general electromagnetic perturbations.

2.1 Introduction.

The linear response of a collisionless plasma to a perturbation is described by the linearised Vlasov-Maxwell equations, which is a set of integro-differential equations. The integrations over the unperturbed trajectories of the charged particles leads to the integral nature of these equations. When the scale lengths of the inhomogeneities are large, the perturbed quantities appearing in the orbit integrals are usually approximated by their Taylor expansions around the local positions of the particles. This leads to the eigenmode equations which are now differential equations. However, in the case of equilibria where the spatial inhomogeneities of the fields and currents are large, this 'local-approximation' is not justified. It is therefore necessary in such cases to consider a non-local theory for studying the modes of the system, namely, an integral formulation of the stability analysis. In such theories, the eigenmodes of the system are

linearised Vlasov-Maxwell set of equations yields a matrix dispersion relation. Such a theory has been developed for the rigid-rotor equilibria of a theta-pinch by Davidson[1], wherein the perturbations were expressed in terms of Bessel functions. A similar integral approach was used by Sharma[2] to study the stability of Bennett equilibrium when most of the particles execute betatron orbits. In recent times the integral approach to the stability analysis has been used to study various physical situations.

The ion-gyro instability associated with the flow of ions encircling the magnetic axis in an inhomogeneous mirror-plasma has been studied by Catto,et al [3]. Myra et al. [4] studied the stability of an inhomogeneous cylindrical plasma to electrostatic flute perturbations in the ion-cyclotron and lower-hybrid frequency range. For large growth rates they were able to reduce the integral equation for the radial eigenmodes to a differential equation in the limit of straight line ion orbits. Marchand et al [5] have used the integral formulation to study the drift-type electrostatic perturbations of a collisionless cylindrical plasma with an axial magnetic field.They have solved the integral equation for the lower hybrid mode and the low-frequency drift mode numerically by the Gaussian quadrature method. In a series of papers Lewis et al [6-8] have presented a general formulation for the study of linear stability of inhomogeneous plasmas. By expanding the perturbed distribution function in terms of the eigenfunctions of the unperturbed Liouville operator they

obtained a dispersion matrix which yields the eigenmodes of the problem. The dispersion matrix is expressed in terms of a dynamic spectral matrix which is dependent on the unperturbed particle orbits. This method was applied to study the stability of multi-species Vlasov plasmas and the Vlasov-fluid model, and a necessary and sufficient condition for the stability of the latter was derived [7-8].

The drift and drift cyclotron instability in a cylindrical plasma has been studied by Ferraro et al [9] using the integral approach. The eigenfunctions in this case were expanded in terms of the Associated Laguerre functions. The tearing instability of a neutral sheet was recently studied by Chen and Lee[10] using the Galerkin method to solve the integral equations.

The Bennett equilibrium [11] is a particular example of a class of axially and azimuthally symmetric equilibria with an equilibrium axial current.These equilibria which are characterised by strong spatial inhomogeneities have been studied extensively earlier [2, 11-13]. They are in general described in terms of an equilibrium distribution function which is an arbitrary function of the single-particle constants of motion. These constants of motion are determined by the symmetries in the equilibrium configuration. For a given system the equilibrium fields and currents can be obtained self-consistently by solving the Vlasov-Maxwell system of equations, with appropriate boundary conditions. The integral stability analysis for electrostatic perturbations of the Bennett equilibrium was

developed by Sharma [2].

In this chapter we consider the stability of a Bennett configuration against general electromagnetic perturbations with arbitrary azimuthal mode number and develop a non-local perturbative theory to obtain a dispersion relation. This dispersion relation is quite general and is applicable to all cylindrical plasmas with Bennett profile and perturbations with arbitrary scale lengths including those comparable to the spatial scale lengths of the equilibrium. We have applied this dispersion relation to the study of electrostatic and electromagnetic instabilities in a pure Z-pinch, the plasma focus and the resistive instability of a beam propagating in a background plasma channel. In the next section we outline the derivation of the equilibrium , its properties and the particle orbits in this equilibrium.

2.2 Equilibrium and particle orbits

Consider an infinitely long cylindrical plasma column consisting of electrons and ions counterstreaming along the axis of the cylinder with a uniform velocity V_j. We choose a cylindrical polar coordinate system (r, θ, z) with its z-axis along the axis of the cylinder. We assume that the equilibrium quantities are independent of z and θ, so that

$$\frac{\partial}{\partial z} = 0 \quad \text{and} \quad \frac{\partial}{\partial \theta} = 0$$

The equilibrium drift of the charged particles gives rise to an axial current and consequently to an azimuthal magnetic field which can be represented by a single component $A_z(r)$ of the vector potential:

$$\bar{A} = (0, 0, A_z(r))$$

In addition we assume that the equilibrium is charge-neutral so that $\phi = 0$, ϕ being the scalar potential. The Lagrangian of a particle with charge q_j in this field can be written as

$$\begin{aligned} L &= \frac{1}{2} m_j v^2 + \frac{q_j}{c} \bar{v} \cdot \bar{A} \\ &= \frac{m_j}{2} \left(\dot{r}^2 + r^2 \dot{\theta}^2 + \dot{z}^2 \right) + \frac{q_j}{c} \dot{z} A_z \end{aligned} \tag{2.1}$$

where 'j' refers to the particle species and dots represent time derivatives. From equation (2.1) it is clear that θ and z are cyclic coordinates. It therefore follows from the Lagrange's equations that the axial and azimuthal conjugate

momenta are constants of the motion. Also for a conservative system the Hamiltonian or energy H_{0j} is a constant of the motion. These are given by:

$$P_{zj} = m_j \dot{z} + \frac{q_j}{c} A_z(r) \tag{2.2}$$

$$P_{\theta j} = m r^2 \dot{\theta} \tag{2.3}$$

$$\& \quad H_{0j} = \tfrac{1}{2} m_j V^2 \tag{2.4}$$

From these constants of motion one can construct distribution functions $f_{0j}(\bar{x}, \bar{v})$, all of which would satisfy the Vlasov equation. For a given equilibrium the choice of the functional form of f_0 is governed by the specific properties of that equilibrium. For the Bennett-type equilibria where the particles have temperature T_j and axial drift V_j, the equilibrium distribution function is chosen to be of the rigid-drift type:

$$f_{0j}(\bar{x}, \bar{v}) = c_1 \exp -\left(\frac{H_{0j} - P_{zj} V_j}{T_j}\right) \tag{2.5}$$

where c_1 is a constant determined by the normalisation condition. This is called the rigid-drift distribution because it leads to an average macroscopic drift of each species along the z-axis, and is appropriate for describing

high-beta collisionless plasmas [13].

The equilibrium density is given by:

$$n_j = \int d^3v \, f_{0j} \tag{2.6}$$

Substituting for f_{0j} from (2.5) we obtain

$$n_j = \hat{n}_0 \exp\left(\frac{q_j V_j}{c T_j} A_z(r)\right) \tag{2.7}$$

From the charge neutrality condition, viz.,

$$n_i q_i + n_e q_e = 0$$

We obtain:

$$\exp \frac{e A_z}{c}\left(\frac{V_i}{T_i} + \frac{V_e}{T_e}\right) = 1$$

This implies that

$$\frac{V_i}{T_i} + \frac{V_e}{T_e} = 0 \tag{2.8}$$

Defining $T_e/T_i = \tau$, $T_e = T$ and $V_e = -V\hat{z}$

we obtain from the above relation $V_i = V/\tau$ and $T_i = T/\tau$

The equilibrium current is given by

$$\bar{j}_0 = \sum_j q_j \int d^3v \, \bar{v} \, f_{0j}$$

$$= \hat{n}_0 e V \left(\frac{1+\tau}{\tau}\right) \exp\left(\frac{eV}{cT} A_z(r)\right) \tag{2.9}$$

The vector potential $A_z(r)$ is given by the equilibrium Ampere's law:

$$\nabla \times \bar{B}_0 = \frac{4\pi}{c} \bar{J}_0$$

Choosing the Coulomb gauge viz., $\nabla \cdot \bar{A} = 0$ and expressing $\bar{J}_0$ in terms of A_z we have

$$-\nabla^2 A_z = \frac{4\pi}{c} \hat{n}_0 eV \left(\frac{1+\tau}{\tau}\right) \exp\left(\frac{eV}{cT} A_z(r)\right)$$

In the cylindrical coordinates with θ and z symmetry, we have

$$\frac{1}{r} \frac{\partial}{\partial r}\left(r \frac{\partial A_z}{\partial r}\right) + \frac{4\pi}{c} n_0 e \frac{(1+\tau)}{\tau} V \exp\left\{\frac{eV}{cT} A_z\right\} = 0 \qquad (2.10)$$

Introducing the variables $x = Kr$ and $y = eVA_z/cT$ we obtain from equation (2.10)

$$\frac{1}{x} \frac{d}{dx}\left(x \frac{dy}{dx}\right) + 2e^y = 0 \qquad (2.11)$$

The general solution of equation(2.11) is given by [12]:

$$A_z(r) = -\frac{cT}{eV} \ln\left\{\frac{K^2 r^2}{4\eta^2}\left[\left(\frac{r}{r_0}\right)^{\eta} + \left(\frac{r_0}{r}\right)^{\eta}\right]^2\right\} \qquad (2.12)$$

Equation (2.12) represents the generalised Bennett equilibria. The constants r_0 and η are arbitrary constants and depend on the boundary conditions. The constant r_0 represents a scale length associated with the radial variation of the beam profile. η is a shaping parameter. Figure(2.1) shows the density profiles for different values of η. For $\eta \neq 1$ the solution is not physical. In such cases additional current is needed to balance internal forces in the beam. The case with $\eta = 1$ and $r_0 = 1/K$ corresponds to the Bennett equilibrium. Here the self-pinching due to the

magnetic field just compensates for the tendency of the thermal motion to make the like-charges fly apart. Substituting $\eta = 1$ and $r_0 = 1/K$ in equation (2.12) we obtain the solutions for the Bennett profile:

$$A_{0z}(r) = -\frac{cT}{eV} \ln\left(1 + \frac{K^2 r^2}{4}\right)^2$$

$$= -\frac{2cT}{eV} \ln\left(1 + \frac{K^2 r^2}{4}\right) \qquad (2.13)$$

The density and current profiles in this case are obtained by substituting for A_{0z} from (2.13) in (2.7) and (2.9) respectively:

$$n(r) = \hat{n}_0 \exp\left(\frac{eV}{cT} A_{0z}(r)\right)$$

$$= \frac{\hat{n}_0}{\left(1 + \frac{1}{4} K^2 r^2\right)^2} \qquad (2.14)$$

$$J_{0z}(r) = \hat{n}_0 eV\left(\frac{1+\tau}{\tau}\right) \exp\left(\frac{eV}{cT} A_{0z}\right)$$

$$= \hat{n}_0 eV\left(\frac{1+\tau}{\tau}\right) \frac{1}{\left(1 + \frac{1}{4} K^2 r^2\right)^2} \qquad (2.15)$$

The magnetic field profile corresponding to equation (2.13) is given by

$$B_0 \hat{\theta} = -\frac{dA_z}{dr} \hat{\theta} = \frac{\hat{B}_0 K r}{\left(1 + \frac{1}{4} K^2 r^2\right)} \hat{\theta} \qquad (2.16)$$

From the above profiles it is clear that the density

and current have their peak values on the axis. The magnetic field peaks at r= 2/K and the peak value is given by B_0=cTK/eV Figure (2. 2) shows the plot of the density and the magnetic field profiles as functions of the radial coordinate r. It is clear that for particles near the axis the magnetic field is almost linear in r and goes as B_0Kr. As the density of the particles peaks on the axis, most of the particles are located in the small r region and therefore experience a linear field. The orbits of such particles are betatron oscillations and have been analysed in detail by Gratreau[15]. These orbits have large radial excursions comparable to the lateral dimensions of the plasma and their exact shape and extent depends on the initial radial positions and velocities of the particles.

To obtain the exact trajectories of the particles, consider the approximate magnetic field $\bar{B}=B_0Kr$ for $K^2r^2/4<<1$. Transforming to Cartesian coordinates(x,y) which are given by x=r cosθ and y=r sinθ we can write the magnetic field in Cartesian coordinates as

$$\bar{B} = B_0 K(-\hat{x}\, y + x\, \hat{y}) \qquad (2.17)$$

Writing down the Cartesian components of the force equation for a particle of charge q_j and m_j we have

$$m_j \ddot{x}' = \frac{q_j}{c}(-v_z' B_y) = -\frac{q_j}{c} B_0 K x' v_z'$$

$$m_j \ddot{y}' = \frac{q_j}{c}(v_z' B_x) = -\frac{q_j}{c} B_0 K y' v_z' \qquad (2.18)$$

For small r, the z component of force can be neglected and the axial velocity is nearly constant. Therefore the x and y components of the force equation can be written as:

$$\ddot{x}' + \omega_{\beta j}^2 x' = 0 \qquad (2.19)$$
$$\ddot{y}' + \omega_{\beta j}^2 y' = 0$$

where $\omega_{\beta j} = \left(\frac{B_0 q_j k V_{z0}}{m_j c}\right)^{1/2}$ is the betatron frequency. The solutions to equations (2.19) define the charged particle trajectories in the equilibrium field. With the boundary conditions

$$x'(t'=t) = x \; ; \quad y'(t'=t) = y$$

$$V_x'(t'=t) = V \; ; \quad V_y'(t'=t) = V_y \qquad (2.20)$$

these solutions are given by

$$x' = x \cos \omega_{\beta j}(t'-t) + \frac{V_x}{\omega_{\beta j}} \sin \omega_{\beta j}(t'-t)$$
$$y' = y \cos \omega_{\beta j}(t'-t) + \frac{V_y}{\omega_{\beta j}} \sin \omega_{\beta j}(t'-t) \qquad (2.21)$$
$$z' = z + V_{z0}(t'-t)$$

The particle orbits in the r-ϕ plane consist of large excursion radial oscillations. The extent and shape of

these oscillations is determined by the initial position and velocity of the particle. Superimposed on these oscillations is an axial drift which leads to helical orbits. For particles having zero angular momentum these oscillations are sinusoidal and confined to a given r-z plane and cross the z-axis. For particles with finite angular momentum these orbits are helical and encircle the axis. Far away from the axis the magnetic field is nearly constant and the particle orbits in this region are the usual Larmor orbits. However such particles constitute a small fraction of the total number. Therefore we assume the dominant particle orbits to be betatron orbits. Figs. (2.3a and 2.3b) show the projections of the betatron and Larmor orbits in the r-z plane. Expressing the perpendicular velocity components in terms of the corresponding polar coordinates so that $v_x = v_\perp \cos\phi$; $v_y = v_\perp \sin\phi$ the orbits given by equation (2.21) can be expressed as

$$x' = r\cos\theta\cos\omega_{\beta j}(t'-t) + \frac{V_\perp}{\omega_{\beta j}}\cos\phi\sin\omega_{\beta j}(t'-t)$$

$$y' = r\sin\theta\cos\omega_{\beta j}(t'-t) + \frac{V_\perp}{\omega_{\beta j}}\sin\phi\sin\omega_{\beta j}(t'-t) \qquad (2.22)$$

$$z' = z + V_{z_0}(t'-t)$$

2.3 Derivation of the non-local dispersion relation

In this section we use the linearised Vlasov-Maxwell equations to investigate the stability of the Bennett equilibrium against small amplitude electromagnetic perturbations in the absence of collisions. For small amplitude perturbations the linearised Vlasov equation can be written as

$$\frac{\partial f_1}{\partial t} + \bar{v}\cdot\frac{\partial f_1}{\partial \bar{x}} + \frac{q_j}{m_j}\left(\frac{\bar{v}\times\bar{B}_0}{c}\right)\cdot\frac{\partial f_1}{\partial \bar{v}} = -\frac{q_j}{m_j}\left(\frac{\bar{v}\times\bar{B}_1}{c} + \bar{E}_1\right)\cdot\frac{\partial f_0}{\partial \bar{v}} \qquad (2.23)$$

The perturbed fields $\bar{E}_1$ and $\bar{B}_1$ can be expressed in terms of scalar and vector potentials ϕ_1 and $\bar{A}_1$ as

$$\bar{E}_1 = -\nabla\phi_1 - \frac{1}{c}\frac{\partial \bar{A}_1}{\partial t}$$
$$\bar{B}_1 = \nabla\times\bar{A}_1 \qquad (2.24)$$

The perturbed electric and magnetic fields are given by the linearised Poisson's and Ampere's equations respectively:

$$\nabla\cdot\bar{E}_1 = 4\pi\rho_1 = 4\pi\sum_j q_j\int f_{1j}\,d^3v \qquad (2.25)$$

$$\nabla\times\bar{B}_1 = \frac{4\pi}{c}\bar{J}_1 + \frac{1}{c}\frac{\partial \bar{E}_1}{\partial t} \qquad (2.26)$$

For low frequency electromagnetic modes the

displacement current term in equation (2.26) can be neglected. Substituting for $\bar{B}_1$ and $\bar{E}_1$ from (2.24) in (2.25) and (2.26) we have:

$$\nabla \cdot \left(-\nabla \phi_1 - \frac{1}{c} \frac{\partial \bar{A}_1}{\partial t} \right) = \frac{4\pi}{c} \sum_j \int q_j f_{1j} \, d^3v \qquad (2.27)$$

and

$$\nabla \times (\nabla \times \bar{A}_1) = \frac{4\pi}{c} \sum_j q_j \int \bar{v} \, f_{1j} \, d^3V \qquad (2.28)$$

Using the Coulomb gauge ($\nabla \cdot A = 0$) in (2.27) and (2.28) we have

$$-\nabla^2 \phi_1 = \frac{4\pi}{c} \sum_j q_j \int f_{1j} \, d^3V = \frac{4\pi}{c} \sum_j q_j n_{1j}$$

$$-\nabla^2 \bar{A}_1 = \frac{4\pi}{c} \sum_j q_j \int \bar{v} \, f_{1j} \, d^3V = \frac{4\pi}{c} \bar{j}_1 \qquad (2.29)$$

The perturbed distribution $f_{1j}(\bar{x}, \bar{v}, t)$ is obtained by integrating equation (2.23) over the unperturbed particle trajectories which in the present case are the betatron orbits given by (2.22). Thus we have:

$$f_{1j}(\bar{x}, \bar{v}, t) = \int_{-\infty}^{t} \frac{q_j}{m_j} \left(\bar{E}_1 + \frac{\bar{v} \times \bar{B}_1}{c} \right)' \cdot \frac{\partial f_{0j}}{\partial \bar{v}} \, dt' \qquad (2.30)$$

The primes within the integral indicate that the quantities are to be evaluated at the unperturbed particle orbits. f_{0j} is the normalised equilibrium distribution function given by

$$f_{0j}(\bar{x},\bar{v}) = \hat{n}_0\left(\frac{m_j}{2\pi T_j}\right)^{3/2} exp\left\{-\frac{1}{T_j}\left(H_{0j} - P_{z_j}V_j + \frac{m_j V_j^2}{2}\right)\right\}$$

$$= \hat{n}_{0j}\left(\frac{m_j}{2\pi T_j}\right)^{3/2} exp\left(\frac{q_j V_j}{c T_j} A_{0z}\right) exp\left\{-\frac{m_j}{2T_j}\left(V_x^2 + V_y^2 + (V_z - V_j)^2\right)\right\} \qquad (2.31)$$

From (2.24) we have

$$\frac{\bar{V}\times\bar{B}_1}{c} = \frac{\bar{V}\times(\bar{\nabla}\times\bar{A}_1)}{c} = \frac{1}{c}\left\{\nabla(\bar{V}.\bar{A}_1) - \frac{d\bar{A}_1}{dt} + \frac{\partial\bar{A}_1}{\partial t}\right\}$$

$$\therefore \bar{E}_1 + \frac{\bar{V}\times\bar{B}_1}{c} = \left[-\nabla\phi_1 - \frac{1}{c}\cancel{\frac{\partial\bar{A}_1}{\partial t}} + \frac{1}{c}\nabla(\bar{V}.\bar{A}_1) + \frac{1}{c}\cancel{\frac{\partial\bar{A}_1}{\partial t}} - \frac{1}{c}\frac{d\bar{A}_1}{dt}\right] \qquad (2.32)$$

Also

$$\frac{\partial f_{0j}}{\partial\bar{V}} = -\frac{m_j}{T_j}(\bar{v} - \bar{V}_j) f_{0j}$$

substituting in (2.30) we obtain

$$f_{1j}(\bar{x},\bar{v},t) = \frac{q_j}{T_j}\int_{-\infty}^{t}(\bar{V}' - \bar{V}_j')\, f_{0j}\left[-\nabla\phi_1 + \frac{1}{c}\nabla(\bar{V}.\bar{A}_1) - \frac{1}{c}\frac{d\bar{A}_1}{dt}\right]' dt'$$

$$= \frac{q_j}{T_j} f_{0j}\left(-\phi_1 + \frac{V_j A_{1z}}{c}\right) +$$

$$\frac{q_j}{T_j} f_{0j}\int_{-\infty}^{t}\left\{\frac{\partial\phi_1}{\partial t} + (\bar{V}_j\cdot\nabla)\phi_1 - \frac{1}{c}\frac{\partial}{\partial t}(\bar{V}.\bar{A}_1) - \frac{1}{c}(\bar{V}_j\cdot\nabla)(\bar{V}.\bar{A}_1)\right\}' dt' \qquad (2.33)$$

The particle trajectories satisfy the equations

$$\frac{d}{dt'}\bar{x}' = \bar{V}' \quad ; \quad \frac{d\bar{V}'}{dt'} = \frac{q_j}{m_j}\left(\frac{\bar{V}'\times B_0\hat{\theta}}{c}\right)$$

$$\bar{x}'(t'=t) = \bar{x} \quad ; \quad \bar{V}'(t'=t) = \bar{V} \qquad (2.34)$$

Each of the perturbed quantities can be expressed as a sum over Fourier components of the form:

$$\begin{aligned}\phi_1(r', \theta', z', t') &= \sum \bar{\phi}_1(r')\, e^{i(kz' + m\theta' - \omega t')} \\ \bar{A}_1(r', \theta', z', t') &= \sum \bar{A}_1(r')\, e^{i(kz' + m\theta' - \omega t')}\end{aligned} \tag{2.35}$$

where k, m, and ω are respectively the axial wavenumber, azimuthal mode number and frequency of the perturbation. Substituting in (2.33) we have:

$$f_{1j} = -\frac{q_j}{T_j} f_{0j}\left(\phi_1 - \frac{V_j A_{1z}}{c}\right) - i\frac{q_j}{T_j} f_{0j} \int_{-\infty}^{t} (\omega - kV_j)\left(\phi_1 - \frac{\bar{V}\cdot\bar{A}_1}{c}\right) dt' \tag{2.36}$$

The perturbed density and current are obtained by taking the velocity moments:

$$\begin{aligned} n_{1j} &= \int f_{1j}\, d^3v = -\frac{q_j}{T_j}\left[\int\left(\phi_1 - \frac{V_j A_{1z}}{c}\right) f_{0j}\, d^3v + (\omega - kV_j)\right. \\ &\left. \int_{-\infty}^{t} f_{0j}\left(\phi_1 - \frac{V\cdot A_1}{c}\right) dt'\, d^3v\right] \\ &= -\frac{q_j}{T_j}\left[\left(\phi_1 - \frac{V_j A_{1z}}{c}\right) n_{0j} + i(\omega - kV_j)\int_{-\infty}^{t} f_{0j}\left(\phi_1 - \frac{\bar{V}\cdot\bar{A}_1}{c}\right) dt'\, d^3v\right. \end{aligned} \tag{2.37}$$

$$\begin{aligned} \bar{J}_1 &= \sum_j q_j \int d^3v\, \bar{v}\, f_{1j} \\ &= -\sum_j^q q_j \int d^3v\, \bar{v}\left[\frac{q_j}{T_j} f_{0j}\left(\phi_1 - \frac{V_j A_{1z}}{c}\right) + i\frac{q_j}{T_j}(\omega - kV_j) f_{0j} \int_{-\infty}^{t} dt'\left(\phi_1 - \frac{\bar{V}\cdot\bar{A}_1}{c}\right)\right. \end{aligned} \tag{2.38}$$

The perturbed current j_1 is predominantly in the z-direction which can be written as

$$j_{1z} = -\sum_j q_j \int d^3v\, v_z \left[\frac{q_j}{T_j} f_{0j} \left(\phi_1 - \frac{v_j A_{1z}}{c} \right) + i \frac{q_j}{T_j} (\omega - k v_j) f_{0j} \int_{-\infty}^{t} \left(\phi_1 - \frac{\bar{v}.\bar{A}_1}{c} \right) dt' \right] \quad (2.39)$$

For low frequency perturbations the transverse components of the perturbed current can be neglected, as compared to j_{1z}. Equation (2.39) can be written as

$$j_{1z} = -\sum_j q_j \int d^3v\, v_z \left[\frac{q_j}{T_j} f_{0j} \left(\phi_1 - \frac{v_j A_{1z}}{c} \right) + i \frac{q_j}{T_j} (\omega - k v_j) f_{0j} \int_{-\infty}^{t} \left(\phi_1 - \frac{\bar{v}.\bar{A}_1}{c} \right) dt' \right]$$

$$= \frac{e^2 v^2}{c T} \left(\frac{1+\zeta}{\zeta} \right) n_0(n) A_{1z} - i \sum_j \frac{q_j^2}{T_j} (\omega - k v_j) \int v_z f_{0j}\, d^3v \int_{-\infty}^{t} \left(\phi_1 - \frac{v_z A_{1z}}{c} \right) dt' \quad (2.40)$$

Substituting for the perturbed density and current from eq. (2.37) and (2.40) in the eq.(2.29) we have:

$$\nabla^2 \phi_1 = \sum_j 4\pi \frac{q_j^2}{T_j} \left[\left(\phi_1 - \frac{v_j A_{1z}}{c} \right) n_{0j} + i (\omega - k v_j) \int_{-\infty}^{t} f_{0j} \left(\phi_1 - \frac{\bar{v}.\bar{A}_1}{c} \right) dt' d^3v \right] \quad (2.41)$$

and

$$-\nabla^2 A_1 = -\frac{4\pi}{c} \sum_j q_j \int d^3v\, \bar{v} \frac{q_j}{T_j} \left[f_{0j} \left(\phi_1 - \frac{v_j A_{1z}}{c} \right) + i(\omega - k v_j) f_{0j} \int_{-\infty}^{t} \left(\phi_1 - \frac{\bar{v}.\bar{A}_1}{c} \right) dt' \right] \quad (2.42)$$

Taking the z-component of this equation we have:

$$-\nabla^2 A_{1z} = -\frac{4\pi}{c} \sum_j q_j \int d^3v\, v_z \left\{ \frac{q_j}{T_j} f_{0j} \left(\phi_1 - \frac{v_j A_{1z}}{c} \right) \right\}$$

$$1 - \frac{4\pi i}{c}\sum_j \frac{q_j^2}{T_j}\int d^3v\, v_z(\omega - kv_j) f_{0j}\int_{-\infty}^{t}\left(\phi_1 - \frac{\bar{v}\cdot\bar{A}_1}{c}\right)dt'$$

$$= -\frac{4\pi}{c}\sum_j \frac{q_j^2}{T_j} n_{0j} v_j\left(\phi_1 - \frac{v_j A_{1z}}{c}\right) - \sum_j \frac{4\pi i q_j^2}{c T_j} \times$$

$$\int d^3v\, v_z(\omega - kv_j) f_{0j}\int_{-\infty}^{t}\left(\phi_1 - \frac{\bar{v}\cdot\bar{A}_1}{c}\right)dt' \qquad (2.43)$$

Substituting for ϕ_1, A_{1z} from equation (2.35) in (2.41) and (2.43) and expanding the ∇^2 operator in cylindrical coordinates we obtain

$$\left[\frac{1}{r}\frac{\partial}{\partial r}\left(r\frac{\partial}{\partial r}\right) + \frac{1}{r^2}\frac{\partial^2}{\partial\theta^2} + \frac{\partial^2}{\partial z^2}\right]\phi_1(r)\, e^{i(kz + m\theta - \omega t)}$$

$$= \sum_j \frac{4\pi q_j^2}{T_j}\left(\tilde{\phi}_1 - \frac{v_j \tilde{A}_{1z}}{c}\right) e^{i(kz + m\theta - \omega t)} n_{0j} + 4\pi i \sum_j \frac{q_j^2}{T_j}\int_{-\infty}^{t} f_{0j}$$

$$\left(\phi_1 - \frac{\bar{v}\cdot\bar{A}_1}{c}\right) e^{i(kz' + m\theta' - \omega t')}\, dt'\, d^3v \Big] \qquad (2.44)$$

and

$$\left[\frac{1}{r}\frac{\partial}{\partial r}\left(r\frac{\partial}{\partial r}\right) + \frac{1}{r^2}\frac{\partial^2}{\partial\theta^2} + \frac{\partial^2}{\partial z^2}\right] A_{1z}(r)\, e^{i(kz + m\theta - \omega t)}$$

$$= -\frac{4\pi}{c}\left[\frac{e^2 v^2}{cT}\frac{1+\tau}{\tau} n_0(r) A_{1z}(r) e^{i(kz + m\theta - \omega t)} - i\sum_j \frac{q_j^2}{T_j}(\omega - kv_j)\int v_z f_{0j}\, d^3v \times\right.$$

$$\left.\int_{-\infty}^{t}\left(\phi_1 - v_z\frac{\tilde{A}_{1z}}{c}\right) e^{i(kz' + m\theta' - \omega t')}\, dt'\right] \qquad (2.45)$$

replacing $\frac{\partial}{\partial\theta}$ and $\frac{\partial}{\partial z}$ in the operators with 'im' and 'ik' and multiplying through with $e^{-i(kz+m\theta-\omega t)}$ we obtain:

$$\left[\frac{1}{r}\frac{\partial}{\partial r}\left(r\frac{\partial}{\partial r}\right)-\frac{m^2}{r^2}-k^2\right]\phi_1(r)=4\pi\sum_j\frac{q_j^2}{T_j}\left(\phi_1-\frac{V_j A_{1z}}{c}\right)n_{0j}$$

$$+4\pi i\sum_j\frac{q_j^2}{T_j}(\omega-kV_j)\int f_{0j}\,d^3v\int_{-\infty}^{t}\left(\tilde{\phi}_1-\frac{\bar{v}.\tilde{A}_1}{c}\right)\times$$

$$\exp\left\{ik(z'-z)+im(\theta'-\theta)-i\omega(t'-t)\right\}dt' \qquad (2.46)$$

and

$$\left[\frac{1}{r}\frac{\partial}{\partial r}\left(r\frac{\partial}{\partial r}\right)-\frac{m^2}{r^2}-k^2\right]A_{1z}(r)=-\frac{4\pi}{c^2}\frac{e^2V^2}{T}\left(\frac{1+\tau}{\tau}\right)$$

$$n_0(r)A_{1z}(r)+\frac{4\pi i}{c}\sum_j\frac{q_j^2}{T_j}(\omega-kV_j)\int V_z f_{0j}\,d^3v\times$$

$$\int_{-\infty}^{t}\left(\tilde{\phi}_1-\frac{V_z\tilde{A}_{1z}}{c}\right)e^{i\{k(z'-z)+m(\theta'-\theta)-\omega(t'-t)\}} \qquad (2.47)$$

Substituting for z'-z from equation (2.18) and changing the variable in the time integration to t'-t=τ we obtain:

$$\left\{\frac{1}{r}\frac{\partial}{\partial r}\left(r\frac{\partial}{\partial r}\right)-\frac{m^2}{r^2}-k^2\right\}\phi_1(r)=4\pi\sum_j\frac{q_j^2 n_{0j}}{T_j}\phi_1(r)+$$

$$4\pi i \sum_j \frac{q_j^2}{T_j}(\omega - kV_j)\int V_z f_{0j}\, d^3V \int_{-\infty}^{0}\left(\phi_1(r') - \frac{V_z A_{1z}(r')}{c}\right) e^{im(\theta'-\theta)}\, e^{-i(\omega-kV_{z0})\tau}\, d\tau \qquad (2.48)$$

and,

$$\left\{\frac{1}{r}\frac{\partial}{\partial r}\left(r\frac{\partial}{\partial r}\right) - \frac{m^2}{r^2} - k^2\right\} A_{1z}(r) =$$

$$-\frac{4\pi e^2}{T}\frac{V^2}{c^2}\left(\frac{1+\tau}{\tau}\right) n_0(r)\, A_{1z}(r) \quad + \frac{4\pi i}{c}\sum_j \frac{q_j^2}{T_j}(\omega - kV)\cdot$$

$$\int V_z f_{0j}\, d^3V \int_{-\infty}^{0}\left(\tilde{\phi}_1(r') - \frac{V_z \tilde{A}_{1z}(r')}{c}\right) e^{im(\theta'-\theta)}\, e^{-i(\omega-kV_{z0})\tau}\, d\tau \qquad (2.49)$$

Equations (2. 48) and(2. 49) represent two coupled integro-differential equations for the eigenmodes of the system. The time integrals on the right hand sides are the orbit integrals to be evaluated over the unperturbed trajectories of the charged particles.These trajectories are described by equation (2. 18) and consist of large excursion radial oscillations whose extent and shape is determined by the initial conditions. Due to these large excursions the particles traversing these orbits will see large gradients in the electric and magnetic fields.Hence the usual 'local- approximation' in which the perturbed fields and potentials are expressed by a Taylor expansion around the local positions of the particles is not applicable. The appropriate way to evaluate the orbit integral for such orbits is the non-local method given by

Davidson [1]. It consists in expressing the radial amplitudes of the perturbations over a complete set of basis functions. In a cylindrical geometry it is convenient to take these basis functions as the Bessel functions. If we assume that the plasma is surrounded by a grounded conducting cylinder of radius R_c then the radial amplitudes can be expressed in terms of the vacuum eigenfunctions $\phi_m(r)$ of the cylinder where the ϕ_m's are given by the equation,

$$\left\{\frac{1}{r}\frac{\partial}{\partial r}\left(r\frac{\partial}{\partial r}\right)-\frac{m^2}{r^2}\right\}\phi_m(r) = -\lambda_m^2\phi_m(r) \qquad (2.50)$$

where λ_m's are the eigenvalues corresponding to the eigenfunctions $\phi_m(r)$. The boundary conditions are given by

$$r\left.\frac{d\phi_m}{dr}\right|_{r=0} = 0 \quad ; \quad \phi_m(r=R_c) = 0 \qquad (2.51)$$

The first boundary condition is obtained by demanding that the solutions be regular at the origin while the second condition follows from the fact that the field vanishes on the boundary. From equation(2.50) we have:

$$\phi_m(r) = A_m J_m(\lambda_m r) \qquad (2.52)$$

where $J_m(\lambda_n r)$ is the m^{th} order Bessel function of the first kind and eigenvalues λ_m are given by the condition:

$$\phi_n(r = R_c) = J_m(\lambda_n R_c) = 0 \tag{2.53}$$

The eigenfunctions $\phi_n(r)$ form an orthonormal set such that

$$\int_0^{R_c} dr\, r\, \phi_{n'}(r)\, \phi_n(r) = \delta_{n'n} \tag{2.54}$$

where $\delta_{n'n}$ is a Kronecker delta function, and A_n's are the normalisation coefficients defined as:

$$A_n = \frac{\sqrt{2}}{R_c J_{m+1}(\lambda_n R_c)} \tag{2.55}$$

Expanding the radial amplitudes $A_{1}(r)$ and $A_{1z}(r)$ in terms of the eigenfunctions ϕ_n of equation (2.50) we have

$$\tilde{\phi}_1(r) = \sum_n \alpha_n \phi_n \; ; \; \tilde{A}_{1z}(r) = \sum_n \beta_n \phi_n \tag{2.56}$$

where α_n and β_n are the expansion coefficients. Substituting from (2.56) in equations (2.48) and (2.49) and using (2.50) we have

$$\sum_n (-\lambda_n^2 - k^2)\, \alpha_n \phi_n(r) = \sum_j \frac{4\pi n_{0j} q_j^2}{T_j} \sum_n \alpha_n \phi_n +$$

$$4\pi i \sum_j \frac{q_j^2}{T_j} (\omega - kV_j) \int V_{zj} f_{0j}\, d^3V \int_{-\infty}^{0} \sum_n \left(\alpha_n \phi_n - \frac{V_z \beta_n \phi_n}{c}\right) \times$$

$$e^{im(\theta'-\theta)} \; e^{-i(\omega-kV_{z_0})\tau} \, d\tau$$

$$\Rightarrow \sum_n \left(-\lambda_m^2 - k^2\right) \alpha_m \phi_m(r) = \sum_j \frac{4\pi n_{0j} q_j^2}{T_j} \sum_n \alpha_m \phi_m +$$

$$4\pi i \sum_j \frac{q_j^2}{T_j} (\omega - kV_j) \int V_z f_{0j} \, d^3v \sum_n \hat{I}_m \qquad (2.57)$$

and

$$\sum_n \left(-\lambda_m^2 - k^2\right) \beta_m \phi_m(r) = -\frac{4\pi e^2 n_0(r)}{T} \frac{V^2}{c^2} \left(\frac{1+\tau}{\tau}\right) \sum_n \beta_m \phi_m(r)$$

$$+ \frac{4\pi i}{c} \sum \frac{q_j^2}{T_j} (\omega - kV_j) \int V_z f_{0j} \, d^3v \sum_n \hat{I}_m \qquad (2.58)$$

where,

$$\hat{I}_m = \int_{-\infty}^{0} d\tau \left(\alpha_m - \frac{V_z \beta_m}{c}\right) \phi_m(r') e^{im(\theta'-\theta)} e^{-i(\omega-kV_z)\tau} \, d\tau \qquad (2.59)$$

is the orbit integral evaluated over the unperturbed particle orbits which in this case are the betatron orbits. The orbit trajectories are given by equation (2.22). In terms of these can be written as

$$x' = \frac{r}{2} \left\{ \cos(\theta + \omega_{\beta j}\tau) + \cos(\theta - \omega_{\beta j}\tau) \right\} + \frac{V_\perp}{2\omega_{\beta j}} \left\{ \sin(\phi + \omega_{\beta j}\tau) - \right.$$

$$\sin(\phi - \omega_{pj}\tau)\Big\}$$

$$y' = \frac{r}{2}\Big\{\sin(\theta+\omega_{pj}\tau) + \sin(\theta-\omega_{pj}\tau)\Big\} +$$

$$\frac{V_\perp}{2\omega_{pj}}\Big\{\cos(\phi-\omega_{pj}\tau) - \cos(\phi+\omega_{pj}\tau)\Big\} \qquad (2.60)$$

The orbit integral $\hat{I}_n$ can be evaluated as follows:

We have

$$\hat{I}_m = \int_{-\infty}^{0} d\tau\, \phi_m(r')\, e^{im(\theta'-\theta)}\, e^{-i\tau(\omega-kV_z)} \left(\alpha_m - \frac{V_z \beta_m}{c}\right)$$

Substituting for $\phi_n(r')$ we obtain

$$\hat{I}_m = A_m \int_{-\infty}^{0} d\tau\, J_m(\lambda_m r')\, e^{im\theta'}\, e^{-im\theta}\, e^{-i\tau(\omega-kV_z)} \times$$

$$\left(\alpha_m - \frac{V_z \beta_m}{c}\right)$$

Making use of the identity

$$e^{im\theta'} J_m(\lambda_m r') = \int_0^{2\pi} \frac{d\alpha}{2\pi} \exp im\left(\alpha - \frac{\pi}{2}\right) \exp i\{\lambda_m r' \cos(\theta'-\alpha)\}$$

& $\lambda_m r' \cos(\theta'-\alpha) = \lambda_m (x' \cos\alpha + y' \sin\alpha)$ (2.61)

we have from (2.60)

$$\lambda_m r' \cos(\theta' - \alpha) = \frac{\lambda_m r}{2} \cos(\theta - \alpha + \omega_{pj}\tau) +$$

$$\frac{\lambda_m r}{2} \cos(\alpha - \theta + \omega_{pj}\tau) + \frac{\lambda_m V_\perp}{2\omega_{pj}} \sin(\phi - \alpha + \omega_{pj}\tau)$$

$$+ \frac{\lambda_m V_\perp}{2\omega_{pj}} \sin(\alpha - \phi + \omega_{pj}\tau) \qquad (2.62)$$

substituting in (2.61) we obtain

$$e^{im\theta'} J_m(\lambda_m r') = \int_0^{2\pi} \frac{d\alpha}{2\pi} \exp im\left(\alpha - \frac{\pi}{2}\right) \exp\left[i\left\{ \frac{\lambda_m r}{2} \cos(\theta - \alpha + \omega_{pj}\tau) \right.\right.$$

$$\left.\left. + \cos(\alpha - \theta + \omega_{pj}\tau)\right\} + \frac{\lambda_m V_\perp}{2\omega_{pj}} \left\{ \sin(\phi - \alpha + \omega_{pj}\tau) + \sin(\alpha - \phi + \omega_{pj}\tau)\right\}\right]$$

Therefore

$$\hat{I}_m = A_m\left(\alpha_n - \frac{V_z \beta_n}{c}\right) \int_{-\infty}^{0} d\tau \int_0^{2\pi} \frac{d\alpha}{2\pi} \exp im\left(\alpha - \frac{\pi}{2}\right) e^{-im\theta} \cdot$$

$$e^{-i(\omega - k V_{z0})\tau} \exp\left[i\left\{ \frac{\lambda_m r}{2} \cos(\theta - \alpha + \omega_{pj}\tau) + \frac{\lambda_m r}{2} \cos(\alpha - \theta + \omega_{pj}\tau) \right.\right.$$

$$\left.\left. + \frac{\lambda_m V_\perp}{2\omega_{pj}} \left(\sin(\phi - \alpha + \omega_{pj}\tau) + \sin(\alpha - \phi + \omega_{pj}\tau)\right)\right\}\right] \qquad (2.63)$$

Using the identities

$$e^{iz\sin\theta} = \sum_{n=-\infty}^{\infty} J_n(z)\, e^{in\theta}$$

$$e^{iz\cos\theta} = \sum_{n=-\infty}^{\infty} J_n(z)\, e^{in\left(\theta + \pi/2\right)} \qquad (2.64)$$

we can write

$$\exp\left\{ i\,\frac{\lambda_m r}{2}\cos(\theta-\alpha+\omega_{pj}\tau)\right\} = \sum_s \exp i\left(\frac{\pi}{2}+\theta-\alpha+\omega_{pj}\tau\right) s\, J_s\left(\frac{\lambda_m r}{2}\right)$$

$$\exp\left\{ i\,\frac{\lambda_m r}{2}\cos(\alpha-\theta+\omega_{pj}\tau)\right\} = \sum_l \exp i\left(\frac{\pi}{2}+\alpha-\theta+\omega_{pj}\tau\right) l\; J_l\left(\frac{\lambda_m r}{2}\right)$$

$$\exp\left\{ i\,\frac{\lambda_m V_\perp}{2\omega_{pj}}\sin(\phi-\alpha+\omega_{pj}\tau)\right\} = \sum_q \exp i(\phi-\alpha+\omega_{pj}\tau) q\; J_q\left(\frac{\lambda_m V_\perp}{2\omega_{pj}}\right)$$

$$\exp\left\{ i\,\frac{\lambda_m V_\perp}{2\omega_{pj}}\sin(\alpha-\phi+\omega_{pj}\tau)\right\} = \sum_p \exp i(\alpha-\phi+\omega_{pj}\tau) p\; J_p\left(\frac{\lambda_m V_\perp}{2\omega_{pj}}\right) \quad (2.65)$$

Substituting above we obtain

$$\hat{I}_m = \sum_{s,l,p,q} A_m\left(\alpha_m - \frac{V_z\beta_m}{c}\right)\int_0^{2\pi} d\alpha \int_{-\infty}^{0} d\tau\; e^{-i m\theta}\, e^{i\alpha(m+l-s+p-q)}$$

$$e^{i\frac{\pi}{2}(s+l-m)}\, e^{i\theta(s-l)}\, e^{i\phi(q-p)}\, J_s\left(\frac{\lambda_m r}{2}\right) J_l\left(\frac{\lambda_m r}{2}\right) \times$$

$$J_p\left(\frac{\lambda_m V_\perp}{2\omega_{pj}}\right) J_q\left(\frac{\lambda_m V_\perp}{2\omega_{pj}}\right) e^{-i(\omega-kV_z)\tau}\, e^{i(s+l+p+q)\omega_{pj}\tau}\, d\tau$$

The α integration gives $m+l+p = s+q$ because

$$\int_0^{2\pi} \frac{dx}{2\pi}\, e^{iax} = \delta_{a,0} \quad (2.66)$$

Therefore we have

$$\hat{I}_m = \sum_{l,q,p} A_m \left(\alpha_m - \frac{V_z \beta_m}{c}\right) \int_{-\infty}^{0} d\tau\, e^{i\frac{\pi}{2}(2l+p-q)} e^{i\theta(p-q)} e^{i\phi(q-p)}$$

$$J_{m+l+p-q}\left(\frac{\lambda_m r}{2}\right) \cdot J_l\left(\frac{\lambda_m r}{2}\right) \cdot J_p\left(\frac{\lambda_m V_\perp}{2\omega_{\beta j}}\right) J_q\left(\frac{\lambda_m V_\perp}{2\omega_{\beta j}}\right) e^{-i\tau(\omega - kV_{z0}) + i\tau\left(m+2l+2p\right)\frac{\omega_{\beta j}}{\omega_{\beta j}}} \quad (2.67)$$

Expressing d^3v as $\int d\phi\, V_\perp\, dV_\perp dV_z$ and noting that $\int d\phi$ operates on only in equation

(2.57) we have

$$\int_0^{2\pi} d\phi\, \hat{I}_m = \sum_{l,p,q} 2\pi \delta_{pq} A_m \left(\alpha_m - \frac{V_z \beta_m}{c}\right) e^{i\frac{\pi}{2}(p-q+2l)} e^{i\theta(p-q)} \times$$

$$\int_{-\infty}^{0} J_l\left(\frac{\lambda_m r}{2}\right) J_{m+l+p-q}\left(\frac{\lambda_m r}{2}\right) J_p\left(\frac{\lambda_m V_\perp}{2\omega_{\beta j}}\right) J_q\left(\frac{\lambda_m V_\perp}{2\omega_{\beta j}}\right) \exp -i\tau\left(\omega - kV_{z0} - (m+2l+2p)\omega_{\beta j}\right) d\tau$$

where we have made use of (2.66) to do the ϕ integration.

Thus we have

$$\int_0^{2\pi} d\phi\, \hat{I}_m = \sum_{l,p} 2\pi A_m \left(\alpha_m - \frac{\beta_m V_z}{c}\right) e^{i\pi l} J_l\left(\frac{\lambda_m r}{2}\right) J_{m+l}\left(\frac{\lambda_m r}{2}\right)$$

$$J_p^2\left(\frac{\lambda_m V_\perp}{2\omega_{\beta j}}\right) \int_{-\infty}^{0} d\tau\, \exp\left\{-i\tau\left(\omega - kV_{z0} - (m+2l+2p)\omega_{\beta j}\right)\right\}$$

$$= \sum_{l,p} \frac{2\pi i A_m \left(\alpha_m - \frac{\beta_m V_z}{c}\right)(-1)^l J_l\left(\frac{\lambda_m r}{2}\right) J_{m+l}\left(\frac{\lambda_m r}{2}\right) J_p^2\left(\frac{\lambda_m V_\perp}{2\omega_{\beta j}}\right)}{\omega - kV_z - (m+2l+2p)\omega_{\beta j}} \quad (2.68)$$

Substituting in (2.57) and (2.58) we have

$$\sum_n \left(-\lambda_n^2 - k^2\right) \alpha_n \phi_n(r) = \sum_j \frac{4\pi n_{0j} q_j^2}{T_j} \sum_n \alpha_n \phi_n(r) +$$

$$\sum_{j,n} \frac{4\pi i q_j^2}{T_j} (\omega - kV_j) \int V_\perp dV_\perp \int V_z dV_z f_{0j} \left(\alpha_n - \frac{V_z \beta_n}{c}\right) \times$$

$$\sum_{\ell,p} \frac{2\pi i A_n (-1)^\ell J_\ell\left(\frac{\lambda_n r}{2}\right) J_{m+\ell}\left(\frac{\lambda_n r}{2}\right) J_p^2\left(\frac{\lambda_n V_\perp}{2\omega_{pj}}\right)}{\omega - kV_{z0} - (m+2\ell+2p)\omega_{pj}}$$

and,

$$-\sum_n \left(\lambda_n^2 + k^2\right) \beta_n \phi_n(r) = \frac{4\pi n_0 e^2}{T} \frac{1+\tau}{\tau} \sum_n \alpha_n \phi_n(r) +$$

$$\sum_{j,\ell,p,n} \frac{4\pi i^2 q_j^2}{T_j} (\omega - kV_j) \cdot 2\pi A_n (-1)^\ell \int V_\perp dV_\perp J_p^2\left(\frac{\lambda_n V_\perp}{2\omega_{pj}}\right) \times$$

$$\int \frac{V_z dV_z f_{0j} \left(\alpha_n - \frac{V_z \beta_n}{c}\right)}{\omega - kV_z - (m + 2\ell + 2p)\omega_{pj}} \cdot J_\ell(\lambda_n r) J_{m+\ell}\left(\frac{\lambda_n r}{2}\right)$$

writing f_{0j} as $\hat{f}_{0j}\, n_{0j}(r)$ and operating both sides of the two equations with $\int_0^{R_c} r\phi_{n'} dr$ we obtain

$$-\sum_n \alpha_n \left(k^2 + \lambda_n^2\right) \int_0^{R_c} \phi_{n'} \phi_n \, r \, dr = \sum_{j,n} \alpha_n \int_0^{R_c} \frac{1}{\lambda_{Dj}^2(r)} \phi_{n'} \phi_n \, dr$$

$$-\sum_{j,n} (\omega - kV_j) \int V_\perp dV_\perp \int V_z dV_z \hat{f}_{0j} \left(\alpha_n - \frac{V_z \beta_n}{c}\right) 2\pi A_n (-1)^\ell \cdot$$

$$\int_0^{R_c} r \, dr \, \frac{\phi_{n'} J_\ell\left(\frac{\lambda_n r}{2}\right) J_{m+\ell}\left(\frac{\lambda_n r}{2}\right)}{\lambda_{Dj}^2(r)} \qquad (2.69)$$

and,

$$-\sum_n (k^2+\lambda_m^2)\beta_m \int_0^{R_c} \phi_{n'}\,\phi_m\, r\,dr = -\frac{4\pi e^2 \hat{n}_0}{T}\frac{V^2}{c^2}\frac{1+\tau}{\tau}\sum_n \beta_n \int_0^{R_c} \frac{\phi_{n'}\,\phi_m\, r\,dr}{\left(1+\frac{1}{4}k^2r^2\right)^2}$$

$$-\sum_j \frac{4\pi q_j^2}{cT_j}(\omega - kV_j)\sum_{n,l,p} 2\pi A_n\left(\alpha_n - \frac{\beta_n V_z}{c}\right).(-1)^l \cdot \int_0^{\infty} dV_\perp\, V_\perp J_p^2\left(\frac{\lambda_n V_\perp}{2\omega_{pj}}\right)$$

$$\int_{-\infty}^{\infty} \frac{V_z\, dV_z\, \hat{f}_{oj}}{\omega - kV_z - (m+2l+2p)\omega_{pj}} \int_0^{R_c} \frac{dr\, r\,\phi_{n'}\, J_l\left(\frac{\lambda_{n'}r}{2}\right) J_{m+l}\left(\frac{\lambda_n r}{2}\right)}{\left(1+\frac{1}{4}k^2r^2\right)^2} \qquad (2.70)$$

Rearranging the terms we can write

$$\sum_n \alpha_n\left(k^2+\lambda_n^2\right)\int_0^{R_c} r\,\phi_{n'}\,\phi_n\,dr + \sum_n \alpha_n \frac{(1+\tau)}{\lambda_{De}^2(0)}\int_0^{R_c} \frac{r\,\phi_{n'}\,\phi_n\,dr}{\left(1+\frac{1}{4}k^2r^2\right)^2}$$

$$-\sum_{l,p,n,j} 2\pi A_n (-1)^l \frac{(\omega - kV_j)}{\lambda_{Dj}^2(0)} \int_0^{R_c} r\,\phi_{n'}\, J_l\left(\frac{\lambda_{n'}r}{2}\right) J_{m+l}\left(\frac{\lambda_n r}{2}\right) \times$$

$$\int_{-\infty}^{\infty} \hat{f}_{oj}\, \frac{V_z\left(\alpha_n - \frac{V_z\beta_n}{c}\right) dV_z}{\omega - kV_z - (m+2l+2p)\omega_{pj}} \int_0^{\infty} \frac{J_p^2\left(\lambda_n V_\perp / 2\omega_{pj}\right)}{1}\, V_\perp\, dV_\perp = 0 \qquad (2.71)$$

and

$$\sum_n \beta_n\left(k^2+\lambda_n^2\right)\int_0^{R_c} r\,\phi_{n'}\,\phi_n\,dr - \frac{1}{\lambda_{De}^2(0)}\frac{V^2}{c^2}\left(\frac{1+\tau}{\tau}\right)\sum_n \beta_n \int_0^{R_c} \frac{\phi_{n'}\,\phi_n\, r\,dr}{\left(1+\frac{1}{4}k^2r^2\right)^2}$$

$$-\sum_j \frac{(\omega - kV_j)}{\lambda_{Dj}^2(0)}\sum_{n,l,p} 2\pi A_n (-1)^l \int_0^{R_c} \frac{r\,\phi_{n'}\, J_l\left(\frac{\lambda_{n'}r}{2}\right) J_{m+l}\left(\frac{\lambda_n r}{2}\right) dr}{\left(1+\frac{1}{4}k^2r^2\right)^2} \times$$

$$\int_{-\infty}^{\infty} \frac{dv_z\, v_z \left(\alpha_n - \beta_n \frac{v_z}{c}\right) \hat{f}_{oj}}{\omega - k v_z - (m+2l+2p)\omega_{pj}} \int_0^{\infty} v_\perp dv_\perp J_p^2\left(\frac{\lambda_m v_\perp}{2\omega_{pj}}\right) = 0 \qquad (2.72)$$

Now

$$\hat{f}_{oj} = \left(\frac{m_j}{2\pi T_j}\right)^{3/2} \exp\left\{-\frac{1}{T_j}\left(H_{oj} - P_{zj} V_j + \frac{m_j V_j^2}{2}\right)\right\}$$

$$= \left(\frac{m_j}{2\pi T_j}\right)^{3/2} \exp\left(-\frac{m_j}{2T_j} v_\perp^2\right) \exp\left\{-\frac{m_j}{2T_j}(v_z - V_j)^2\right\}$$

We now carry out the $v_\perp$ integral:

We have

$$\int_0^{\infty} v_\perp dv_\perp \exp\left(-\frac{m_j}{2T_j} v_\perp^2\right) J_p^2\left(\frac{\lambda_m v_\perp}{2\omega_{pj}}\right)$$

Using the standard integral

$$\int_0^{\infty} e^{-\rho^2 x^2} J_p^2(\alpha x)\, dx = \frac{1}{2\rho^2} e^{-\alpha^2/2\rho^2} I_p\left(\frac{\alpha^2}{2\rho^2}\right)$$

where $|\arg| < \pi/4$, Re $p > -1$ and $\alpha > 0$ we have

$$\int_0^{\infty} e^{-\frac{m_j v_\perp^2}{2T_j}} J_p^2\left(\frac{\lambda_m v_\perp}{2\omega_{pj}}\right) v_\perp dv_\perp = \frac{T_j}{m_j} \exp\left(-\frac{T_j}{m_j}\frac{\lambda_m^2}{4\omega_{pj}^2}\right) I_p\left(\frac{T_j}{m_j}\frac{\lambda_m^2}{4\omega_{pj}^2}\right) \qquad (2.73)$$

Substituting in (2.71) and (2.72) we have

$$\sum_n a_n \left\{ k_m^2 \delta_{n'n} + \frac{1+\tau}{\lambda_{De}^2(0)} A_{n'n} \right\} - \sum_j \frac{\omega - kV_j}{\lambda_{Dj}^2(0)} \left(\frac{m_j}{2\pi T_j} \right)^{1/2} \exp\left(- \frac{T_j}{m_j} \frac{\lambda_m^2}{4\omega_{pj}^2} \right) \times$$

$$\sum_{n,l,p} I_{R,l} \Gamma_p^j \int_{-\infty}^{\infty} \frac{(\alpha_n - \beta_n V_z/c) \left(m_j/2\pi T_j \right)^{3/2}}{\omega - kV_z - (m+2l+2p)\omega_{pj}} \exp - \frac{m_j}{2T_j} (V_z - V_j)^2 \qquad (2.74)$$

$$= 0$$

and

$$\sum_n \beta_n \left\{ k_m^2 \delta_{n'n} - \frac{1}{\lambda_{De}^2(0)} \left(\frac{1+\tau}{\tau} \right) \frac{V^2}{c^2} A_{n'n} \right\}$$

$$- \sum_j \frac{(\omega - kV_j)}{\lambda_{Dj}^2(0)} \sum_{n,l,p} I_{R,l} \Gamma_p^j \int_{-\infty}^{\infty} \frac{dV_z \, V_z (\alpha_n - \beta_n V_z/c) \left(\frac{m_j}{2\pi T_j} \right)^{1/2}}{\omega - kV_z - (m+2l+2p)\omega_{pj}} \exp - \frac{m_j}{2T_j} (V_z - V_j)^2 \qquad (2.75)$$

$$= 0$$

where

$$k_m^2 = k^2 + \lambda_m^2 \; ; \quad \lambda_{De}^2(0) = \frac{T_e}{4\pi n_0 e^2} \; ; \quad \tau = \frac{T_e}{T_i}$$

$$A_{n'n} = \int_0^{R_c} \frac{r \phi_{n'} \phi_n \, dr}{\left(1 + \frac{1}{4} k^2 r^2 \right)^2}$$

$$I_{R,l} = (-D)^l A_m \int_0^{R_c} \frac{dr \, r \, \phi_{n'}(r) J_l\left(\frac{\lambda_m r}{2} \right) J_{m+l}\left(\frac{\lambda_m r}{2} \right)}{\left(1 + \frac{1}{4} k^2 r^2 \right)^2}$$

$$\Gamma_p^j = I_p \left(\frac{T_j}{m_j} \frac{\lambda_n^2}{4\omega_{pj}^2} \right) \exp\left(- \frac{T_j}{m_j} \frac{\lambda_n^2}{4\omega_{pj}^2} \right)$$

We now evaluate the orbit integrals:

$$\int_{-\infty}^{\infty} \left(\alpha_n - \beta_n \frac{V_z}{c} \right) \frac{\exp - \frac{m_j}{2T_j} (V_z - V_j)^2 \, dV_z}{\omega - kV_z - (m+2l+2p)\omega_{pj}}$$

$$= -\alpha_n \frac{\sqrt{\pi}}{k} Z(\zeta_j) + \frac{\beta_n}{ck}\sqrt{\frac{2\pi T_j}{m_j}} +$$

$$\frac{\beta_m}{ck^2}\sqrt{\pi}\ \frac{\omega-(m+2l+2p)\omega_{pj}}{l}\ Z(\zeta_j) \qquad (2.76)$$

$$\zeta_j = \frac{\omega - kV_j - (m+2l+2p)\omega_{pj}}{\sqrt{2}\,k\,V_{thj}} \quad ; \quad V_{thj} = \sqrt{\frac{T_j}{m_j}}$$

$Z(\zeta_j)$ is the plasma dispersion function.

The v_z integral in the Ampere's equation is given by

$$\int_{-\infty}^{\infty} \frac{V_z\left(\alpha_n - \beta_n \frac{V_z}{c}\right)\exp - \frac{m_j}{2T_j}(V_z - V_j)^2 dV_z}{\omega - kV_z - (m+2l+2p)\omega_{pj}}$$

The first part is from (2.76)

$$-\alpha_n\left[\sqrt{\frac{2\pi T_j}{m_j}}\ \frac{1}{k} + \frac{1}{k^2}\left(\omega-(m+2l+2p)\omega_{pj}\right)\sqrt{\pi}\ Z(\zeta_j)\right] \qquad (2.77)$$

The second part is given by

$$\frac{\beta_m}{ck}\left\{\left[\frac{\omega-(m+2l+2p)\omega_{pj}}{k} + V_j\right]\sqrt{2\pi}\,V_{thj} + \sqrt{\pi}\left(\frac{\omega-(m+2l+2p)\omega_{pj}}{k}\right)^2 Z(\zeta_j^{lp})\right\}$$

$$(2.78)$$

Substituting from (2.76), (2.77) and (2.78) in equation (2.74) and (2.75) we obtain

$$\sum_m \alpha_n \left[k_m^2 \delta_{m'm} + \frac{1+\tau}{\lambda_{De}^2(o)} A_{m'm} + \sum_j \frac{(\omega - kV_j)}{\lambda_{Dj}^2(o)} \frac{1}{\sqrt{2}kV_{thj}} \sum_{l,p} Z(\zeta_j^{lp}) I_{RI}\, I_p^{lj} \right]$$

$$-\sum_n \beta_n \left[\sum_{j,l,p} \frac{(\omega - kV_j)}{\lambda_{Dj}^2(\omega)} \frac{I_{Rl} \Gamma_p^j}{ck} \left\{ 1 + \frac{\omega - (m+2l+2p)\omega_{pj}}{\sqrt{2}\, k V_{thj}} Z(\zeta_j^{lp}) \right\} = 0 \right. \quad (2.79)$$

and

$$\sum_n \alpha_n \left[\frac{(\omega - kV_j)}{\lambda_{Dj}^2(\omega)\sqrt{2}kV_{thj}} \sum_{l,p} I_{Rl} \Gamma_p^j \left\{ \frac{1}{ck} + \frac{\omega - (m+2l+2p)\omega_{pj}}{ck} Z(\zeta_j^{lp}) \right\} \right] +$$

$$\sum_n \beta_n \left[k_n^2 \delta_{n'n} - \frac{V_e^2}{c^2} \frac{1+\tau}{\tau} \cdot \frac{A_{n'n}}{\lambda_{De}^2(\omega)} - \sum_j \frac{(\omega - kV_j)}{\lambda_{Dj}^2(\omega)} \sum_{l,p} I_{Rl} \Gamma_p^j \times \right. \quad (2.80)$$

$$\left. \frac{1}{c^2 k^2} \left\{ (\omega - (m+2l+2p)\omega_{pj} + kV_j) + \frac{(\omega - (m+2l+2p)\omega_{pj})^2}{\sqrt{2}\, k V_{thj}} Z(\zeta_j^{lp}) \right\} = 0 \right]$$

Equations (2.79) and (2.80) represent two infinite sets of algebraic equations in α_n and β_n. In the matrix form these can be written as

$$\begin{bmatrix} D_{n'n}^{(1)} \end{bmatrix} \begin{bmatrix} \alpha_n \end{bmatrix} + \begin{bmatrix} D_{n'n}^{(2)} \end{bmatrix} \begin{bmatrix} \beta_n \end{bmatrix} = 0$$

$$\begin{bmatrix} D_{n'n}^{(3)} \end{bmatrix} \begin{bmatrix} \kappa \end{bmatrix} + \begin{bmatrix} D_{n'n}^{(4)} \end{bmatrix} \begin{bmatrix} \beta_n \end{bmatrix} = 0 \quad (2.81)$$

where $D_{n'n}^{(1)}$, $D_{n'n}^{(2)}$, $D_{n'n}^{(3)}$, $D_{n'n}^{(4)}$ are infinite matrices given by:

$$D_{n'n}^{(1)} = k_n^2 \delta_{n'n} + \frac{1+\tau}{\lambda_{De}^2(\omega)} A_{n'n} + \sum_j \frac{\omega - kV_j}{\sqrt{2}kV_{thj}\, \lambda_{Dj}^2(\omega)} \sum_{l,p} Z(\zeta_j^{lp}) I_{Rl} \Gamma_p^j$$

$$D_{n'n}^{(2)} = -\sum_{j,l,p} \frac{(\omega - kV_j)}{\lambda_{Dj}^2(\omega)} \frac{I_{Rl} \Gamma_p^j}{ck} \left\{ 1 + \frac{\omega - (m+2l+2p)\omega_{pj}}{\sqrt{2}\, k V_{thj}} Z(\zeta_j^{lp}) \right\}$$

$$D_{n'n}^{(3)} = -D_{n'n}^{(2)}$$

$$D^{(4)}_{n'm} = k_m^2 \delta_{n'm} - \frac{V^2}{c^2}\,\frac{1+\zeta}{\zeta}\cdot\frac{A_{n'm}}{\lambda_{De}^2(o)} - \sum_j \frac{(\omega - k\cdot V_j)}{\lambda_{Dj}^2(o)\, k_j^2} \sum_{\ell,p} I_{n\ell}\, \Gamma^j_p \qquad (2.82)$$

$$\frac{1}{c^2k^2}\left[(\omega - (m+2\ell+2p)\omega_{pj} + kV_j) + \frac{(\omega-(m+2\ell+2p)\omega_{pj})^2}{\sqrt{2}\,kV_{thj}}\, Z(\zeta_j^{\ell p})\right.$$

Equation (2.81) determines the eigenmodes of the system. The condition that these equations have non-trivial solutions for α_n's and β_n's is that the determinant of the coefficient matrix is zero. Thus we have

$$\text{Det}\left[\begin{array}{c|c} D^{(1)} & D^{(2)} \\ \hline D^{(3)} & D^{(4)} \end{array}\right] = 0 \qquad (2.83)$$

This is a transcendental equation in ω and k, and represents the electromagnetic modes of the plasma.

2.4 Summary

We have derived a kinetic non-local dispersion relation for the most general low freqency eletromagnetic perturbations of a cylindrical plasma represented by the Bennett equilibrium, taking into account the non-local and wave-particle effects. The non-local effects arising from the inhomogeneity are represented by the coefficients of the infinite matrix and the wave particle interactions are given by the plasma dispersion functions.

In the case of general electromagnetic perturbations the electrostatic and electromagnetic effects are coupled and it is difficult to obtain the results in a simple analytic form. However there may be situations where either of the two effects may become dominant as compared to the other and electrostatic and electromagnetic effects may get decoupled. In such limits the matrix dispersion relation gets simplified and in eq. (2. 83) only D^1 in the electrostatic case, and D^4 in the electromagnetic case are relevant. Further approximations may be used to convert the matrix dispersion relation into a simple analytic form where the non-local and wave-particle effects on the modes can be understood in a more systematic manner. The present method of analysis which has been carried out for the specific case of the Bennett equilibrium can be easily extended to other inhomogeneous equilibria with diffuse profiles. In subsequent chapters, we shall discuss the various limiting forms of the dispersion relation (2.83)

obtained here and apply it to the study of various experimental situations.

References

1. Davidson, R.C., Phys. Fluids 19, 1189 (1976).

2. Sharma, A.S., Nucl. Fusion 23, 1493 (1983).

3. Catto, P. J., Aamodt, R.E., Rosenbluth, M.N., Byers, J.A. & Pearlstein, L.D., Phys. Fluids 23, 764 (1980).

4. Myra, S. R., Catto, P.J. & Aamodt, R.J., Phys. Fluids 24, 651 (1981)

5. Marchand, R., Zhang, C.F. & Lee, E.P., Phys. Fluids 26, 194 (1983).

6. Symon, K. R., Seyler, C.E. & Lewis, H.R., J. Plasma Phys. 27, 13 (1982).

7. Lewis, H. R. & Seyler, C. E., J. Plasma Phys. 27, 25 (1982).

8. Seyler, C. E. & Lewis, H. R., J. Plasma Phys. 27, 37 (1982).

9. Ferraro, R.D., Sanuki, H., Littlejohn, R.G. & Fried, B.D., Phys. Fluids 28, 2181 (1985).

10. Chen, J. & Lee, Y.C., Phys. Fluids 28, 2137 (1985).

11. Bennett, W. H., Phys. Rev. 45, 890 (1934); 98, 1584 (1955).

12. Benford, G. & Book, D. L., in Advances in Plasma

Physics(Interscience,New York) 4, 153 (1971).

13. Buneman, O., in Plasma Physics, Ed. W. E. Drummond (Chapter 7).

14. Morse, R. L. & Friedberg, J.P., Phys. Fluids 13, 531 (1970).

15. Gratreau,P., Phys. Fluids 21, 1302 (1978).

Figure captions for chapter 2

Fig. (2. 1) Density profiles for generalised Bennett Equilibria.

Fig. (2. 2) Normalised density and magnetic field profile for the Bennett Equilibrium.

Fig. (2. 3) a) Betatron orbit and b) Larmor orbit projection in the r-z plane.

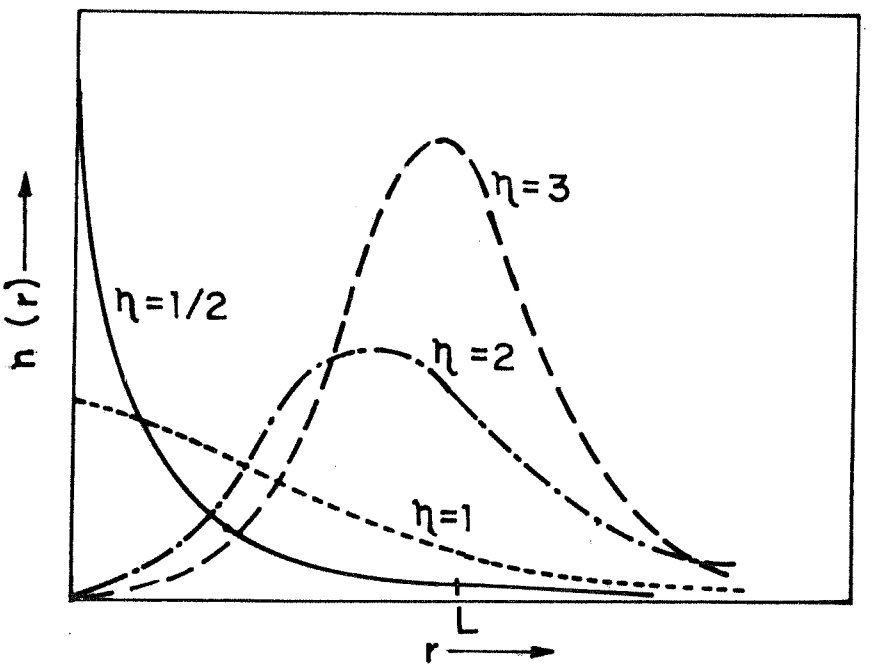

FIG. 2.1

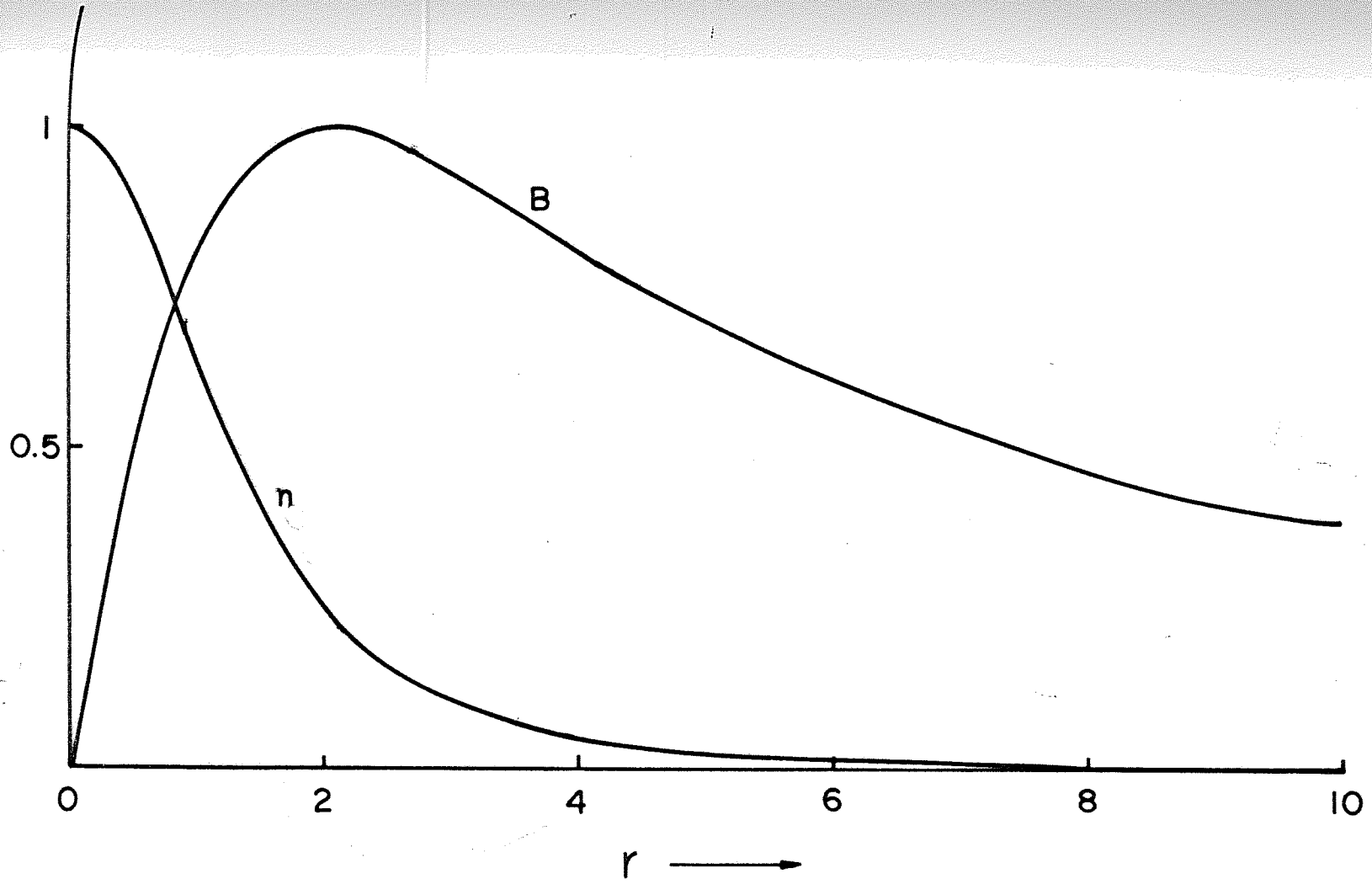

FIG. 2.2

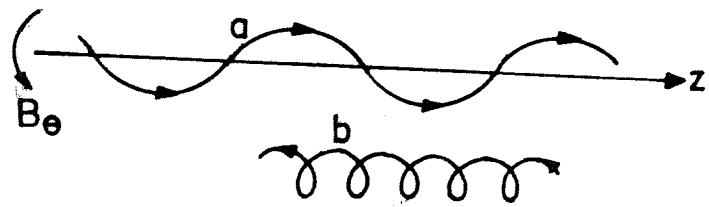

FIG. 2.3

CHAPTER 3

Electromagnetic m=1 kink instability

3.1 Introduction

The kink instability is one of the earliest known instabilities of a cylindrical plasma column and has been studied quite extensively by several workers. In a pure Z-pinch a lateral displacement of the plasma column leads to a decrease in magnetic pressure in front of the displacement and an increase behind it. This enhances the plasma displacement, leading to the kink instability which has an azimuthal mode number m=1. Using the ideal MHD theory Kruskal & Schwarzchild [1] first predicted the kink instability of a cylindrical plasma column. This instability was experimentally observed in a Z-pinch discharge by Carruthers & Davenport [2] and subsequently by others [3,4].

The hydromagnetic energy principle developed by Bernstein et al [5] using a variational formulation of the

linearised ideal MHD equations also predicts this instability. The first order variations of all physical quantities with respect to their equilibrium values are retained in the equations, and expressed in terms of a Lagrangian displacement vector $\bar{\xi}(\bar{r}_0, t)$. This vector represents the displacement of a given fluid element from its equilibrium position $\bar{r}_0$ at time t. From the ideal MHD equations a second order differential equation for the displacement $\bar{\xi}$ is obtained as

$$\rho_0 \frac{\partial^2 \bar{\xi}}{\partial t^2} = F(\bar{\xi}) \qquad (3.1)$$

where $F(\bar{\xi})$ represents a force density operator and is a complicated function of the equilibrium profiles of current, magnetic field, pressure etc. This equation is frequently employed in studying the linear growth for given plasma profiles. Kruskal and Schwarzchild [1] have studied the m=1 kink mode for a linear pinch assuming infinite conductivity and a surface current model. They have shown that for any given wavelength the mode is always unstable, the growth increasing monotonically with k. Taylor [6] investigated the stability of the Z-discharge against m=1 perturbation assuming a volume current with a power law distribution. He showed that the volume current model was more stable with respect to the surface current model. Later he included an external axial magnetic field and conducting walls and showed that the mode could be stabilized provided all the

current flowed on the surface of the cylinder, and the wall radius does not exceed the discharge radius by more than a factor of five [7].Newcomb [8] used the energy principle to obtain the necessary and sufficient conditions for the hydromagnetic stability of a diffuse linear pinch with distributed current. For diffuse current models the growth rate calculations based on ideal MHD equations have also been carried out by several other workers [9-11] and these are found to depend sensitively on the current profile used.

The various studies of the hydromagnetic stability has been reviewed by Kadomtsev [12] and more recently by Friedberg [13].

As a result of these theoretical investigations efforts were made to find more stable configurations for the confinement of thermonuclear plasma. These include the addition of an axial external magnetic field for the suppression of magnetohydrodynamic instabilities and introduction of toroidal discharges to eliminate end losses.

This led to the class of discharges known as the tokamak and the stabilized pinch.However, for practical values of the magnetic fields (5-10T) and at fusion temperatures this restricted the density to about $10^{14} cm^{-3}$ [14]. In order to satisfy the Lawson criterion, therefore, the confinement time has to be roughly one second which is quite high.The Z pinch, on the other hand, has the advantage of producing much higher plasma density and therefore requires a much shorter confinement time. Moreover under the reactor conditions the ion orbit size is of the order of the pinch

radius and this is expected to have a strong stabilizing influence [15]. Recent Z-pinch experiments have shown [16] remarkable stability properties. The experiments on compression Z-pinch at Imperial College [17] show that the plasma is stable for the duration of the discharge. The pinch plasma in Extrap [18] have been found to be stable for 100 Alfven times. The plasma focus which in its compression phase closely resembles the Z-pinch configuration yields a density of 10^{19} cm^{-3} and a temperature of about 1 KeV in a narrow filament of radius 1 mm. It also exhibits enhanced stability properties which are attributed to finite ion orbits [19]. The experimentally observed growth times of the instability in the Z-pinch are found to be much larger than those predicted by fluid theory [16]. This discrepancy is attributed to the fact that the fluid theory does not take into account the finite particle orbit effects and therefore the predicted growth rates from MHD calculations cannot be compared with these experiments. It is therefore necessary to have a realistic theory which would account for the finite particle orbits and their effect on the growth rates of the instabilities. This would lead to a better understanding of the observed stability of the pinch and enable a closer comparison between theoretical predictions and observations of the growth rates.

One of the attempts in this direction is the Vlasov fluid model of Friedberg for high β plasmas [20]. In this model the ions are treated as collisionless and described

by the Vlasov equation, while the electrons are treated as a simple cold fluid described by Ohm's law. Using this model Friedberg obtained a comparison theorem for the stability of the $m \neq 0$ mode. He also obtained approximate growth rates for a θ-pinch using a surface current model. This model was later used by Coppins et al [21] to study the stability of the axisymmetric perturbations in Z-pinches.

In this chapter, we investigate the m=1 kink mode of a Z-pinch with the Bennett profile in cylindrical geometry in both magnetohydrodynamic as well as the kinetic limits. From the magnetohydrodynamic stability theory it is found that the modes with any m number except for the case m=1 can be stabilised by an appropriate choice of the diffuse profile [12]. This makes the study of the m=1 mode particularly important. The magnetohydrodynamic case has been investigated for a pure Z-pinch using a normal mode analysis of the ideal MHD equations. The eigenvalues and eigenfunctions are obtained by a shooting method using a Bennett profile. It is important to use realistic diffuse profiles like the Bennett profile as the growth rates for such profiles have been found to be about one-third of that given by sharp boundary current profiles [11]. These results have been compared with a calculation by Nycander et al[22] which is based on a perturbation theory. For the kinetic limit we adopt the approach developed in Chapter 2. The dispersion relation is considered for the limit of pure electromagnetic perturbations with m=1 and growth rates are

obtained both numerically and in approximate analytic limits.

3.2 The m=1 ideal MHD eigenmodes of a pure Z-pinch

We consider an axially and azimuthally symmetric cylindrical plasma carrying a uniform axial current. As discussed in Chapter 2, such a configuration can be described by the Bennett equilibrium. The current and magnetic field profiles are then respectively given by

$$J_{0z}(r) = \frac{p_0 e V \left(1+\frac{1}{c}\right)}{\left(1+\frac{1}{4}K^2 r^2\right)^2} \; ; \quad B_0 = \frac{\hat{B}_0 K r}{\left(1+\frac{1}{4}K^2 r^2\right)} \tag{3.2}$$

They are related through the relation

$$J_0(r) = \frac{B_0}{r} + \frac{dB_0}{dr} \tag{3.3}$$

The equilibrium pressure is given by

$$\frac{dp_0}{dr} = -\frac{B_0}{4\pi r}\frac{d}{dr}(r B_0) \tag{3.4}$$

We assume that the plasma is infinitely conducting and the pressure is isotropic. To investigate the stability of the plasma against small amplitude perturbations the linearised ideal MHD equations are used. Following the earlier derivation [8, 5] the eigenmode equation may be derived as follows. Let ρ, p, and θ represent the first

order variations of the density, pressure and magnetic field from their equilibrium values ρ_0, p_0 and B_0 respectively. Then the linearised MHD equations can be written as

$$\frac{\partial \rho}{\partial t} + \nabla \cdot (\rho_0 \bar{V}) = 0 \tag{3.5}$$

$$\rho_0 \frac{\partial \bar{V}}{\partial t} + \nabla p = \frac{1}{4\pi}(\nabla \times \bar{B}_0) \times \bar{B}_1 + \frac{1}{4\pi}(\nabla \times \bar{B}_1) \times \bar{B}_0 \tag{3.6}$$

$$\frac{\partial p}{\partial t} + \bar{V} \cdot \nabla p_0 + \gamma p \nabla \cdot \bar{V} = 0 \tag{3.7}$$

$$\frac{\partial \bar{B}_1}{\partial t} = \nabla \times (\bar{V} \times \bar{B}_0) \tag{3.8}$$

It is usually more convenient to use the plasma displacement $\bar{\xi}$ instead of the perturbed velocity $\bar{V}$ and the two are related as $V = \dot{\xi} = \frac{\partial \bar{\xi}}{\partial t}$. Replacing V by $\dot{\xi}$ in the above equations and integrating with respect to time, we obtain

$$\rho = -\nabla \cdot (\rho_0 \bar{\xi}) \tag{3.9}$$

$$p = -\bar{\xi} \cdot \nabla p_0 - \gamma p_0 \nabla \cdot \bar{\xi} \tag{3.10}$$

$$\bar{B} = \nabla \times (\bar{\xi} \times \bar{B}_0) \tag{3.11}$$

Substitution in eq. (3.6) yields a single second order differential equation in the vector $\bar{\xi}$.

$$\rho_0 \frac{\partial^2 \bar{\xi}}{\partial t^2} = \nabla \left(\bar{\xi} . \nabla p_0 + \gamma p_0 \nabla . \bar{\xi} \right) + \frac{1}{4\pi} \left[\nabla \times \bar{B}_0 \times \left(\nabla \times (\bar{\xi} \times \bar{B}_0) \right) \right]$$

$$+ \frac{1}{4\pi} \left[\left\{ \nabla \times \left(\nabla \times (\bar{\xi} \times \bar{B}_0) \right) \right\} \times \bar{B}_0 \right] \tag{3.12}$$

or

$$\rho_0 \frac{\partial^2 \bar{\xi}}{\partial t^2} = F(\bar{\xi}) \tag{3.1}$$

The right hand side may be interpreted as the force density operator. For a conservative system this operator can be shown to be Hermitian and therefore has real eigenvalues. We assume that the perturbation is incompressible so that

$$\nabla . \bar{\xi} = 0 \tag{3.13}$$

Fourier analysing the displacement $\bar{\xi}$ as exp i(kz + $m\theta - \omega t$) for a perturbation of wave number k, azimuthal wave number m and frequency ω , and eliminating ξ_θ and ξ_z from the above three equations, we obtain a single

second order differential equation in the radial displacement $\xi_r = \xi$; viz., the Euler-Lagrange equation:

$$\frac{d}{dr}\left(f\frac{d\xi}{dr}\right) + g\xi = 0. \tag{3.14}$$

where

$$f = \frac{(B^2 - \omega^2 r^2) r}{1 + k^2 r^2} \tag{3.15}$$

$$g = \frac{k^2 r}{1+k^2 r^2}\left\{2B\frac{dB}{dr}r + \frac{4\omega^2 r^2 - B^2}{B^2 - \omega^2 r^2} + \frac{(3+k^2 r^2)(B^2+\omega^2 r^2)}{1+k^2 r^2}\right\} \tag{3.16}$$

Making the substitution $x = r^2$ we have

$$2r\frac{d}{dx}\left\{2fr\frac{d\xi}{dx}\right\} + g\xi = 0$$

$$\frac{d}{dx}\left\{fr\frac{d\xi}{dx}\right\} + \frac{g}{4r}\xi = 0 \tag{3.17}$$

Defining new variables F and G as

$$F = fr, \qquad G = \frac{g}{4r} \tag{3.18}$$

we have

$$F = \frac{(B^2 - \omega^2 x)\, x}{1 + k^2 x} \tag{3.19}$$

$$G_1 = \frac{k^2}{4(1+k^2x)} \left\{ 4xB\frac{dB}{dx} + \frac{4\omega^2 B^2 x}{B^2 - \omega^2 x} + \frac{(3+k^2x)(b^2+\omega^2 x)}{1+k^2x} \right\} \tag{3.20}$$

Making a substitution $\xi = u/\sqrt{F}$ in equation (3.17) we obtain

$$\frac{d^2u}{dx^2} + Q(x)\, u = 0 \tag{3.21}$$

where

$$Q(x) = \frac{G_1}{F} - \frac{F''}{2F} + \frac{1}{4}\left(\frac{F'}{F}\right)^2 \tag{3.22}$$

The primes here denote differentiation with respect to x. Eq.(3.21) is the radial eigenmode equation which may be solved with appropriate boundary conditions to yield the eigenvalues and eigenfunctions.

Figure (3. 1) shows a plot of Q(x) vs. x for typical values of ω and k. For large values of x it is seen that Q(x) is negative and a slowly varying function of x. In this region, therefore, the solution to Equation(3.21) can

be approximated by the WKB solution

$$u(x) = \frac{c_1}{\sqrt[4]{-Q(x)}} \exp -\int \sqrt{-Q(x)}\, dx \qquad (3.23)$$

In the other limit viz., $x \to 0$ the eq.(3.21) can be solved approximately as follows:

From (3.19), we get

$$F' = \frac{dF}{dx} = F\left\{\frac{1}{x(1+k^2x)} + \frac{2BB' - \omega^2}{B^2 - \omega^2 x}\right\}$$

$$= FP$$

where

$$B' = \frac{dB}{dx}$$

Substitution into (3.22) yields

$$Q(x) = \frac{G_1}{F} - \frac{P^2}{4} - \frac{P'}{2}$$

where

$$P(x) = \frac{1}{x(1+k^2x)} + \frac{2BB' - \omega^2}{B^2 - \omega^2 x}$$

Substituting in the expression for Q(x) we have

$$Q(x) = \frac{k^2BB' - B'^2 - BB''}{B^2 - \omega^2 x} + \frac{4\omega^2 B^2 k^2 + (2BB' - \omega^2)^2}{4(B^2 - \omega^2 x)^2} +$$

$$\frac{k^2(3+k^2x)(B^2+\omega^2 x) - 2(2BB' - \omega^2)}{4x(1+k^2x)(B^2 - \omega^2 x)} + \frac{1+4k^2x}{4x^2(1+k^2x)^2} \qquad (3.24)$$

For the Bennett profile, we have

$$B = \frac{K x^{1/2}}{1 + \frac{1}{4}K^2 x} \; ; \quad B' = \frac{K x^{-1/2}}{2} \frac{(1 - K^2x/4)}{(1+K^2x/4)^2}$$

where K is the inverse scale length

$$B'' = -\frac{K}{4} \frac{x^{-3/2}}{(1+K^2x/4)^3} \left\{ 1 + \frac{3}{2}K^2x - \frac{3}{16}K^4x^2 \right\}$$

Therefore we have

$$BB' = \frac{K^2}{2} \frac{(1 - K^2x/4)}{(1+K^2x/4)^3}$$

$$B'^2 = \frac{K^2}{4x} \frac{(1 - K^2x/4)^2}{(1+K^2x/4)^4}$$

$$BB'' = -\frac{K^2}{4x} \frac{1}{(1+K^2x/4)^4} \left\{ 1 + \frac{3}{2}K^2x - \frac{3}{16}K^4x^2 \right\}$$

so that

$$\frac{k^2BB' - B'^2 - BB''}{B^2 - \omega^2 x} = \frac{\frac{k^2K^2}{2}\left(1 - \frac{K^4x^2}{16}\right) + \frac{K^2}{4x}\left\{\frac{5}{2}K^2x - \frac{1}{4}K^4x^2\right\}}{\left(1 + \frac{K^2x}{4}\right)^4 \left[\frac{K^2x}{(1+K^2x/4)^2} - \omega^2 x\right]}$$

Taking the limit when $x \rightarrow 0$ and rearranging the terms, we have

$$Q(x) = \frac{\lambda^2}{4x}$$

where

$$\lambda^2 = \frac{1}{(k^2-\omega^2)^2}\left[2k^2(k^2-\omega^2)+k^2\left\{2(k^2+\omega^2)+8k^4-8\omega^2k^2\right\}\right]$$

Therefore in the limit $x \rightarrow 0$ the equation (3.21) reduces to

$$\frac{d^2u}{dx^2} + \frac{\lambda^2}{4x}u = 0 \qquad (3.25)$$

The solution is given by [23]

$$u = \sqrt{x}\, J_1(\lambda\sqrt{x}) \qquad x \ll 1 \qquad (3.26)$$

In equation (3.21) the variable x is a function of and k. In principle the eigenvalue ω for a given k is obtained by solving the differential equation in two regions and matching the solutions at some physical boundary. However, in the present case of the Bennett profile the plasma boundary extends to infinity and the transcendental nature of Q(x) does not permit analytic solutions at every radial point. The solutions obtained

above are valid only in the asymptotic limits,and there is no common region where both the solutions are valid. Therefore we have to match the two solutions numerically. This is done by using a numerical shooting method and we adopt the Numerov shooting scheme. We start with a guess value ω_0 for the eigenvalue and evaluate the eigenfunction at a suitably large value of x using the WKB expression given by equation(3.23).We then integrate the differential equation inwards until some point $x<<1$ where the analytic solution given by Equation(3.26) is valid.These solutions and their derivatives are then compared at this point in x. The guess value of ω_0 is now changed and the process of matching repeated. An iteration of this process yields the eigenvalue ω corresponding to a given k. For the iterations Muller's method with deflation is used from the software library package IMSL. For a given set of plasma parameters the growth rates for different wavenumbers are computed,and these are plotted in the curve marked 'a' in Fig.(3.2).It is seen that the mode is unstable at all wavelengths with the growth rate increasing monotonically with increasing wave number. It may be noted that the eigenvalues are purely imaginary. Ideal MHD theory assumes that there are no dissipations present in the system, so the frequency is purely imaginary with Re ω = 0.

The MHD growth rate of the kink mode has been computed for a pure Z-pinch by Nycander et al.[22] By expanding the operator in equation (3. 14) and retaining terms upto the lowest order in k^2 and ω^2 they obtain an approximate

dispersion relation of the form

$$\omega^2 = k^2 \ln k/2 + k^2\left(\gamma - \int_0^1 r B^2 dr\right) \qquad (3.27)$$

where ω and k are the frequency and axial wavenumber of the mode and are normalised to V_A/r_o and r_o respectively. Here V_A is the Alfven speed at the plasma boundary $r = r_o$ and γ is Euler's constant given by $\gamma = .577$. For the sake of comparison we have computed growth rates of the kink mode for the Bennett profile from their dispersion relation (3. 27). However, the integral in eq.(3.27) is divergent for the Bennett profile because the plasma boundary is at infinity. We have therefore assumed the plasma boundary to be truncated at $r = 2L_n$, $L_n = 1/K$ being the characteristic scale length corresponding to the Bennett profile. These growth rates are as shown in Fig.(3. 2b). Also using the same analytic expression[22] the growth rate for a volume current case is obtained and shown in Fig. (3.2c).

The eigenfunctions ξ_r are obtained numerically from the solution of equation (3. 21) and then through the transformation $\xi = u/\sqrt{F}$. A physical solution of Eq.(3.21), viz., an eigenmode that decays for large x, is obtained when Q(x) has a well-like potential structure with negative values for a large x. The displacement ξ_r for the case k = 1. 1 is shown in Fig. (3. 3). It is found that the eigenfunction is peaked on the axis and goes to zero at

large distances. There are no radial oscillations and this corresponds to the radial node number zero. Also it is found that for large axial wavenumbers the displacement is more localised near the axis of the plasma, whereas for small k it has a larger width. For k = 0.1 the whole of the plasma suffers a large displacement and thus is more like a global mode. The displacement of the plasma surface is much reduced for smaller wavelengths and for k = 1.1 (Fig. 3.3) the instability is quite localized to the centre of the pinch. However at the plasma boundary, which may be at a few L_n, the displacement is finite as shown in figure(3.3).

3.3 Kinetic Theory for the m=1 mode instability in Z-pinch

In this section we investigate the stability of a high β cylindrical plasma against small amplitude electromagnetic perturbations with the azimuthal mode number m=1. The plasma is considered collisionless so that this analysis corresponds to the kinetic theory of the m=1 ideal MHD mode discussed in the preceding section. High beta plasmas are characterised by high temperatures, large spatial inhomogeneities and finite size particle orbits (15, 24-26). In Chapter 2, we derived a fully kinetic non-local dispersion relation for a general electromagnetic perturbation of the Bennett equilibrium using the linearised Vlasov-Maxwell equations for both electrons and ions assuming betatron orbits. Without using the local approximation in the orbit integral and expressing the radial amplitude of the perturbations in terms of a complete set of basis functions, a dispersion relation in matrix form was obtained for a given azimuthal mode number m and axial wavenumber k. Here we consider the limiting form of the general matrix dispersion relation for a purely electromagnetic perturbation in the limit ($\phi_1 \to 0$) and investigate the stability of m=1 kink type perturbations. We shall briefly outline the essential steps of the derivation of the dispersion relation for this mode on the lines of the analysis presented in chapter 2. This is followed by a discussion on the numerical computation of

the eigenvalues and the analytic solutions in the limiting cases.

Consider an infinitely long cylindrical plasma carrying an axial current J_{oz}. This current produces an azimuthal magnetic field $B_\theta(r)$. The equilibrium current and the magnetic field are related through the Ampere's equation:

$$\nabla \times \bar{B}_0 = \frac{4\pi}{c} \bar{J}_0 \tag{3.28}$$

For an equilibrium which is axially uniform and azimuthally symmetric we have $\frac{\partial}{\partial z} = 0 = \frac{\partial}{\partial \theta}$. Consequently the equilibrium is one-dimensional and the equilibrium quantities such as the current, magnetic field, etc. are functions of the radial coordinate alone. The equilibrium profiles are obtained by solving the Vlasov-Ampere system of equations self-consistently, as shown in chapter 2. For the Bennett equilibrium these are given by

$$\bar{J}_0 = \frac{n_0 e (V_e + V_i)}{\left(1 + \frac{1}{4} K^2 r^2\right)^2} \hat{z}$$

$$\bar{B}_0 = \frac{\hat{B}_0 K r}{1 + \frac{1}{4} K^2 r^2} \hat{\theta} \tag{3.29}$$

To investigate the stability of the system against small amplitude perturbations, the linearised Vlasov equation and Maxwell's equations form a complete description:

$$\frac{\partial f_{1j}}{\partial t} + \bar{v}\cdot\frac{\partial f_{1j}}{\partial \bar{x}} + \frac{\bar{F}_0}{m_j}\cdot\frac{\partial f_{1j}}{\partial \bar{v}} = -\frac{\bar{F}_1}{m_j}\cdot\frac{\partial f_{0j}}{\partial \bar{v}} \tag{3.30}$$

$$\nabla\times\bar{B}_1 = \frac{4\pi}{c}\bar{J}_1 + \frac{1}{c}\frac{\partial \bar{E}_1}{\partial t} \tag{3.31}$$

$$\nabla\cdot\bar{E}_1 = 4\pi\rho_1 \tag{3.32}$$

For low frequency electromagnetic perturbations described by scalar and vector potentials ϕ_1 and A_{1z} the dispersion relation was obtained in chapter 2, by expanding the radial amplitudes of the perturbations over a complete set of basis functions, and integrating over the unperturbed orbits, namely, the betatron orbits. This is given by:

$$\begin{bmatrix} D^{(1)}_{n'n} & D^{(2)}_{n'n} \\ D^{(3)}_{n'n} & D^{(4)}_{n'n} \end{bmatrix} = 0 \tag{3.33}$$

where $D^{(1)}_{n'n}$, $D^{(2)}_{n'n}$, $D^{(3)}_{n'n}$ and $D^{(4)}_{n'n}$ are submatrices. This is the most general dispersion relation for electromagnetic perturbations. When the perturbation is purely electromagnetic i. e. the charge density perturbations are zero but current perturbations are finite, i. e. , when

$\phi_1 \to 0$ the system can be described by the linearised Vlasov and Ampere's equation alone. The dispersion relation in this case reduces to

$$\text{Det}\left|D^{(4)}_{n'm}\right| = 0 \qquad (3.34)$$

where

$$D^{(4)}_{n'm} = (k^2+\lambda_m^2)\delta_{n'm} - \frac{\omega^2}{c^2k^2}\cdot\frac{1}{\lambda^2_{De(0)}}\left(\frac{1+\tau}{\tau}\right)A_{n'm} + \sum_j \frac{(\omega-kV_j)}{c^2k^2\lambda^2_{Dj}(0)} \sum_{l,p} I_{Rl}\Gamma^j_p \left\{(1+2l+2p)\omega_{pj} - \frac{(\omega-(1+2l+2p)\omega_{pj})^2}{\sqrt{2}kV_{thj}} Z(\zeta^{lp}_j)\right\} \qquad (3.35)$$

Here

$$A_{n'm} = \int_0^{R_c} \frac{r\phi_{n'}\phi_n\,dr}{(1+\frac{1}{4}k^2r^2)^2}$$

$$\lambda^2_{De(0)} = \frac{kT_e}{4\pi\hat{n}_{(0)}e^2} \quad ; \quad I_{Rl} = (-1)^l \int_0^{R_c} \frac{r\phi_{n'}J_m\left(\frac{\lambda_m r}{2}\right)J_{m+l}\left(\frac{\lambda_m r}{2}\right)dr}{(1+\frac{1}{4}k^2r^2)^2}$$

$$\Gamma^j_p = I_p\left(\frac{T_j}{m_j}\frac{\lambda_m^2}{4\omega^2_{pj}}\right)\exp\left(-\frac{T_j}{m_j}\frac{\lambda_m^2}{4\omega^2_{pj}}\right)$$

$$\zeta^{lp}_j = \frac{\omega-kV_j-(1+2l+2p)\omega_{pj}}{\sqrt{2}kV_{thj}} \qquad V_{thj} = \sqrt{\frac{T_j}{m_j}}$$

$$\tau = \frac{T_e}{T_i}$$

The third term in eqn.(3.35) can be simplified as follows:

We have

$$\sum_{l,p} I_{R,l}\, \Gamma_p^{j}(1+2l+2p)$$

$$= \sum_{l,p} I_{R,l}\, \Gamma_p (1+2l) + 2\sum_{l,p} I_{R,l}\, p\, \Gamma_p$$

$$= \sum_{l} I_{Rl}(1+2l) \sum_{p} \Gamma_p + 2 \sum I_{Rl} \sum p\, \Gamma_p$$

Now $I_p = I_{-p}$ for integer p [23] and

$$\sum_{p=-\infty}^{\infty} I_p(x) = e^{x}$$

Therefore it follows that $\sum_p \Gamma_p = 1$ and $\sum_p p\Gamma_p^{j} = 0$

Substituting above we have

$$\sum_{l,p} I_{Rl}\, \Gamma_p^{j}\,(1+2l+2p)$$

$$= \sum_{l} I_{R,l}(1+2l)$$

We will now show that this term vanishes identically. Let

$$S = \sum_{l} I_{Rl}(1+2l)$$

Substituting for I_{RL} we have

$$S = \sum_{l} (-1)^{l} \int_{0}^{Rc} \frac{r\, dr\, \phi_{m'}\, J_l\left(\frac{\lambda_m r}{2}\right) J_{l+m}\left(\frac{\lambda_m r}{2}\right)}{\left(1+\frac{1}{4}k^2 r^2\right)^2} (1+2l)$$

For m=1 modes we have

$$S = \sum_{l} (-1)^{l} \int r\, dr\, \phi_{m'}\, J_l\left(\frac{\lambda_m r}{2}\right) J_{l+1}\left(\frac{\lambda_m r}{2}\right)(1+2l)$$

Substituting $l + l = -q$ we have

$$S = \sum_q (-1)^{-q-1} \int_0^{R_c} \frac{r\,dr\,\phi_m\, J_{-q-1}\, J_q(-2q-1)}{\left(1+\frac{1}{4}k^2\gamma_r^2\right)^2}$$

$$= -\sum_q (-1)^q \int_0^{R_c} \frac{r\,dr\,\phi_m\, J_{q+1}\, J_q(2q+1)}{\left(1+\frac{1}{4}k^2\gamma_r^2\right)^2}$$

$$= -S$$

Therefore it follows that $S = 0$. Hence the third term in equation (3. 35) vanishes identically. The last term can be expanded as follows:

$$-\sum_j \frac{(\omega - kV_j)}{c^2k^2\lambda_{Dj}^2(o)} \sum_{l,p} I_{R,l}\, \Gamma_p^j \frac{(\omega-(1+2l+2p)\,\omega_{pj})^2}{\sqrt{2}\,kV_{thj}}\, Z\left(\xi_j^{lp}\right)$$

Substituting for ξ_j^{lp} and putting $l + p = \alpha$ this gives

$$-\sum_j \frac{(\omega-kV_j)}{c^2k^2\lambda_{Dj}^2(o)} \sum_{l,\alpha} I_{R,l}\, \Gamma_{\alpha-l}^j \frac{(\omega-\omega_{pj})^2}{\sqrt{2}\,kV_{thj}}\, Z\left(\frac{\omega-kV_j-(1+2\alpha)\,\omega_{pj}}{\sqrt{2}\,kV_{thj}}\right)$$

On carrying out the α— summation and writing down the first few terms we have

$$-\sum_j \frac{(\omega-kV_j)}{c^2k^2\lambda_{Dj}^2(o)}\left[\frac{(\omega-\omega_{pj})^2}{\sqrt{2}\,kV_{thj}}\, Z\left(\frac{\omega-kV_j-\omega_{pj}}{\sqrt{2}\,kV_{thj}}\right) \sum_l I_{R,l}\, \Gamma_{-l}^j\right.$$

$$+\frac{(\omega+\omega_{pj})^2}{\sqrt{2}kV_{thj}}\,Z\left(\frac{\omega-kV_j+\omega_{pj}}{\sqrt{2}kV_{thj}}\right)\sum_l I_{Rl}\,\Gamma_{-1-l}$$

$$+\frac{(\omega-3\omega_{pj})^2}{\sqrt{2}kV_{thj}}\,Z\left(\frac{\omega-kV_j-3\omega_{pj}}{\sqrt{2}kV_{thj}}\right)I_{Rl}\,\Gamma_{1-l}$$

$$+\frac{(\omega+3\omega_{pj})^2}{\sqrt{2}kV_{thj}}\,Z\left(\frac{\omega-kV_j+3\omega_{pj}}{\sqrt{2}kV_{thj}}\right)I_{Rl}\,\Gamma_{-2-l}+\cdots$$

$$=-\sum_j\frac{(\omega-kV_j)}{c^2k^2\lambda_{Dj}^2(\omega)}\left[\frac{(\omega-\omega_{pj})^2}{\sqrt{2}kV_{thj}}\,Z\left(\frac{\omega-kV_j-\omega_{pj}}{\sqrt{2}kV_{thj}}\right)P_{n'm}^{(0)}+\frac{(\omega+\omega_{pj})^2}{\sqrt{2}kV_{thj}}\times\right.$$

$$\left.Z\left(\frac{\omega-kV_j+\omega_{pj}}{\sqrt{2}kV_{thj}}\right)P_{n'm}^{(-1)}\right]+\frac{(\omega-3\omega_{pj})^2}{\sqrt{2}kV_{thj}}\,Z\left(\frac{\omega-kV_j-3\omega_{pj}}{\sqrt{2}kV_{thj}}\right)P_{n'm}^{(1)}$$

$$+\frac{(\omega+3\omega_{pj})^2}{\sqrt{2}kV_{thj}}\,Z\left(\frac{\omega-kV_j+3\omega_{pj}}{\sqrt{2}kV_{thj}}\right)P_{n'm}^{(-2)}+\cdots\cdots$$

where

$$P_{n'm}^{(\alpha)}=\sum_l I_{Rl}\,\Gamma_{\alpha-l}$$

It can be shown that $P_{n'm}^{\alpha}=P_{n'm}^{-\alpha-1}$ where $\alpha=0,1,2,$ .....We have

$$P_{n'm}^{(\alpha)}=\sum_l(-1)^l\int_0^{R_c}\phi_{n'}\,r\,dr\,J_l\,\frac{J_{l+1}\left(\frac{\lambda_{mn}r}{2}\right)}{\left(1+\frac{1}{4}k^2r^2\right)^2}\,\Gamma_{\alpha-l}$$

Putting $l=-q-1$ we have

$$P_{n'm}^{(\alpha)}=\sum_q(-1)^{-q-1}\int_0^{R_c}\frac{r\phi_{n'}\,dr\,J_{-q-1}\,J_{-q}}{\left(1+\frac{1}{4}k^2r^2\right)^2}\,\Gamma_{\alpha+q+1}$$

$$= \sum_q (-1)^{-q-1} (-1)^{2q+1} \int_0^{R_c} \frac{r\phi_{m'} \, dr \, J_{q+1} \, J_q}{\left(1+\frac{1}{4}k^2r^2\right)^2} \Gamma_{\alpha+q+1}$$

$$= \sum_q (-1)^{-q} \int_0^{R_c} \frac{r\phi_{m'} \, dr \, J_{q+1} \, J_q}{\left(1+\frac{1}{4}k^2r^2\right)^2} \Gamma_{-\alpha-q-1} = P_{m'm}^{-\alpha-1}$$

Therefore we can write the equation (3.35) as

$$D^{(4)}_{m'm} = \left(k^2+\lambda_m^2\right)\delta_{m'm} - \frac{\omega^2}{c^2k^2} \frac{1}{\lambda_{De}^2} \frac{1+\tau}{\tau} A_{m'm}$$

$$- \sum_j \frac{(\omega - kV_j)}{\sqrt{2}kV_{th_j} \lambda_{Dj}^2(0)} \sum_{\alpha=0}^{\infty} P^{(\alpha)}_{m'm} \left[\left(\frac{\omega - (1+2\alpha)\omega_{\beta j}}{ck} \right)^2 Z(\zeta_\alpha^-) + \left(\frac{\omega + (1+2\alpha)\omega_{\beta j}}{ck} \right)^2 Z(\zeta_\alpha^+) \right] \quad (3.36)$$

where $P_{n'n}$ is a matrix defined by

$$P^{(\alpha)}_{m'n} = \sum_l (-1)^l \int_0^{R_c} \frac{r\phi_{m'} \, J_l\left(\frac{\lambda_m r}{2}\right) J_{l+1}\left(\frac{\lambda_m r}{2}\right) dr}{\left(1+\frac{1}{4}k^2r^2\right)^2} \Gamma_{\alpha-l} \quad (3.37)$$

The index α now takes on positive integral values only.

Equation (3. 34) therefore represents the general dispersion relation with the matrix $D_{n'n}$ given by equation (3. 36). Because of the nature of the betatron orbit, the

particles execute helical orbits whose pitch depends on the initial position of the particle. Thus a perturbation with a given pitch, i.e. m and k, will resonate only with particles with a particular initial position. This makes the wave-particle resonance localised, and this effect is represented in the above matrix elements by the combination of the plasma dispersion function and the matrix elements $P_{n'n}$. The wave-particle resonance represented by $Z(\zeta)$ is non-local but is weighted by $P_{n'n}$ to yield the effect of the profile. The first term in the α-summation represents the fundamental betatron resonance and the successive terms represent higher harmonics resonances. The strength of these successive harmonics becomes smaller and smaller as α is increased. For an m=1 mode it is found that only the odd harmonics are present. Retaining only the fundamental resonance term and writing down the electron and ion terms separately we have in (3.36)

$$\text{Det}\,|D_{n'n}| = (k^2+\lambda_n^{-2})\,\delta_{n'n} - \frac{\omega^2}{c^2k^2}\,\frac{1}{\lambda_{De(o)}^2}\left(\frac{1+\tau}{\tau}\right)A_{n'n}$$

$$-\left\{\frac{\omega+kV}{\sqrt{2}kV_{the}\lambda_{De}^2}\left[\left(\frac{\omega-\omega_{pe}}{ck}\right)^2 Z(\zeta_e^-) + \left(\frac{\omega+\omega_{pe}}{ck}\right)^2 Z(\zeta_e^+)\right] + \right.$$

$$\left.\frac{\omega-kV/\tau}{\sqrt{2}kV_{thi}}\,\lambda_{Di(o)}^2\left[\left(\frac{\omega-\omega_{pi}}{ck}\right)^2 Z(\zeta_i^-) + \left(\frac{\omega+\omega_{pi}}{ck}\right)^2 Z(\zeta_i^+)\right]\right\} P_{n'n} \qquad (3.38)$$

The matrix $D_{n'n}$ is in principle of infinite order with n and n' extending upto infinity. However in practice it is

usually possible to truncate the matrix at suitably large n depending on the convergence of the matrix elements and solve the resulting determinant numerically.

We have solved the matrix dispersion relation by taking a typical matrix size of 20. The matrix D can be expressed as a sum over coefficient matrices P_0 , P_1 etc. multiplied by functions of ω and k. These coefficient matrices depend on the equilibrium parameters and are independent of ω. For a given set of equilibrium parameters these matrices are evaluated only once. To solve for the ω's we follow the following procedure:

We write equation (3.38) in the form

$$\text{Det}\left[D - \lambda_i K\right] = 0$$

where the λ_i's are eigenvalues of the complex matrix D. Now

$$\text{Det } D = \prod_{i=1}^{n} \lambda_i$$

and solving equation(3. 38) reduces to obtaining λ_i's and iterating till their product is small enough. We now start with an initial guess value ω_0, and obtain the matrix D(ω, k). In order to obtain the eigenvalues λ_i the original matrix was first balanced and then transformed to the complex upper Hessenberg form using elementary similarity transformations. This leads to an increased accuracy and numerical stability of the eigenvalues[28]. The eigenvalues are then obtained by the modified LR method. In this method a sequence of complex upper Hessenberg matrices, similar to the input matrix is generated, which converges to a

triangular matrix. The eigenvalues are then determined from the diagonal elements of the triangular matrix[29]. From the product of the eigenvalues the determinant $|D|$ is obtained. This process is repeated for a new value of ω and iterated using Muller's method[30] till convergence is achieved. The real and imaginary parts of $\omega = \omega_r + i\gamma$ obtained by this method are shown by the solid curves in Fig. (3. 4). Relative convergence of the product of the eigenvalues was used as the criterion for the roots. The root-finding process in the complex ω-plane based on Muller's method is quite sensitive to the initial guess value ω_0. Therefore it is important to have a good initial guess value for ω in order to obtain convergence. Two different methods viz., Nyquist and graphic methods, have been used before solving for ω in a given parameter region.

The Nyquist method[31] is based on the residue theorem in complex analysis. Though it does not determine the actual root of the given function, it is still useful because it tells us whether there exists a root in the upper half ω-plane with Im $\omega > 0$. In order to determine whether such a root exists for a function $D(\omega)$ we consider a contour in the complex ω-plane defined by the real axis from $-\infty$ to $+\infty$ and the semicircle in the upper half plane in an anti-clockwise manner. Then the integral:

$$I = \oint_{\omega} \frac{dD/d\omega}{D} \, d\omega$$

taken over this contour will have a finite value according to Cauchy's residue theorem if $D = 0$ for some ω along the

contour, assuming D has no poles. In the D-plane the integral may be written as

$$I = \oint_D \frac{dD}{D}$$

where the integration contour is mapped into the D-plane. In the D-plane the pole occurs at D = 0, hence I has a value when the mapped contour in the D-plane encircles the origin in the D-plane. In other words instability occurs when the mapping into the D-plane of the contour that encircles the upper half ω-plane encircles the origin in the D- plane. The contribution from the semicircle at infinity vanishes, so it is necessary to do the mapping for the real axis from $-\infty$ to $+\infty$ and see if the contour encloses the origin. However, this method only tells us whether or not there exists a root with $Im\omega > 0$ in a given region. In order to obtain rough estimate of where a root lies, in the ω-plane we used the graphic method[32]. In this method the complex ω-plane is divided into a series of grids and the real and imaginary parts of the given function whose root is desired, are obtained at each grid point. From the change of sign of the function, the roots are obtained to an accuracy of the order of the width of the grid. Repeating this method for smaller and smaller grid size the contours of Re $f(\omega)=0$ and Im $f(\omega)=0$ are obtained and plotted in the ω-plane. The intersections of these curves determine points in the ω-plane where Re $(f)=0$ and Im $(f)=0$ and therefore yield an estimate of the roots. These roots are fed as initial guess in the Muller's method for obtaining an actual root.

The above procedure for finding the roots of equation (3.38) is quite general but involves extensive computations. In some particular cases it is possible to reduce the matrix dispersion relation to a more convenient form which is easier to handle numerically as well as analytically. This can be done as follows:

We first show that the matrices $A_{n'n}$ and $P_{n'n}$ are related.

We have (from chapter 2):

$$A_{n'n} = A_{n'} A_n \int_0^{R_c} \frac{dr\, r\, J_1(\lambda_{n'} r)\, J_1(\lambda_n r)}{(1+\frac{1}{4}K^2 r^2)^2}$$

Using the addition theorem for Bessel functions

$$J_l(\lambda_n r) = \sum_p J_{l-p}\left(\frac{\lambda_n r}{2}\right) J_p\left(\frac{\lambda_n r}{2}\right)$$

and the Bessel function identity

$$e^x = I_0(x) + 2\sum_{p=1}^{\infty} I_p(x)$$

we can write

$$A_{n'n} = A_{n'} A_n \int_0^{R_c} \frac{dr\, r\, J_1(\lambda_{n'} r) \sum_p J_{1-p}\left(\frac{\lambda_n r}{2}\right) J_p\left(\frac{\lambda_n r}{2}\right)}{\left(1+\frac{1}{4}K^2 r^2\right)^2}$$

$$= \sum_{\alpha,p} A_{n'} A_n \int_0^{R_c} \frac{dr\, r\, J_1(\lambda_{n'} r)\, J_{1-p}\left(\frac{\lambda_n r}{2}\right) J_p\left(\frac{\lambda_n r}{2}\right) \Gamma_{\alpha-p}}{\left(1+\frac{1}{4}K^2 r^2\right)^2}$$

$$= \sum_{\alpha=0}^{\infty} 2\, P^{(\alpha)}_{n'n} \qquad (3.39)$$

Using (3.39) we can now write down $D_{n'n}$ as

$$D_{n'm} = k_n^2 \lambda_{De}^2 \delta_{n'm} + \frac{\omega^2}{c^2 k^2}\left(\frac{1+\tau}{\tau}\right) A_{n'm}$$

$$- P_{n'm}\left[\frac{\omega+kV}{\sqrt{2}kV_{the}}\left\{\left(\frac{\omega-\omega_{pe}}{ck}\right)^2 Z\left(\frac{\omega+kV-\omega_{pe}}{\sqrt{2}kV_{the}}\right)+\left(\frac{\omega+\omega_{pe}}{ck}\right)^2 Z\left(\frac{\omega+kV+\omega_{pe}}{\sqrt{2}kV_{the}}\right)\right\}\right.$$

$$\left.+\frac{\omega\tau-kV}{\sqrt{2}kV_{thi}}\left\{\left(\frac{\omega-\omega_{pi}}{ck}\right)^2 Z\left(\frac{\omega-kV/\tau-\omega_{pi}}{\sqrt{2}kV_{thi}}\right)+\left(\frac{\omega+\omega_{pi}}{ck}\right)^2 Z\left(\frac{\omega-kV/\tau+\omega_{pi}}{\sqrt{2}kV_{thi}}\right)\right\}\right] \tag{3.40}$$

The second term on the right hand side can be neglected for low frequency waves. The resulting matrix can be written as

$$[D] = [K - f(\omega) P] \tag{3.41}$$

where K is a diagonal matrix with the matrix elements $k^2 \lambda_{De}^2 \delta_{n'n}$. P is the matrix with the elements $P_{n'n}$ and $f(\omega)$ is given by

$$f(\omega) = \frac{\omega+kV}{\sqrt{2}kV_e}\left[\left(\frac{\omega-\omega_{pe}}{ck}\right)^2 Z(\zeta_e^-) + \left(\frac{\omega+\omega_{pe}}{ck}\right)^2 Z(\zeta_e^+)\right] +$$

$$\frac{\omega\tau-kV}{\sqrt{2}kV_{thi}}\left[\left(\frac{\omega-\omega_{pi}}{ck}\right)^2 Z(\zeta_i^-) + \left(\frac{\omega+\omega_{pi}}{ck}\right)^2 Z(\zeta_i^+)\right] \tag{3.42}$$

The determinant of the matrix P is non-zero so that its inverse exists. Then operating with P^{-1} we have

$$\left[P^{-1}.D\right] = \left[P^{-1}K - f(\omega)\,I\right]$$

Therefore Det D x Det P^{-1} = Det $[P^{-1}$ K - f(ω) I] or Det D = 0 implies

$$\text{Det}\left[P^{-1}.K - f(\omega)\,I\right] = 0 \qquad (3.43)$$

This equation can be compared with the eigenvalue equation of the matrix P^{-1}. K which is given by

$$\text{Det}\left[P^{-1}.K - \mu_i\,I\right] = 0 \qquad (3.44)$$

where μ_i are the eigenvalues of the matrix P^{-1}.K. From Eqs.(3.43) and (3.44) we have

$$f(\omega) - \mu_i = 0. \qquad (3.45)$$

Equation (3. 45) is the reduced dispersion relation for the electromagnetic modes and may be solved for given μ_i and k. For a given set of plasma parameters the elements of the matrix P^{-1}. K are functions of k, and therefore the eigenvalues μ_i of this matrix are functions of k. The numerical solution of equation (3.45) has been obtained for various parameter regions using the following scheme:First

the plasma parameters are fixed so that the matrix P and therefore P^{-1} is evaluated. Then a specific value of k is taken. Using the numerical algorithms for finding the eigenvalues of a general complex matrix described earlier the complex eigenvalues are obtained. On taking one of the eigenvalues, typically the small one, equation (3.45) becomes an equation in the complex frequency ω. Starting with a guess value of ω_0, equation (3.45) is now solved iteratively using the Muller's method. To obtain another value of ω, we change the value of k and repeat the whole cycle of computations. The real and imaginary parts of ω thus obtained is plotted as the dashed curve in Fig. (3.4). It is seen that the values of ω obtained thus is very close to the values obtained previously by the matrix method. This provides a good check on these two methods of solving eq. (3. 45). The advantage of the latter method is that the simple function $f(\omega)$, rather than the complex matrix $[D_{m'm}]$ is evaluated at each iteration step. This yields considerable saving of computer time. On the DEC 1091 system which was used for all the computations, the typical CPU times for obtaining a single value by these two methods are 2.6min. and 0.36sec respectively. It is seen in Fig. (3. 5) that the growth rate increases linearly with k for small wavenumbers while the real part of the frequency remains nearly zero. At large values of k the kinetic effects e. g. , Landau damping, become important, and the growth rate decreases after reaching a maximum and eventually becomes negative for still higher k. As the

particle drift velocity V is increased the growth rate for a given k increases and the peak shifts to higher k values. The position of maximum growth as well as the threshold k for damping are found to increase with the electron drift velocity. The increase in the growth rate with V may be understood from the fact that the drift velocity is a source of free energy in the system and therefore higher V would yield faster growth.

To understand the above results physically we solve the dispersion relation (3. 45) approximately in appropriate limits. In the low frequency limit and for small values of k we can approximate the Z-functions in (3.45) by their corresponding large argument expansions. Substituting in (3. 44) and retaining only the first term in the power series expansion we obtain:

$$\frac{\omega+kV}{\sqrt{2}kV_e}\left[\left(\frac{\omega-\omega_{pe}}{ck}\right)^2\left\{\frac{-\sqrt{2}kV_{the}}{\omega+kV-\omega_{pe}}+i\pi^{1/2}\exp-\left(\frac{\omega+kV-\omega_{pe}}{\sqrt{2}kV_{the}}\right)^2\right\}\right.$$

$$+\left(\frac{\omega+\omega_{pe}}{ck}\right)^2\left\{\frac{-\sqrt{2}kV_{the}}{\omega+kV+\omega_{pe}}+i\pi^{1/2}\exp-\left(\frac{\omega+kV+\omega_{pe}}{\sqrt{2}kV_{the}}\right)^2\right\}$$

$$+\frac{\omega\tau-kV}{\sqrt{2}kV_{thi}}\left[\left(\frac{\omega-\omega_{pi}}{ck}\right)^2\left\{\frac{-\sqrt{2}kV_{thi}}{\omega-kV/\tau-\omega_{pi}}+i\pi^{1/2}\exp-\left(\frac{\omega-kV/\tau-\omega_{pi}}{\sqrt{2}kV_{thi}}\right)^2\right\}\right.$$

$$\left.\left.+\left(\frac{\omega+\omega_{pi}}{ck}\right)^2\left\{\frac{-\sqrt{2}kV_{thi}}{\omega-kV/\tau+\omega_{pi}}+i\pi^{1/2}\exp-\left(\frac{\omega-kV/\tau+\omega_{pi}}{\sqrt{2}kV_{thi}}\right)^2\right\}\right]-\mu_i=0$$

For $\omega \ll \omega_{pi}, \omega_{pe}$ we can neglect the exponential terms in the above expansion. The dispersion relation then approximates to

$$\frac{(\omega+kV)}{c^2k^2}\left[\frac{(\omega-\omega_{pe})^2}{\omega+kV-\omega_{pe}}+\frac{(\omega+\omega_{pe})^2}{\omega+kV+\omega_{pe}}\right]+$$

$$\frac{(\omega\tau-kV)}{c^2k^2}\left[\frac{(\omega-\omega_{pi})^2}{\omega-kV/\tau-\omega_{pi}}+\frac{(\omega+\omega_{pi})^2}{\omega-kV/\tau+\omega_{pi}}\right]+\mu_i=0$$

Multiplying through with c^2k^2 we have

$$c^2k^2\mu_i+(\omega+kV)\left[\frac{(\omega-\omega_{pe})^2(\omega+kV+\omega_{pe})+(\omega+\omega_{pe})^2(\omega+kV-\omega_{pe})}{(\omega+kV)^2-\omega_{pe}^2}\right]$$

$$+(\omega\tau-kV)\left[\frac{(\omega-\omega_{pi})^2(\omega-kV/\tau+\omega_{pi})+(\omega+\omega_{pi})^2(\omega-kV/\tau-\omega_{pi})}{(\omega-kV/\tau)^2-\omega_{pi}^2}\right]$$

$$=0$$

or

$$c^2k^2\mu_i+(\omega+kV)\frac{\{2(\omega^2+\omega_{pe}^2)(\omega+kV)-4\omega\omega_{pe}^2\}}{(\omega+kV)^2-\omega_{pe}^2}+$$

$$(\omega\tau-kV)\frac{\{2(\omega^2+\omega_{pi}^2)(\omega-kV/\tau)-4\omega\omega_{pi}^2\}}{(\omega-kV/\tau)^2-\omega_{pi}^2}=0$$

or

$$c^2k^2\mu_i+\frac{2\omega^2(\omega+kV)^2+2\omega_{pe}^2(k^2V^2-\omega^2)}{(\omega+kV)^2-\omega_{pe}^2}+$$

$$\tau\cdot\frac{2\omega^2(\omega-kV/\tau)^2+2\omega_{pi}^2(k^2V^2/\tau^2-\omega^2)}{(\omega-kV/\tau)^2-\omega_{pi}^2}=0$$

$$\Rightarrow c^2k^2\mu_i + 2\omega^2(1+\tau) + \frac{2\omega_{pe}^2 k^2V^2}{(\omega+kV)^2-\omega_{pe}^2} + \frac{2\omega_{pi}^2\tau\cdot k^2V^2/\tau^2}{(\omega-kV/\tau)^2-\omega_{pi}^2}$$

$$= 0$$

$$\Rightarrow \frac{k^2c^2\mu_i}{2} + \omega^2(1+\tau) - k^2V^2\left\{1-\left(\frac{\omega+kV}{\omega_{pe}}\right)^2\right\}^{-1} -$$

$$\frac{k^2V^2}{\tau}\left\{1-\left(\frac{\omega-kV/\tau}{\omega_{pi}}\right)^2\right\}^{-1} = 0$$

Taylor-expanding the brackets for $\omega \ll \omega_{pe}, \omega_{pi}$ we obtain

$$\frac{\mu_i c^2}{2V^2} + \frac{\omega^2}{k^2V^2}(1+\tau) - \frac{1+\tau}{\tau} - \left(\frac{\omega+kV}{\omega_{pe}}\right)^2 - \frac{(\omega-kV/\tau)^2}{\tau\omega_{pi}^2} = 0$$

From the equilibrium we have the following relation between V^2, τ and λ_D^2:

$$\frac{V^2}{c^2}\left(\frac{1+\tau}{2\tau}\right) = \frac{\lambda_{De}^2}{L_n^2}$$

Substituting above for V^2/c^2 we have

$$\frac{\mu_i}{4}\left(\frac{1+\tau}{\tau}\right)\frac{L_n^2}{\lambda_{De}^2} + \frac{\omega^2}{k^2V^2}(1+\tau) - \frac{1+\tau}{\tau} - \omega^2\left(\frac{1}{\omega_{pe}^2} + \frac{1}{\tau\omega_{pi}^2}\right)$$

$$+ 2\omega\left(-\frac{kV}{\omega_{pe}^2} + \frac{kV}{\tau^2\omega_{pi}^2}\right) - \frac{k^2V^2}{\omega_{pe}^2} - \frac{k^2V^2/\tau^2}{\tau\omega_{pi}^2} = 0$$

$$\Rightarrow \omega^2\left(\frac{1+\tau}{k^2V^2} - \frac{1}{\omega_{pe}^2} - \frac{1}{\tau\omega_{pi}^2}\right) + 2\omega\left(-\frac{kV}{\omega_{pe}^2} + \frac{kV}{\tau^2\omega_{pi}^2}\right) +$$

$$\left(\frac{\mu_i}{4}\frac{L_n^2}{\lambda_\beta^2} - 1\right)\frac{1+\tau}{\tau} - \frac{k^2V^2}{\omega_{pe}^2} - \frac{k^2V^2\tau^3}{\omega_{pi}^2\tau} = 0$$

Retaining only the leading terms for small k we have

$$\frac{\omega^2(1+\tau)}{k^2V^2} + \frac{2\omega kV/\tau}{\tau\omega_{pi}^2} + \left(\frac{\mu_i}{4\lambda_{De}^2} - 1\right)\frac{1+\tau}{\tau} \simeq 0$$

multiplying through with $\frac{k^2V^2}{1+\tau}$ we have

$$\omega^2 + 2\omega\frac{k^3V^3}{\tau^2(1+\tau)}\frac{1}{\omega_{pi}^2} + \left(\frac{\mu_i}{4}\frac{L_n^2}{\lambda_{De}^2} - 1\right)\frac{k^2V^2}{\tau} \simeq 0$$

$$\Rightarrow \omega = -\frac{k^3V^3}{\tau^2(1+\tau)}\frac{1}{\omega_{pi}^2} \pm \sqrt{\frac{k^6V^6}{\tau^4(1+\tau)^2}\frac{1}{\omega_{pi}^4} - \frac{k^2V^2}{\tau}\left(\frac{\mu_i}{4\lambda_{De}^2} - 1\right)} \qquad (3.46)$$

These solutions are shown by the dashed curves in Fig. (3. 6b) and are in good agreement with the general solutions (Fig.(3.6a)).

3.4 Discussion

We have investigated the stability of a Bennett equilibrium for m=1 electromagnetic perturbations in the magnetohydrodynamic as well as kinetic limits. In the MHD limit we have solved for the linear growth rates numerically and obtained the radial eigenfunctions. These indicate that the displacement is peaked at the centre of the pinch especially for short wavelengths. From the plot of ξ_r vs. r it is clear that the eigenfunction ξ_r does not cross the axis at any finite radial point and this has zero node number. For a given m and k value this is the most unstable eigenmode [27]. Though the instability of the m=1 mode in the Z-pinch has been well known since the work of Kruskal and Schwarzchild [1], it is nevertheless important to compute the growth rates for realistic profiles such as the Bennett profile due to the fact that the growth rate for the sharp boundary pinch is about three times that of a diffuse pinch. From Fig.(3.2) it is seen that the growth rate obtained by the numerical integration of the eigenvalue equation is considerably lower than those obtained from approximate analytic expressions for the same or other equilibrium profiles.

In the kinetic case , we have used a non-local theory to study the m=1 kink mode in a current carrying plasma with a diffuse profile. The numerical solution of the dispersion relation using different methods yields a mode which is driven basically by the plasma current. At small

wavenumbers the mode is unstable and the growth is linear. For these small values of k approximate analytic expressions for γ are obtained and these coincide with the numerically computed values. As k is increased the two depart from each other, as would be expected. At higher values of k the kinetic effects become important and the Landau damping is strong enough to stabilize the mode completely. This is a new feature of the instability that the inclusion of the kinetic effects has yielded. In the MHD analysis the growth rate monotonically increases with k and there are no stabilizing effects that would provide saturation. It may be noted that for $m \neq 1$ the ideal MHD gross instabilities may be stabilized by an appropriate choice of equilibrium profiles[12]. However for $m = 1$ this is not possible and the present study shows that the kinetic damping effect can stabilize the instability, at least for higher k.

References

1. Kruskal, M. & Schwarzchild,M., Proc. Phys. Soc. A223, 348 (1954).

2. Carruthers, R. & Davenport,P.A., Proc. Phys. Soc. B70, 49 (1957)

3. Curzon, F. L. , Folkierski,A., Lathem,R. & Nation,J.A., Proc. Roy.Soc. Lond. A257, 386 (1960).

4. Cousins, S. W. & Ware,A.A., Proc. Phys. Soc. B64, 159 (1957).

5. Bernstein,I.B., Frieman,E.A., Kruskal,M.D. & Kulsrud,R. M., Proc. Roy. Soc. Lond. A244, 17 (1958).

6. Taylor,R.J., Proc. Phys. Soc. B70, 31 (1957).

7. Taylor,R.J., Proc. Phys. Soc. B70, 1049 (1957).

8. Newcomb,W.A., Annals of Physics (N.Y.) 10, 232 (1960).

9. Hain,V.K. & Lust,R., Z. Naturforch. 13a, 936 (1958).

10. Goedbloed, J. P. & Hagebeuk,H.J.I., Phys. Fluids 15, 1090 (1972).

11. Friedberg,J.P., Phys. Fluids 13, 1812 (1970).

12. Kadomtsev, B. B. in Reviews of Plasma Physics,edited by

M. A. Leontovich (Consultants bureau, N. Y.) II, 153 (1966)..

13. Friedberg,J.P., Rev. Mod. Phys. 54, 801 (1982).

14. Haines,M.G., Phys. Scripta T2/2, 380 (1982).

15. Haines,M.G., J. Phys. D: Appl. Phys. 11, 1709 (1978).

16. Struve, K. W. , Ph. D. Thesis, Lawrence Livermore Laboratory, (1980).

17. Choi, P., Dangor,A.E., Folkierski,A., Kahan,E., Potter, D. E. , Slade, P. D. & Webb,S.J., Plasma Physics and Controlled Nuclear Fusion,IAEA,II, 69 (1978).

18. Drake,J.R., Plasma Phys. 26, 387 (1984).

19. Haines, M. G. , Phil. Trans. Roy. Soc. Lond. A300, 649 (1981).

20. Friedberg,J.P., Phys. Fluids 25, 1102 (1972).

21. Coppins,M.,Bond,D.J. & Haines,M.G., J. Plasma phys. 32, 1 (1984).

22. Nycander, J. & Wahlberg, C. , Nucl. Fusion 24, 1357 (1984).

23. Abramowitz, M. & Stegun,I.A., Handbook of Mathematical Functions,Dover Publications, (N.Y.) (1970).

24. Symon, K. R. , Seyler,C.E., Lewis,H.R., J. Plasma Phys. 27, 13 (1982).

25. Lewis, H. R. & Seyler, C. E., J. Plasma Phys. 27, 25 (1982).

26. Lewis, H. R. & Seyler, C. E., J. Plasma Phys. 27, 37 (1982).

27. Batemann, G. in "MHD Instabilities" MIT press (1980).

28. Wilkinson, J. H. & Reinsch, C., Handbook for automatic computation, II, "Linear Algebra", Springer-Verlag (1971).

29. Smith, B.T., Boyle, J.M., Garbow, B.S., Ikebe, Y., Klema, V. C. & Moler, C.B., Lecture notes in Computer Science 6, "Matrix eigensystem Routines- Eispack guide", Springer-Verlag (1974).

30. Conte, S.D. & DeBoor, C., Elementary numerical analysis, McGraw-Hill (1972).

31. Krall, N. A. & Trivelpiece, A.W., Principles of Plasma Physics, McGraw-Hill (1973).

32. Pfeiffer, W. , General Atomic company Report, San Diego, California (Unpublished) (1978).

Figure captions for chapter 3

Fig. (3.1) Plot of Q(x) vs. x for a typical and k.

Fig. (3.2) Plot of γ vs. k: a) Bennett Profile (numerical solution) b) Nycander et al's approximate solution for Bennett profile. c) Nycander et al's approximate solution for a uniform volume current.

Fig. (3.3) Plot of ξ_n vs. r for k=1.1.

Fig. (3.4) Plot of ω_n and γ vs. k .Matrix solution (solid curve).Reduced dispersion relation (dashed curve).

FIg. (3.5) Plot of γ vs. k for V = 1 , 2 and 5.

Fig. (3.6) Plot of ω_n and γ vs. k .Numerical solution (solid curve).Analytical solution (dashed curve).

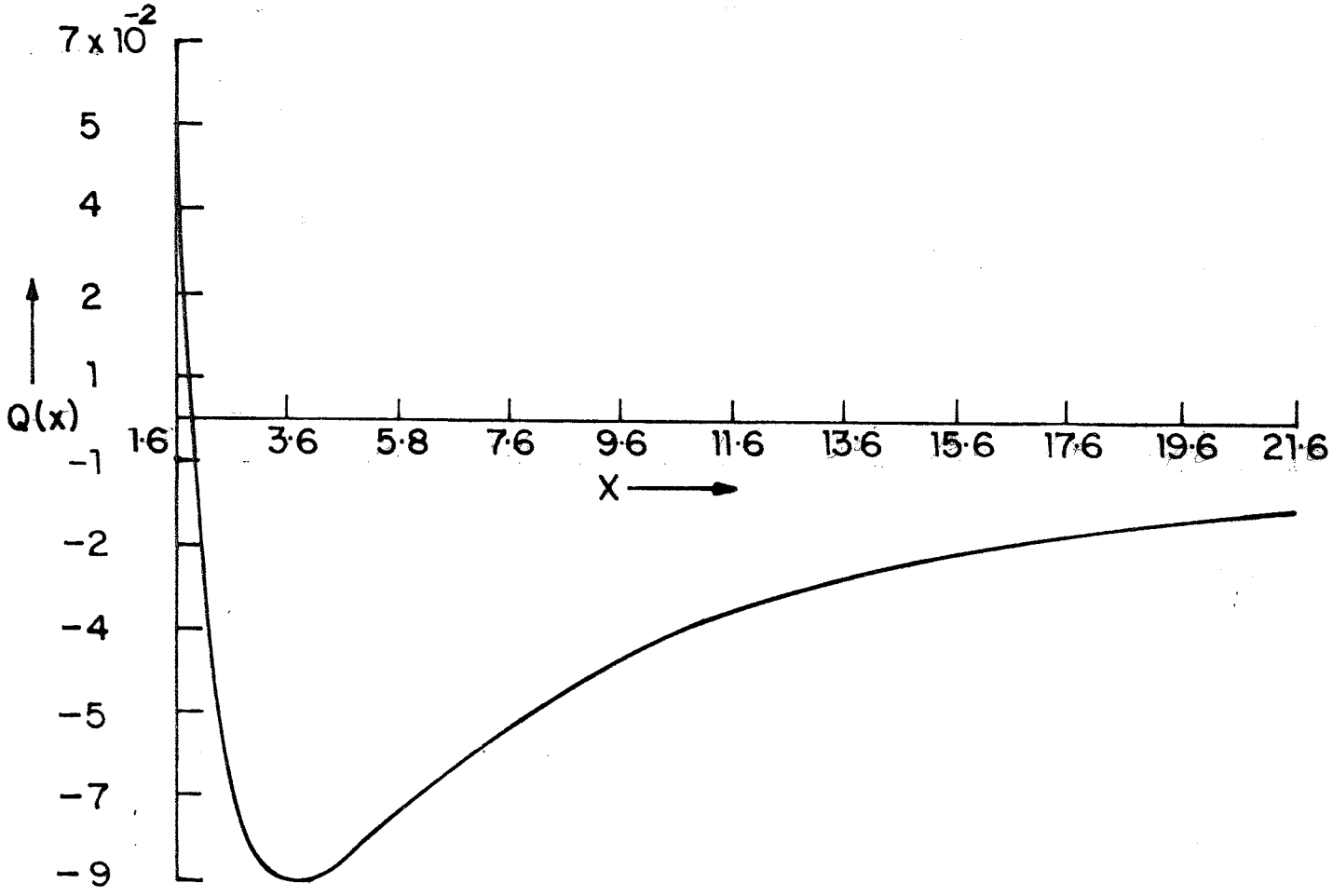

FIG. 3.1

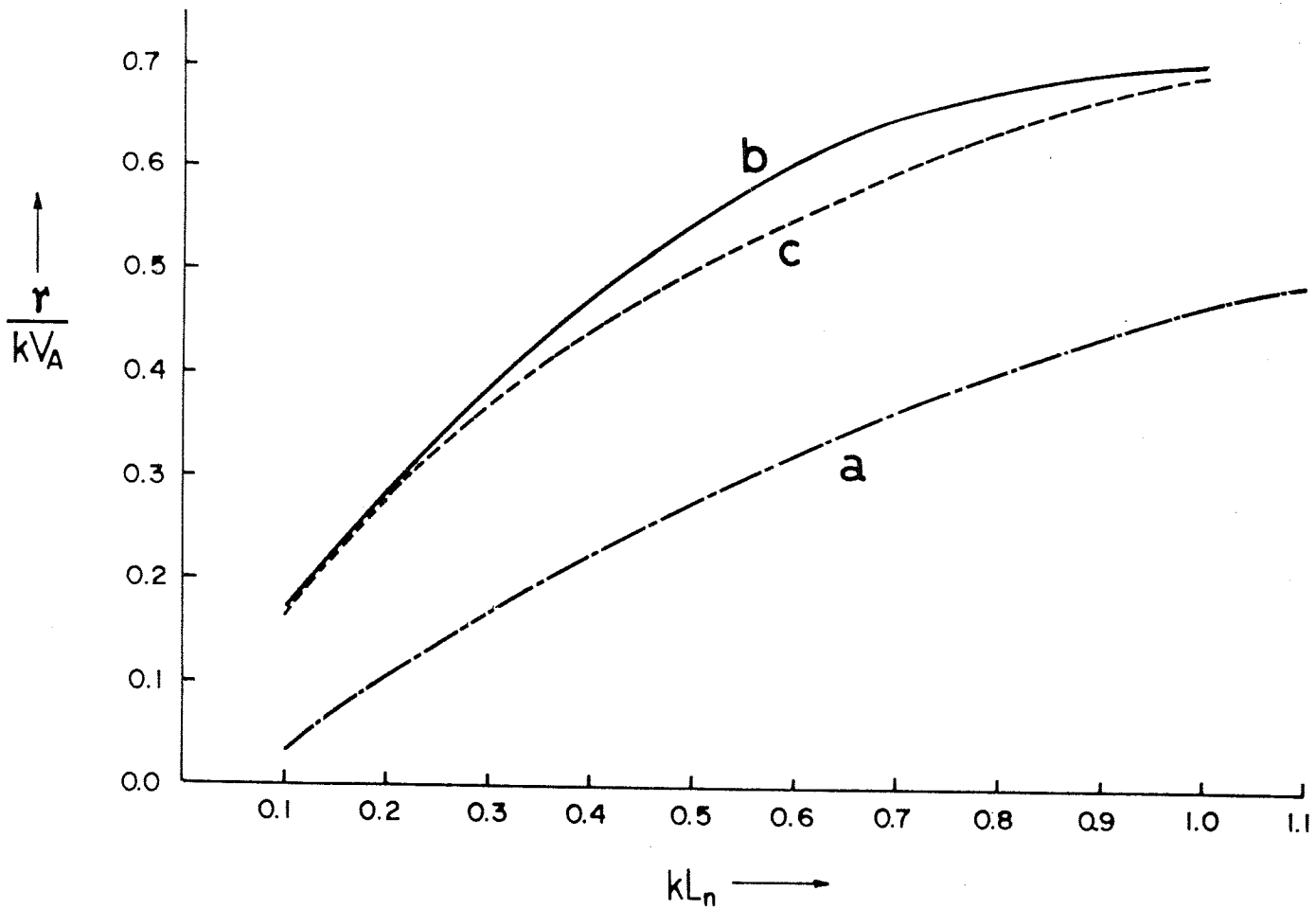

FIG. 3.2

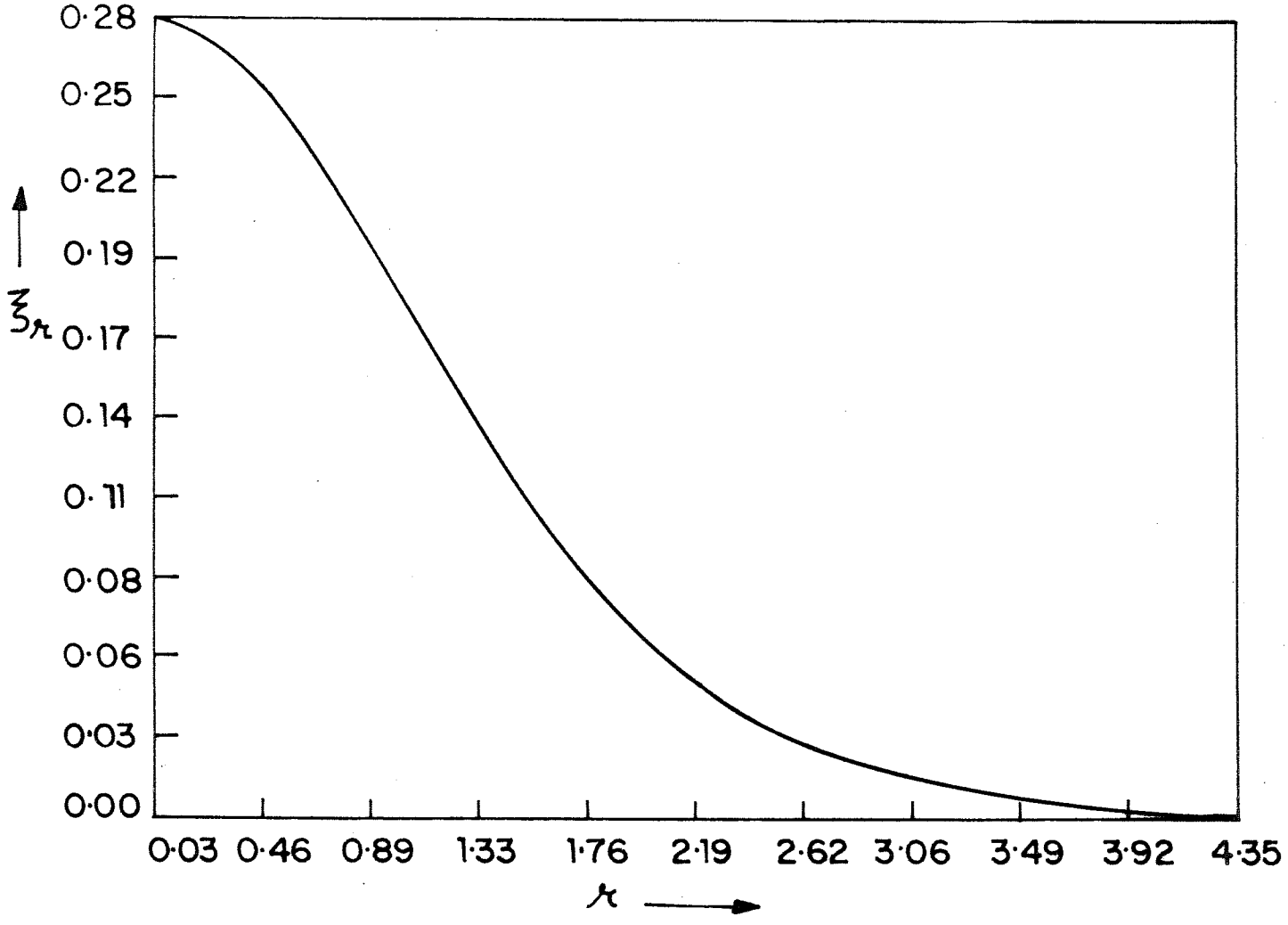
0·28
0·25
0·22
0·19
ξ_r
0·17
0.14
0·11
0·08
0·06
0·03
0·00
0·03 0·46 0·89 1·33 1·76 2·19 2·62 3·06 3·49 3·92 4·35
r

FIG. 3.3

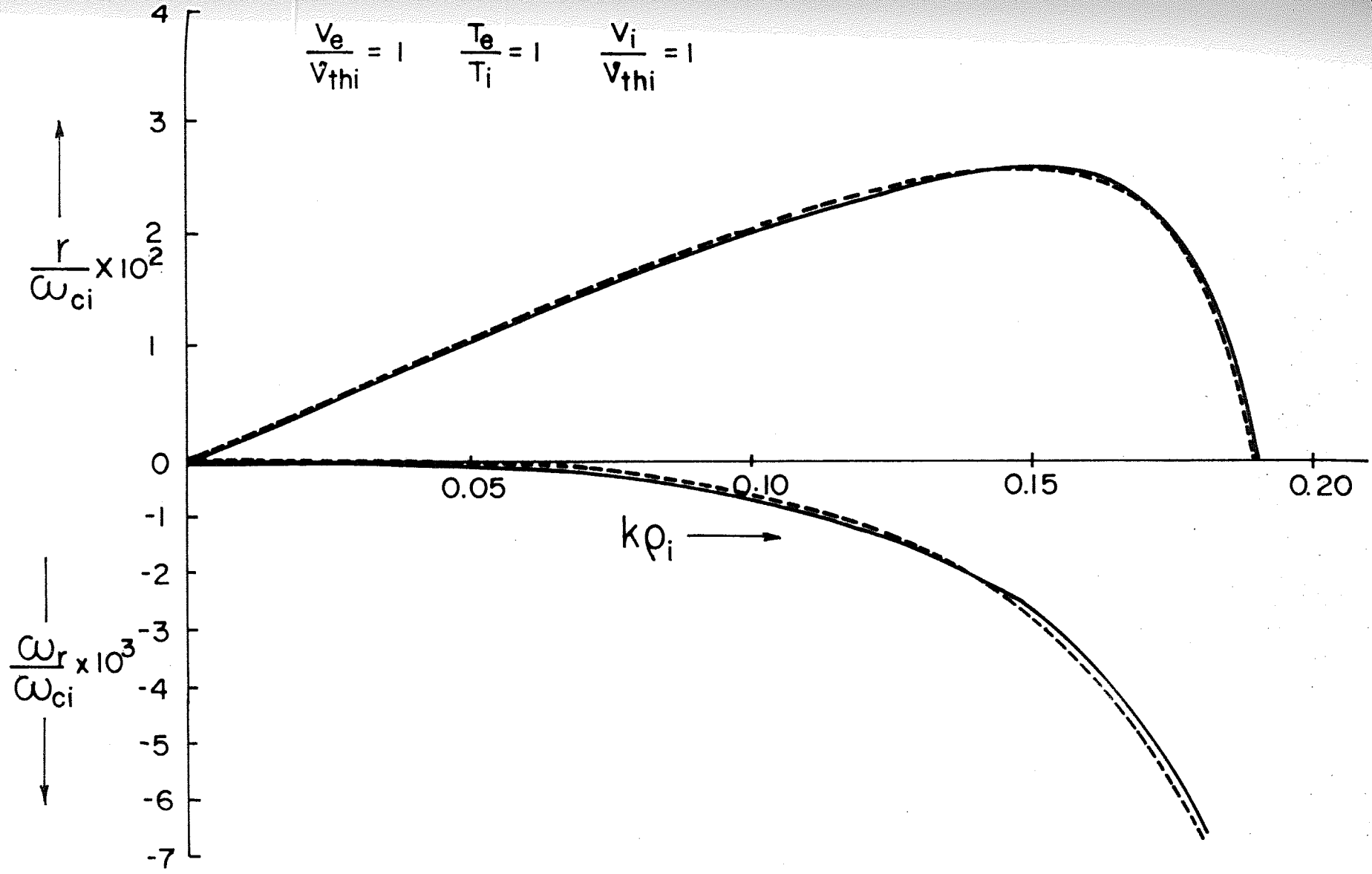
$\frac{V_e}{V_{thi}} = 1$
$\frac{T_e}{T_i} = 1$
$\frac{V_i}{V_{thi}} = 1$
$\frac{r}{\omega_{ci}} \times 10^2$
$\frac{\omega_r}{\omega_{ci}} \times 10^3$
4
3
2
1
0
-1
-2
-3
-4
-5
-6
-7
0.05
0.10
0.15
0.20
$k\rho_i$

FIG. 3.4

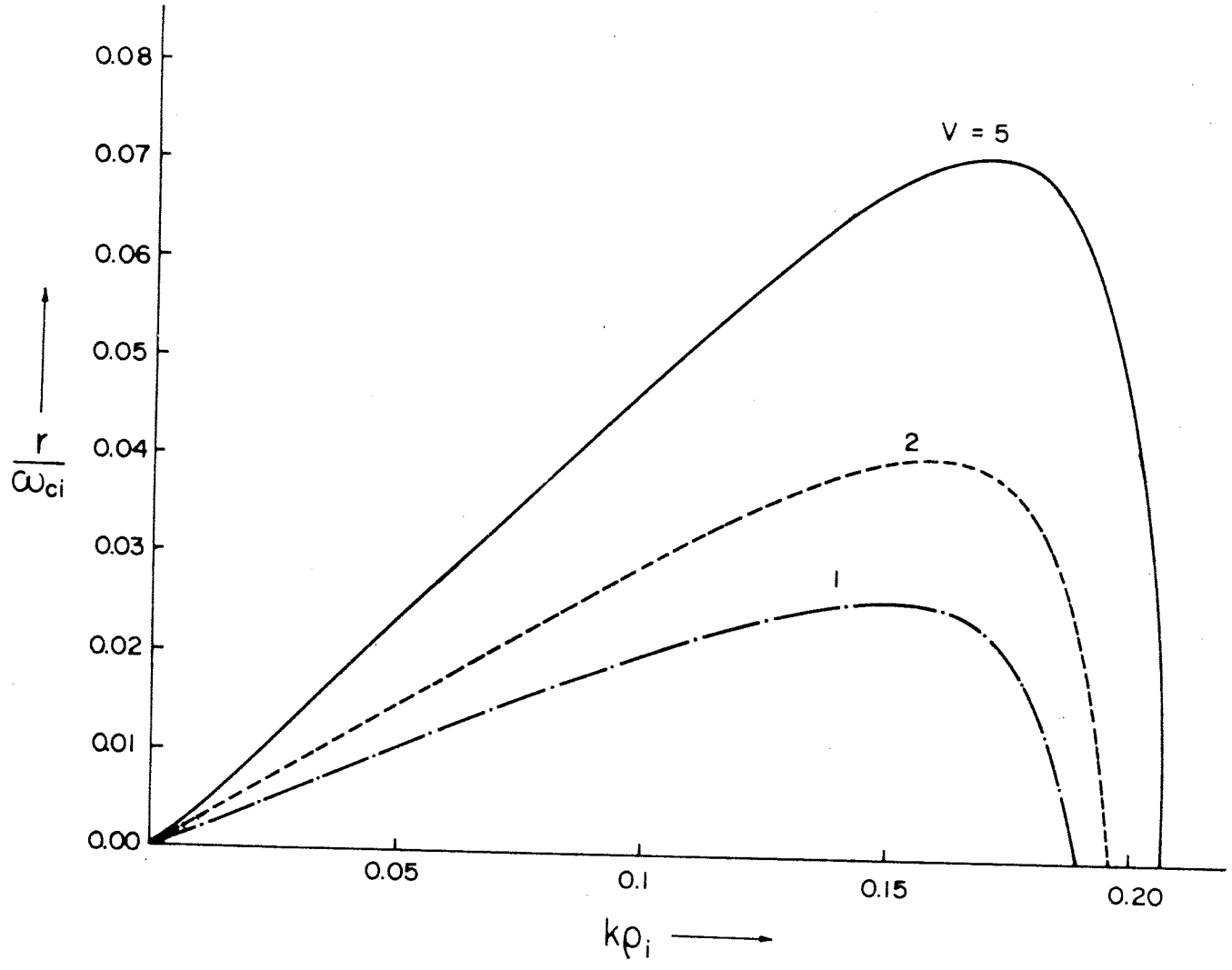

FIG. 3.5

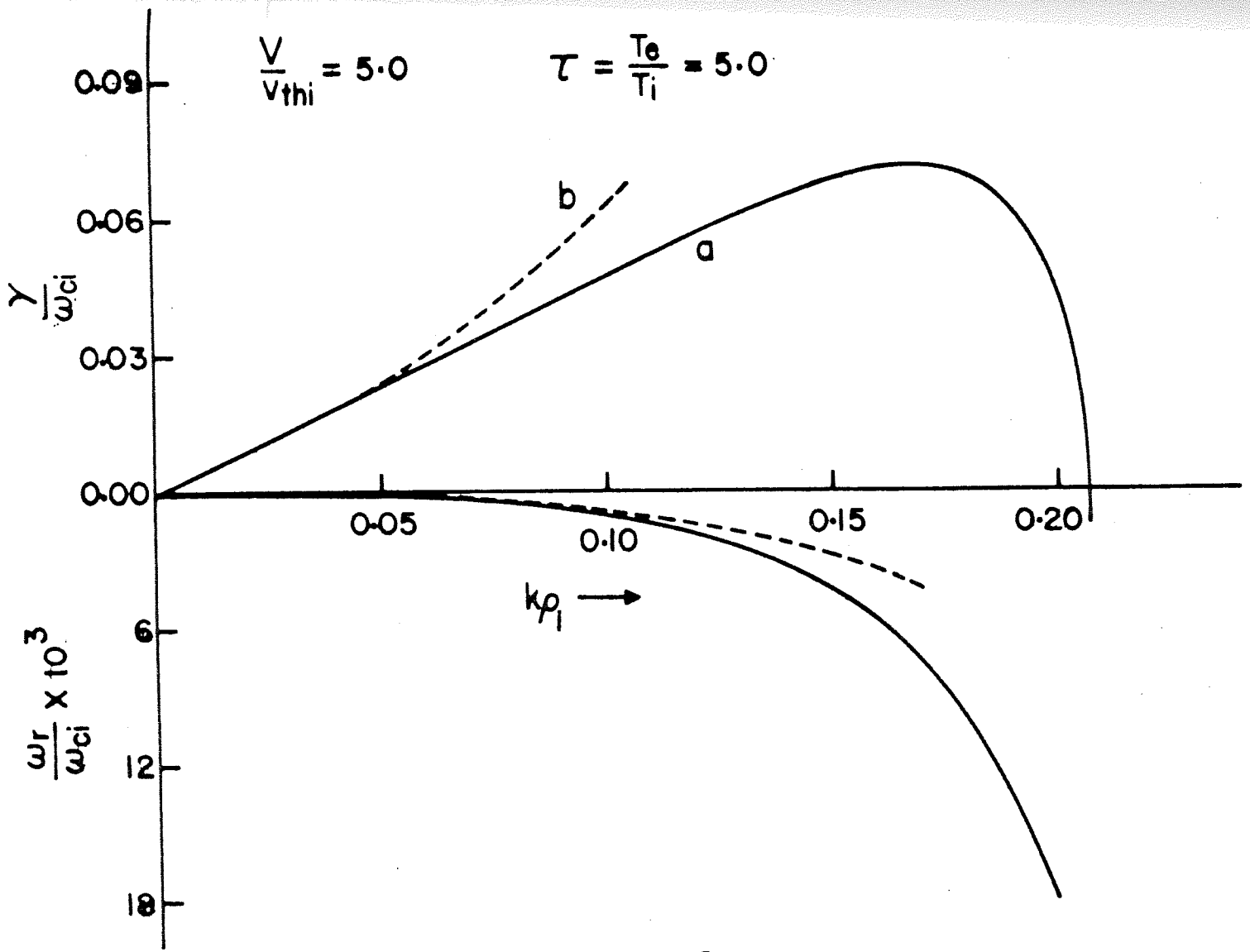
$\frac{V}{V_{thi}} = 5.0$
$\tau = \frac{T_e}{T_i} = 5.0$
0.09
0.06
0.03
0.00
$\frac{\gamma}{\omega_{ci}}$
b
a
0.05
0.10
0.15
0.20
$k\rho_i \rightarrow$
6
12
18
$\frac{\omega_r}{\omega_{ci}} \times 10^3$

FIG. 3.6

Chapter 4

Betatron modified Ion-acoustic instability

4.1 Introduction

The presence of gross MHD modes in the Z-pinch has been known since early times and these are the most dangerous modes for confinement. As a result of these instabilities the earlier pinch configurations were found to be highly unstable. However, recent experiments performed in the low line density pinches reveal remarkable stability [1,2]. This parameter region which corresponds to low line densities and low atomic number is being exploited for the consideration of a Z-pinch reactor [3,4] where stability is attributed to the finite particle orbit effects. Under these conditions it is believed that microinstabilities could play an important role in determining the dynamics of the pinch. Some experiments have reported the observation of microinstabilities in the pinch and the plasma focus in

the later stages of compression [5-8]. These could possibly give rise to turbulence, enhanced resistivity and thereby cause heating and expansion of the pinch. Some of the important microinstabilities which could arise in the pinch are the Buneman, Ion-acoustic, lower hybrid drift instability etc. These have been studied by some workers [9, 10]. Each of these has a specific threshold value for its excitation. The lower hybrid drift instability has a threshold $V_e > V_{thi}$ where V_{thi} is the ion thermal speed. The ion-acoustic instability on the other hand requires $V_e > C_s$, the ion sound speed and $\frac{T_e}{T_i} \gg 1$. The Buneman instability requires $V_e > V_{the}$. This instability is less likely to be excited because the threshold is quite high. In this chapter we have studied this aspect by looking at the electrostatic limit of our general dispersion relation. In the limit $k^2\lambda_D^2 \ll 1$ where k is the wavenumber and λ_D is the Debye length we are able to reduce the matrix dispersion relation to a simple analytic form which makes it possible to clearly understand the various physical processes responsible for the growth or damping of the eigenmodes. We have solved the dispersion relation to obtain a new low frequency electrostatic instability. This instability is in the ion-acoustic range and has characteristics similar to the ion-acoustic instability of a two-component plasma with a relative drift. It is primarily driven by the equilibrium electron drift but has significant modifications from the ion betatron motion. The betatron motion has a stabilizing influence on the mode at long wavelengths and also causes a

shift in the real frequency.

4.2 The electrostatic dispersion relation

For low frequency electrostatic perturbations the system can be described by the linearised Vlasov equation and the Poisson's equation described in chapter 2. A linear perturbation analysis, following the standard procedure outlined earlier and using the non-local approximation to evaluate the orbit integrals leads to a matrix dispersion relation of the form

$$\text{Det}\left[D^{(1)}_{m'm}(\omega, k)\right] = 0 \qquad (4.1)$$

where $D^{(1)}_{n',n}(\omega, k)$ is defined in Chapter 2.

This dispersion relation given by (4.1) is a rather complicated function of ω and k and cannot in general be solved analytically. Its numerical solution is also quite cumbersome, as one has to evaluate a large complex determinant (typically of order 20) over several iterations in the root finding process. The numerical technique for solving the matrix dispersion relation is described in detail in chapter 3. Since each element of the determinant involves evaluation of the plasma dispersion function several times, the numerical calculations are time consuming and prone to cumulative errors. It is also difficult to trace the physical nature of a given root from the complex expression of the determinant.So, although, in

principle, equation (4. 1) represents the complete dispersion relation for linear perturbation of the Bennett equilibrium, it is not a very convenient form for numerical solution or analytical interpretation. We now reduce the matrix dispersion relation to a simpler form in the limit $k^2\lambda_D^2 << 1$.

The matrix $D_{n',n}$ can be written as

$$k_m^2 \delta_{n'm} + \frac{1+\tau}{\lambda_{De}^2(0)} A_{n'm} + \sum_j \frac{(\omega - kV_j)}{\lambda_{Dj}^2(0)} \frac{1}{\sqrt{2}kV_{thj}} \sum_{l,p} Z(\xi_j^{lp}) \, I_{R,l} \, \Gamma_p^j \qquad (4.2)$$

Rewriting the electron and ion terms separately and multiplying with $\lambda_{De}^2(0)$, we have

$$D_{n'm} = k_m^2 \lambda_D^2 \delta_{n'm} + (1+\tau) A_{n'm} + \sum_{l,p} I_{R,l} \left\{ \Gamma_p^e \left(\frac{\omega + kV}{\sqrt{2}kV_{the}} \right) \cdot \right.$$

$$\left. Z\left(\frac{\omega + kV - (m+2l+2p)\omega_{pe}}{\sqrt{2}kV_{the}} \right) + \Gamma_p^i \left(\frac{\omega\tau - kV}{\sqrt{2}kV_{thi}} \right) Z\left(\frac{\omega - kV/c - (m+2l+2p)\omega_{pi}}{\sqrt{2}kV_{thi}} \right) \right\} \qquad (4.3)$$

Here m is the azimuthal mode number. We consider the case m=0 which corresponds to the sausage modes and has no structure in the azimuthal direction. Writing $l + p = \alpha$ and noting that $\Gamma_p^e = \Gamma_p^i = \Gamma_p$, we have

$$D_{n'n} = k_n^2 \lambda_{De}^2 \delta_{n'n} + (1+\tau) A_{n'n} + \sum_{\alpha,\ell} I_{R,\ell}\, \Gamma_{\alpha-\ell}$$

$$\left\{ \frac{\omega + kV}{\sqrt{2}\, k V_{the}}\, Z\left(\frac{\omega + kV - 2\alpha\omega_{pe}}{\sqrt{2}\, k V_{the}}\right) + \left(\frac{\omega\tau - kV}{\sqrt{2}\, k V_{thi}}\right) Z\left(\frac{\omega - kV/\tau - 2\alpha\omega_{pi}}{\sqrt{2}\, k V_{thi}}\right) \right\} \quad (4.4)$$

$$= k_n^2 \lambda_{De}^2 \delta_{n'n} + (1+\tau) A_{n'n} +$$

$$\sum_{\alpha} P_{n'n}^{(\alpha)} \left\{ \frac{\omega + kV}{\sqrt{2}\, k V_{the}}\, Z(\zeta_e^{\alpha}) + \frac{\omega\tau - kV}{\sqrt{2}\, k V_{thi}}\, Z(\zeta_i^{\alpha}) \right\} \quad (4.5)$$

where

$$P_{n'n}^{(\alpha)} = \sum_{\ell} I_{R\ell}\, \Gamma_{\alpha-\ell} \quad (4.6)$$

and

$$\zeta_{\alpha}^{e} = \left(\frac{\omega + kV - 2\alpha\omega_{pe}}{\sqrt{2}\, k V_{the}}\right)$$

$$\zeta_{\alpha}^{i} = \left(\frac{\omega - kV/\tau - 2\omega_{pi}\alpha}{\sqrt{2}\, k V_{thi}}\right) \quad (4.7)$$

Substituting for $I_{R\ell}$ in eq.(4.6) we have

$$P_{n'n}^{(\alpha)} = \sum_{\ell} A_n \int_0^{R_c} \frac{(-1)^{\ell}\, r\, \phi_{n'}\, J_{\ell}^2\left(\frac{\lambda_n r}{2}\right) \Gamma_{\alpha-\ell}}{\left(1 + \frac{1}{4} k^2 r^2\right)^2}$$

Changing 1 to -1 we have

$$P_{n'n}^{(2\alpha)} = \sum_{l} A_n \int_0^{R_0} \frac{(-1)^l r \phi_{n'} J_l^2\left(\frac{\lambda_{n'} r}{2}\right) \Gamma_{\alpha+l}}{\left(1+\frac{1}{4}k^2 r^2\right)^2}$$

$$= P_{n'n}^{(-2\alpha)} \qquad (4.8)$$

Therefore we can write (4.5) as

$$D_{n'n} = k_n^2 \lambda_{De}^2 \delta_{n'n} + (1+\tau) A_{n'n} +$$

$$P_{n'n}^{(0)} \left\{ \frac{\omega+kV}{\sqrt{2}kV_{the}} Z(\zeta_e^0) + \frac{\omega\tau - kV}{\sqrt{2}kV_{thi}} Z(\zeta_i^0) \right\}$$

$$+ \sum_{\alpha=1}^{\infty} \left\{ \frac{\omega+kV}{\sqrt{2}kV_{the}} \left\{ Z\left(\frac{\omega+kV-2\omega_{pe}\alpha}{\sqrt{2}kV_{the}}\right) + Z\left(\frac{\omega+kV+2\omega_{pe}\alpha}{\sqrt{2}kV_{the}}\right) \right\} \right.$$

$$\left. + \frac{\omega\tau - kV}{\sqrt{2}kV_{thi}} \left\{ Z\left(\frac{\omega - kV/\tau - 2\alpha\omega_{pi}}{\sqrt{2}kV_{thi}}\right) + Z\left(\frac{\omega - kV/\tau + 2\alpha\omega_{pi}}{\sqrt{2}kV_{thi}}\right) \right\} \right\}$$

$$= k_n^2 \lambda_{De}^2 \delta_{n'n} + (1+\tau) A_{n'n} + P_{n'n}^{(0)} g_0 + \sum_{\alpha=1}^{\infty} P_{n'n}^{(2\alpha)} g_\alpha \qquad (4.9)$$

where

$$g_0 = \zeta_e^0 Z(\zeta_e^0) + \tau \zeta_i^0 Z(\zeta_i^0) \qquad (4.10)$$

and

$$g_\alpha = \zeta_e^0 \left\{ Z(\zeta_e^\alpha) + Z(\zeta_e^{-\alpha}) \right\}$$

$$+ \tau \zeta_i^0 \left\{ Z(\zeta_i^{\alpha}) + Z(\zeta_i^{-\alpha}) \right\} \qquad (4.11)$$

We shall now show that the matrices $\overset{to}{A}_{n'n}$ and $P_{n'n}^{(2\alpha)}$ are related to each other:

We have

$$A_{n'n} = A_{n'} A_n \int_0^{Rc} \frac{dr\, r\, J_0(\lambda_{n'} r)\, J_0(\lambda_n r)}{\left(1+\frac{1}{4}K^2 r^2\right)^2}$$

$$= A_{n'} A_n \int_0^{Rc} \frac{dr\, r\, J_0(\lambda_{n'} r) \sum_l (-1)^l J_l^2\left(\frac{\lambda_n r}{2}\right)}{\left(1+\frac{1}{4}K^2 r^2\right)^2}$$

$$= \sum_{l,\alpha} (-1)^l A_{n'} A_n \int_0^{Rc} \frac{dr\, r\, J_0(\lambda_{n'} r)\, J_l^2\left(\frac{\lambda_n r}{2}\right) \Gamma_{l+\alpha}(\zeta_n)}{\left(1+\frac{1}{4}K^2 r^2\right)^2}$$

$$= P_{n'n}^{(0)} + 2 \sum_{\alpha=1}^{\infty} P_{n'n}^{(2\alpha)} \qquad (4.12)$$

In deriving the above equation we have made use of the following two Bessel function identities [11]

$$J_n(x) = \sum_m J_{n-m}\left(\frac{x}{2}\right) J_m\left(\frac{x}{2}\right) \qquad (4.13)$$

and

$$e^x = I_0(x) + 2 \sum_{p=1}^{\infty} I_p(x) \qquad (4.14)$$

Using equation (4. 12) we can now write down more compactly as:

$$D_{n'm}(\omega,k) = k_m^2 \lambda_{De}^2 \delta_{n'm} + f_0(\omega) P^{(0)}_{n'm} + \sum_\alpha f_\alpha(\omega,k) P^{(2\alpha)}_{n'm} \qquad (4.15)$$

where

$$f_0 = 1+\tau + g_0 \qquad (4.16)$$

and

$$f_\alpha = 2(1+\tau) + g_\alpha \qquad (4.17)$$

In equation (4. 15) it is easier to understand the physical significance of each term. The first term $k_m^2 \lambda_D^2$ arises from the departure from charge neutrality for the perturbations and is the usual dispersive contribution from Poisson's equation. The term $f_0(\omega)$ represents the homogeneous plasma contribution in the absence of the magnetic field, but includes the contribution from the equilibrium axial drifts. The term f_α contains the effect of the self- magnetic field and displays the contribution from betatron orbits. The constant coefficient matrices $P_{n'm}$ are a manifestation of the non-local character of the stability analysis and arise from the inhomogeneity and large excursion lengths of the particle orbits.

If we now consider the limit of low frequency

perturbations in the range $\omega \lesssim \omega_{\beta i}$ then the α-summation in equation (4.12) can be truncated at $\alpha = 1$. If the number of terms in the expansion for $\phi(r)$ is not too large and $k_m^2 \lambda_D^2 << 1$ we can approximate matrix $D_{m'm}$ by the simple form

$$D_{m'm} \simeq f_0 P^{(0)}_{m'm} + f_1 P^{(2)}_{m'm} \qquad (4.18)$$

The dispersion relation (4.1) can now be expressed as

$$\text{Det} \left| f_0 P^{(0)}_{m'm} + f_1 P^{(2)}_{m'm} \right| = 0$$

i.e.

$$\left| f(\omega) \delta_{m',m} + P_0^{-1} . P_2 \right| = 0 \qquad (4.19)$$

where

$$f(\omega) = \frac{f_0(\omega)}{f_1(\omega)}$$

Here we have assumed that $f_1(\omega) \neq 0$ and the determinant of the matrix $\left| P^{(0)}_{m'm} \right| \neq 0$ so that its inverse is defined. The matrices P_0 and P_2 are constant matrices independent of ω and k and depend only on the scale length of the inhomogeneity, in the equilibrium. The equation (4.19) can be compared with the characteristic equation of the real matrix $P_0^{-1} . P_2$, namely:

$$\left| P_0^{-1} . P_2 - \mu_i \hat{I} \right| = 0 \qquad (4.20)$$

The eigenvalues μ_i are a set of constant numbers and can be evaluated numerically. Thus we can now write the dispersion relation as

$$f(\omega) = -\mu_i$$

or

$$f_0(\omega) + \mu_i f_1(\omega) = 0 \qquad (4.21)$$

Equation (4.21) is the reduced dispersion relation with μ_i a constant number typically of the order unity. The numerical solution of equation (4.21) is much simpler than the solution of eqn.(4.1) and it is also possible to obtain approximate analytic solutions of equation (4. 21) in limiting cases. These solutions help us to understand the physical nature of the instability and the role played by the betatron motion. We shall present the solutions to equation (4.21) in the next section.

4.3 Numerical and analytical solutions

We have carried out a detailed numerical investigation of equation (4.21) in order to obtain unstable solutions of the dispersion relation in the complex ω-plane. Basically we find only one type of unstable mode which is in the low-frequency range and whose characteristics are similar to the ion-acoustic instability of a two component plasma with a relative drift. Figure (4.1) is a typical plot of the growth rate γ and real frequency ω_r versus the wavenumber for a typical set of parameters. The mode is found to be stable for very small as well as very large wavenumbers k. The range of k for which the mode is unstable increases with increasing value of the electron drift V_e. This is shown in Figure (4.2) where the growth rate is plotted as a function of k for different values of the electron drift. There is a threshold velocity for the electrons below which the mode is stable for all wavenumbers. This threshold velocity is around $V_e \gtrsim 6$ in units of the ion thermal speed. Further, it is found that only modes propagating in the direction of electron drift ($\omega_r/k < 0$) are unstable. The plot of real frequency ω_r versus k shows that at large wavenumbers the frequency ω_r goes as $-kC_s$ where C_s is the ion-acoustic speed; however at small k, there is a significant departure from the ion-acoustic frequency. This is a modification arising from

the betatron motion of the ions and the shift is found to be proportional to the ion betatron frequency. The instability threshold ($k > k_c$) is also higher than the usual ion-acoustic instability threshold ($V_e > C_s$), which indicates a stabilizing influence on the ion betatron motion at long wavelengths.

Figs. (4.3a, b, & c) show a plot of γ versus k obtained by solving the dispersion relation (4.21) numerically for three different values of μ_i, but for a fixed value of the electron drift V_e. It is seen that as μ_i is increased, the range of unstable wavenumbers as well as the wavenumber corresponding to maximum growth shift to the right, and the width of the unstable spectrum increases. The magnitude of maximum growth rate increases only by a small amount.

We can understand the abovementioned results more quantitatively by obtaining an approximate analytic solution of equation (4.21) in the appropriate limits. We look for solutions to the dispersion relation in the frequency domain $|\omega\tau - kV| \gg kV_{thi}$ and $|\omega + kV| \ll kV_{the}$ and $\tau >> 1$ which is typical of the ion-acoustic range in plasmas. Making the approximate expansions of the plasma dispersion functions we have

$$Z\left(\frac{\omega + kV}{\sqrt{2}kV_e}\right) \simeq i\sqrt{\pi} - \frac{2(\omega + kV)}{\sqrt{2}kV_{the}}$$

$$Z\left(\frac{\omega\tau - kV}{\sqrt{2}kV_{thi}}\right) \simeq -\left\{\frac{\sqrt{2}kV_{thi}\tau}{\omega\tau - kV} + \frac{1}{2}\left(\frac{\sqrt{2}kV_{thi}\tau}{\omega\tau - kV}\right)^3\right\} + i\sqrt{\pi}$$

$$\exp -\frac{(\omega\tau - kV)^2}{2k^2\tau^2 V_{thi}^2}$$

$$Z\left(\frac{\omega\tau - kV \pm 2\omega_{\beta i}\tau}{\sqrt{2}kV_{thi}}\right) \simeq \frac{-\sqrt{2}kV_{thi}\tau}{\omega\tau - kV \pm 2\tau\omega_{\beta i}} + i\sqrt{\pi}\exp\left(\frac{\omega\tau - kV - 2\omega_{\beta i}\tau}{\sqrt{2}kV_{thi}\tau}\right)^2 \quad (4.22)$$

Substituting these expansions in $f_0(\omega)$ and $f_1(\omega)$ we can write equation (4.21) as

$$(1+\tau)(1+2\mu_i) + \frac{\omega+kV}{\sqrt{2}kV_{the}}\left(i\sqrt{\pi} - \frac{2(\omega+kV)}{\sqrt{2}kV_{the}}\right) - \frac{\omega\tau - kV}{\sqrt{2}kV_{thi}}\left[\left\{\frac{\sqrt{2}kV_{thi}\tau}{\omega\tau - kV} + \frac{1}{2}\left(\frac{\sqrt{2}kV_{thi}\tau}{\omega\tau - kV}\right)^3 + i\sqrt{\pi}\exp -\left(\frac{\omega\tau - kV}{\sqrt{2}kV_{thi}\tau}\right)^2\right\} + \frac{\sqrt{2}kV_{thi}\tau}{\omega\tau - kV + 2\omega_{\beta i}\tau} + \frac{\sqrt{2}kV_{thi}\tau}{\omega\tau - kV - 2\omega_{\beta i}\tau}\right.$$

$$\left. + i\sqrt{\pi}\left\{\exp -\left(\frac{\omega\tau - kV + 2\omega_{\beta i}\tau}{\sqrt{2}kV_{thi}}\right)^2 + \exp -\left(\frac{\omega\tau - kV - 2\omega_{\beta i}\tau}{\sqrt{2}kV_{thi}}\right)^2\right\}\right] = 0$$

Here we have neglected the electron betatron term in $f_1(\omega)$ because it will have a contribution of order $\omega/\omega_{\beta e}$ which is negligibly small. Rearranging the terms above we obtain

$$(1+\tau)(1+2\mu_i) + i\sqrt{\pi}\left(\frac{\omega+kV}{\sqrt{2}kV_{the}}\right) - \left(\frac{\omega+kV}{kV_{the}}\right)^2 - \tau - \frac{k^2\tau^3 V_{thi}^2}{(\omega\tau - kV)^2}$$

$$- \frac{2\tau\mu_i(\omega\tau - kV)^2}{(\omega\tau - kV)^2 - 4\omega_{\beta i}^2\tau^2} + i\sqrt{\pi}\frac{\omega\tau - kV}{\sqrt{2}kV_{thi}}\left\{e^{-S_i^2} + \mu_i\left(e^{-S_i^{-2}} + e^{-S_i^{+2}}\right)\right\}$$

or $$1 + 2\mu_i + 2\mu_i\tau - \frac{2\mu_i\tau(\omega\tau - kV)^2}{(\omega\tau - kV)^2 - 4\omega_{\beta i}^2\tau^2} - \frac{k^2V_{thi}^2\tau^3}{(\omega\tau - kV)^2}$$

$$+ i\sqrt{\pi}\left\{\frac{\omega+kV}{\sqrt{2}kV_{the}} + \frac{\omega\tau-kV}{\sqrt{2}kV_{thi}}\left(e^{-\zeta_i^{-2}} + \mu_i\left(e^{-\zeta_i^{-2}} + e^{-\zeta_i^{+2}}\right)\right)\right\}$$

$$= 0.$$

or

$$1+2\mu_i - \frac{8\mu_i\tau^3\omega_{pi}^2}{(\omega\tau-kV)^2 - 4\omega_{pi}^2\tau^2} - \frac{k^2\tau^2c_s^2}{(\omega\tau-kV)^2}$$

$$+ i\sqrt{\pi}\left\{\frac{\omega\tau-kV}{\sqrt{2}kV_{thi}}\left(e^{-\zeta_i^{2}} + \mu_i\left(e^{-\zeta_i^{-2}} + e^{-\zeta_i^{+2}}\right)\right) + \left(\frac{\omega+kV}{\sqrt{2}kV_{the}}\right)\right\} = 0 \quad (4.23)$$

where $c_s = \tau^{1/2}V_{thi}$ is the ion-acoustic speed.

This equation can be solved perturbatively as follows: We write $\omega = \omega_r + i\gamma$ and assume that $\omega_r >> \gamma$. Substituting in (4.23), we have

$$(1+2\mu_i) - \frac{8\mu_i\tau^3\omega_{pi}^2}{(\omega_r\tau-kV)^2 - 4\omega_{pi}^2\tau^2 + 2i\gamma\tau(\omega_r\tau-kV)} + i\sqrt{\pi}\left(\frac{\omega+kV}{\sqrt{2}kV_e}\right)$$

$$- \frac{k^2c_s^2}{\left(\omega_r - \frac{kV}{\tau}\right)^2 + 2i\gamma\left(\omega_r - \frac{kV}{\tau}\right)} + i\sqrt{\pi}\frac{(\omega_r\tau-kV)}{\sqrt{2}kV_{thi}}\left\{e^{-\zeta_i^{2}} + \right.$$

$$\left.\mu_i\left(e^{-\zeta_i^{-2}} + e^{-\zeta_i^{+2}}\right)\right\} = 0$$

$$\Rightarrow (1+2\mu_i) \neq -\frac{8\lambda\tau\omega_{pi}^2}{(\omega_r - kV/\tau)^2 - 4\omega_{pi}^2}\left(1 - \frac{2i\gamma\left(\omega_r - kV/\tau\right)}{(\omega_r - kV/\tau)^2 - 4\omega_{pi}^2}\right)$$

$$-\frac{k^2 c_s^2}{\left(\omega_r - kV/\tau\right)^2}\left(1 - \frac{2i\gamma}{\omega_r - kV/\tau}\right) + \sqrt{\pi}\left[\frac{\omega_r\tau - kV}{\sqrt{2}kV_{thi}}\left(e^{-\zeta_i^2} + \mu_i e^{-\zeta_i^{\pm 2}}\right) + \frac{\omega_r + kV}{\sqrt{2}kV_{the}}\right] \qquad (4.24)$$

Taking the real and imaginary parts of equation (4.24) we have

$$\left(1 + 2\mu_i\right) - \frac{8\mu_i\tau\omega_{pi}^2}{\left(\omega_r - \frac{kV}{\tau}\right)^2 - 4\omega_{pi}^2} - \frac{k^2 c_s^2}{\left(\omega_r - kV/\tau\right)^2} = 0 \qquad (4.25)$$

and

$$\frac{16\mu_i\tau\omega_{pi}^2\,\gamma\left(\omega_r - kV/\tau\right)}{\left\{\left(\omega_r - \frac{kV}{\tau}\right)^2 - 4\omega_{pi}^2\right\}^2} + \frac{2\gamma k^2 c_s^2}{\left(\omega_r - kV/\tau\right)^2} + \sqrt{\frac{\pi}{2}}\frac{\omega_r + kV}{kV_{the}}$$

$$\sqrt{\frac{\pi}{2}}\left[\frac{\omega_r\tau - kV}{kV_{thi}}\left(e^{-\zeta_i^2} + \mu_i e^{-\zeta_i^{\pm 2}}\right)\right] = 0 \qquad (4.26)$$

From (4.25) the solution for ω_r is given by

$$\left(\omega_r - \frac{kV}{\tau}\right)^2 = \left[k^2 c_s^2 + 8\mu_i\omega_{pi}^2 + 4\left(1+2\mu_i\right)\omega_{pi}^2 \pm \sqrt{\left\{k^2 c_s^2 + 8\mu_i\tau\omega_{pi}^2 + 4\left(1+2\mu_i\right)\omega_{pi}^2\right\}^2 - 16k^2 c_s^2\omega_{pi}^2\left(1+2\mu_i\right)}\right] \times \left\{2\left(1+2\mu_i\right)\right\}^{-1} \qquad (4.27)$$

The corresponding growth rate γ is given by

$$\gamma = \sqrt{\frac{\Delta}{8}} \; \frac{\frac{\omega_r + kV}{kV_{the}} + \frac{\omega_r \tau - kV}{kV_{thi}} \left(e^{-\zeta_i^2} + \lambda e^{-\zeta_i^{+2}} \right)}{\frac{k^2 c_s^2}{\left(\omega_r - \frac{kV}{\tau}\right)^3} + \frac{8\lambda\tau\omega_{pi}^2 \left(\omega_r - kV/\tau\right)}{\left(\omega_r - kV/\tau\right)^2 - 4\omega_{pi}^2}} \qquad (4.28)$$

The solution for ω_r can be approximated as

$$\omega_r \simeq \frac{kV}{\tau} \pm \sqrt{\frac{k^2 c_s^2 + 8\mu_i \tau \omega_{pi}^2}{1+2\mu_i}}$$

$$\simeq \pm \omega_{pi} \sqrt{\frac{8\mu_i \tau}{1+2\mu_i}} \qquad \text{at small k}$$

and

$$kV/\tau \pm \frac{k c_s}{(1+2\mu_i)^{1/2}} \qquad \text{at large k} \qquad (4.29)$$

From equation (4. 29) we see the behaviour of the real frequency in low k and high k regions; this is basically the ion-acoustic mode modified by the ion betatron frequency. The values of ω_r and γ obtained from (4.27) and (4. 28) for typical values of the equilibrium parameters are plotted in Fig. (4.1) and are shown by the dashed curves along with the corresponding numerical solutions of the full dispersion relation (solid curves) It is found that the two are in fair agreement. From equation (4.28) we see

that the mode with negative sign in equation (4.27) is the unstable mode and the instability arises from the electron Landau damping term, which is proportional to $\frac{\omega_r + kV}{kV_{the}}$. The threshold at low k is therefore given by the condition $kv > \omega_r$ which using equation (4.29) for ω_r leads to

$$V > \frac{\omega_{pi}}{k}\sqrt{\frac{8\mu_i\tau}{1+2\mu_i}} \qquad (4.30)$$

This agrees quite well with numerical results. We find that this threshold is higher than C_s which is the usual threshold for the ion-acoustic instability, indicating the stabilizing influence of the ion betatron motion for large wavelength modes.

The stability of the mode at the higher k-values arises from the usual ion Landau damping term i.e. exponential terms in (4. 28); however, it is difficult to obtain a quantitative measure of this upper threshold because of the transcendental nature of the dispersion relation.

4.4 Discussion

We have investigated the kinetic stability of the Bennett equilibrium for low frequency electrostatic perturbations. The analysis is based on the integral formulation which provides a rigorous framework for dealing with inhomogeneous bounded plasmas whose particle trajectories have large excursion lengths, comparable to their radial positions. In the limit $k_n^2 \lambda_D^2 \ll 1$ and with a finite number of terms in the eigenfunction expansion we are able to obtain a simple expression for the dispersion relation, which is convenient for both analytical and numerical computations. We have numerically computed the eigenvalue spectrum for various equilibrium parameters. We find that the Bennett equilibrium has a low-frequency instability that is primarily driven by the electron drift motion. The instability occurs above a minimum threshold value $V > 6V_{thi}$ (in physical units). The mode characteristics of the instability are very similar to the ion-acoustic mode. At small wavenumbers, there is a significant shift in the real frequency, brought about by the ion betatron motion, and thus has a stabilizing effect on the mode.

Our calculations are pertinent to various experimental situations where the Bennett profile provides a close description of the plasma equilibrium e.g. the Z-pinches, Extrap configuration, plasma focus,etc. Ion-acoustic type

turbulence phenomena have been mentioned earlier with reference to observations of density fluctuations in various plasma focus experiments [5-8,12]. However, there has been no realistic identification of these fluctuations. On the basis of conventional slab geometry and Larmor orbit theory estimates, the fluctuations are assumed to have their origin in current driven ion-acoustic instability,or electron cyclotron drift instability or lower hybrid drift instability [10]. We can examine these data in the light of our present theory which takes into account some of the specific features of the Bennett pinch, namely,the large orbits of the particles due to the self consistent confining fields, the cylindrical geometry etc. We note in particular that the average electron drifts reported in these experiments are typically $V \quad V_{thi}$ [6-8] and $V \sim 2.1$ V_{thi} [12] which is well below the threshold value predicted by our theory. Consequently, the observed density fluctuations are unlikely to be due to the ion-acoustic instability. It is interesting to note that even in fusion reactor scenario bases on the Bennett equilibrium of the burning plasma [3, 4, 13] the electron drift would be well below the threshold, since the ion temperatures are estimated to be a few tens of kilo electron volts, whereas the plasma current would be typically the Pease limiting current i.e. 1.35 MA [14]. However, during the current rise phase when the current flows mostly on the outside and the densities are low,the average drift may become large enough to excite the ion-acoustic waves.In the equilibrium pinch

stage also, if the thermal conductivity is high and viscosity is low, the average drift on the outside can become very large [14]. In such situations ion-acoustic turbulence would develop and would contribute to anomalous plasma transport processes.

References

1. Haines,M.G., Phys. Scripta T2/2, 380 (1982).

2. Struve, K. W. , Ph. D. Thesis, Lawrence Livermore Laboratory, (1980).

3. Hartman,C.W., Carlson,G., Hoffman,M., Werner,R.& Cheng, D.Y., Nucl.Fusion 17, 909 (1977).

4. Hagenson, R. L., Tai,A.S., Krakowski,R.A. & Moses,R.W., Nucl. Fusion 21,1351 (1981).

5. Sethian, J. D., Gerber,K.A., Robson,A.E., DeSilva,A.W., Hammel, J. E., Scudder,D.W. & Schlachter,J.S., in Proc. of the tenth International conference on Plasma Physics and Controlled Nuclear Fusion research II, IAEA-CN- 44/D-IV-2, (1984).

6. Bernard, A. , Coudeville,A., Jolas,A., Launspach,J. & DeMascureau,J.,Phys. Fluids 18, 180 (1975).

7. Bernard, A. , Garconnet,J.P., Jolas,A., LeBreton,J.P. & DeMascureau, J. , in Plasma Physics and controlled Nuclear Fusion research,IAEA, II,159 (1979).

8. Haines, M. G. , Phil. Trans. Roy. Soc. Lond. A300, 649 (1981).

9. Liewer,P.C. & Krall,N.A., Phys. Fluids 16, 1953 (1973).

10. Vikhrev, V.V. & Korzhavin,V.M., Sov. J. Plasma Phys. 4, 411 (1978).

11. Abramowitz, A. & Stegun,I.A., Handbook of Mathematical Functions,Dover,N.Y. (1970).

12. Kirk, R. E., Forrest,M.J., Muir,D.G. & Peacock,N.J., in Plasma Focus Research (Proc. of the third Int. workshop, Stuttgart) 119 (1983).

13. Hammel, J. E. , Scudder,D.W. & Schlachter,J.S., Recent results on the dense Z-pinch, Los Alamos National Lab. Rep. LA-UR-82-1494 (1982).

14. Pease,R.S., Proc. Phys. Soc. 70, 11 (1957).

Figure captions for chapter 4

Fig. (4. 1) Plot of ω_n and γ vs. k . a) Solid curve (numerical solution) b) Dashed curve (analytic solution).

Fig. (4.2) Plot of γ vs. k for different values of V.

Figs. (4. 3) Plot of γ vs. k different values of μ_i.
a) μ_i = (.9907,.006) b) μ_i = (.6679,0.) c) μ_i = (.4999,0.).

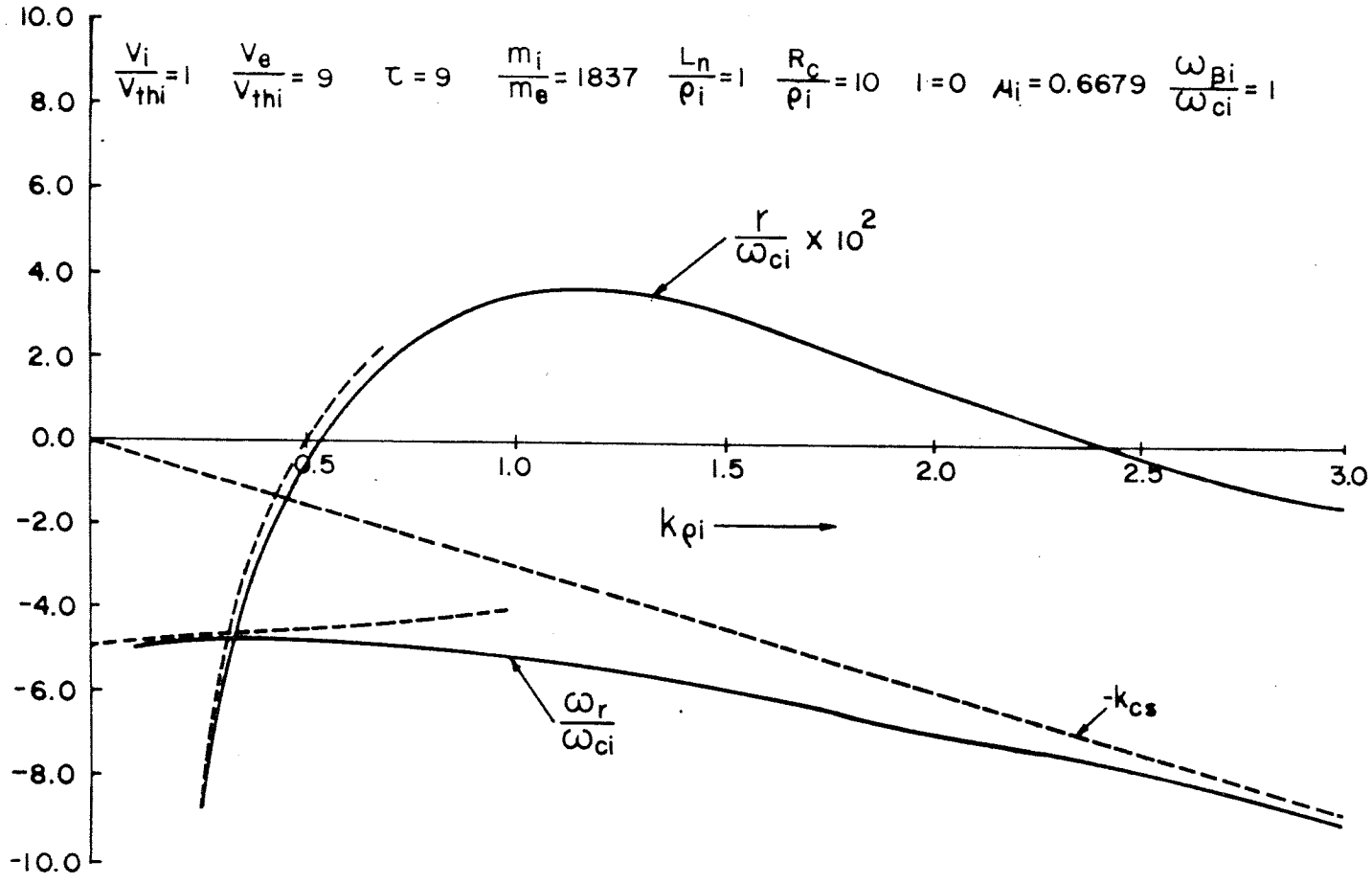
$\frac{V_i}{V_{thi}}=1$ $\frac{V_e}{V_{thi}}=9$ $\tau=9$ $\frac{m_i}{m_e}=1837$ $\frac{L_n}{\rho_i}=1$ $\frac{R_c}{\rho_i}=10$ $l=0$ $\mu_i=0.6679$ $\frac{\omega_{Bi}}{\omega_{ci}}=1$
10.0
8.0
6.0
4.0
2.0
0.0
-2.0
-4.0
-6.0
-8.0
-10.0
0.5
1.0
1.5
2.0
2.5
3.0
$\frac{r}{\omega_{ci}} \times 10^2$
$k_{\rho i}$
$\frac{\omega_r}{\omega_{ci}}$
$-k_{cs}$

FIG. 4.1

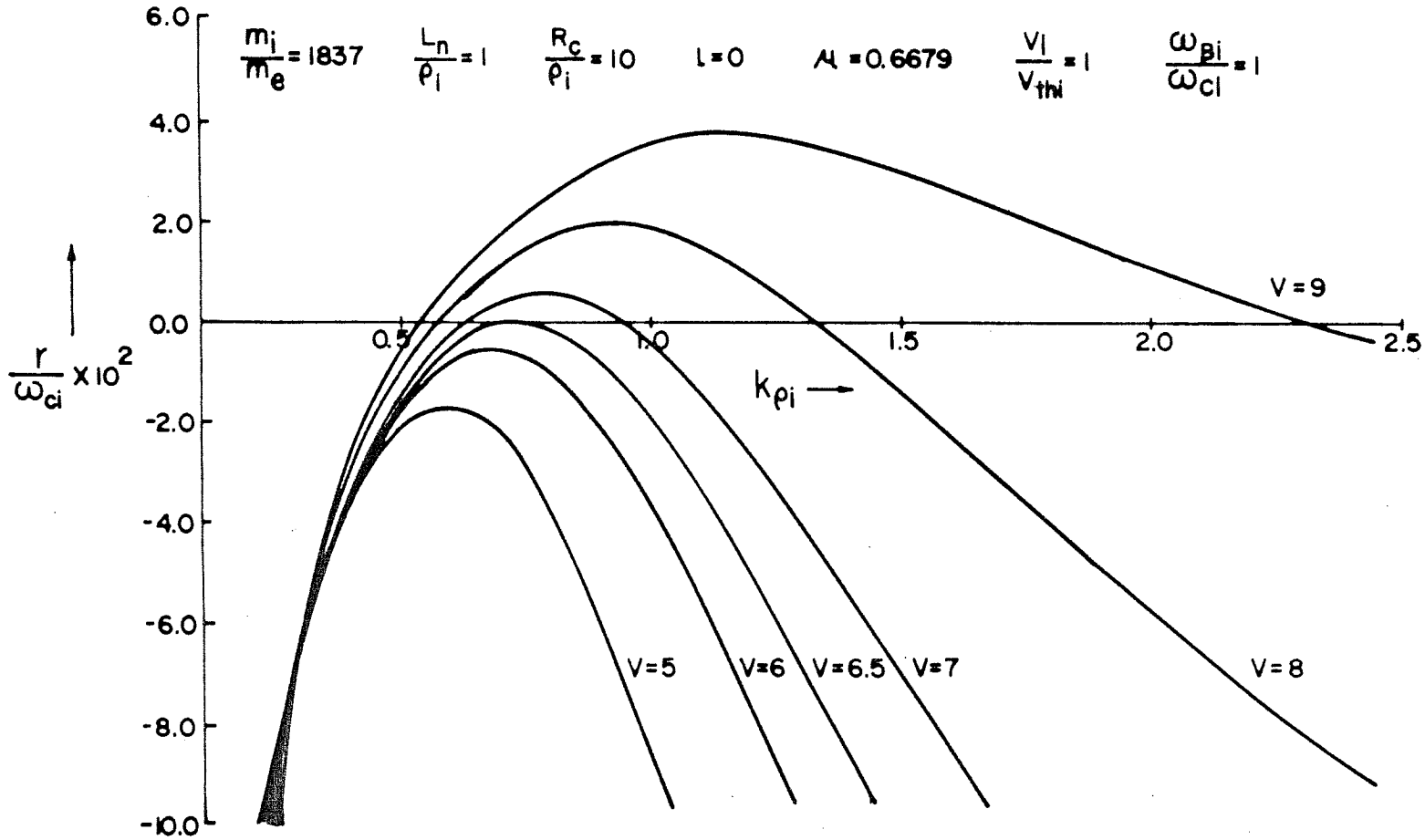
$\frac{m_i}{m_e}$ = 1837
$\frac{L_n}{\rho_i}$ = 1
$\frac{R_c}{\rho_i}$ = 10
l = 0
A = 0.6679
$\frac{V_I}{V_{thi}}$ = 1
$\frac{\omega_{Bi}}{\omega_{ci}}$ = 1
$\frac{r}{\omega_{ci}} \times 10^2$
$k_{\rho i}$
V = 5
V = 6
V = 6.5
V = 7
V = 8
V = 9
6.0
4.0
2.0
0.0
-2.0
-4.0
-6.0
-8.0
-10.0
0.5
1.0
1.5
2.0
2.5

FIG. 4.2

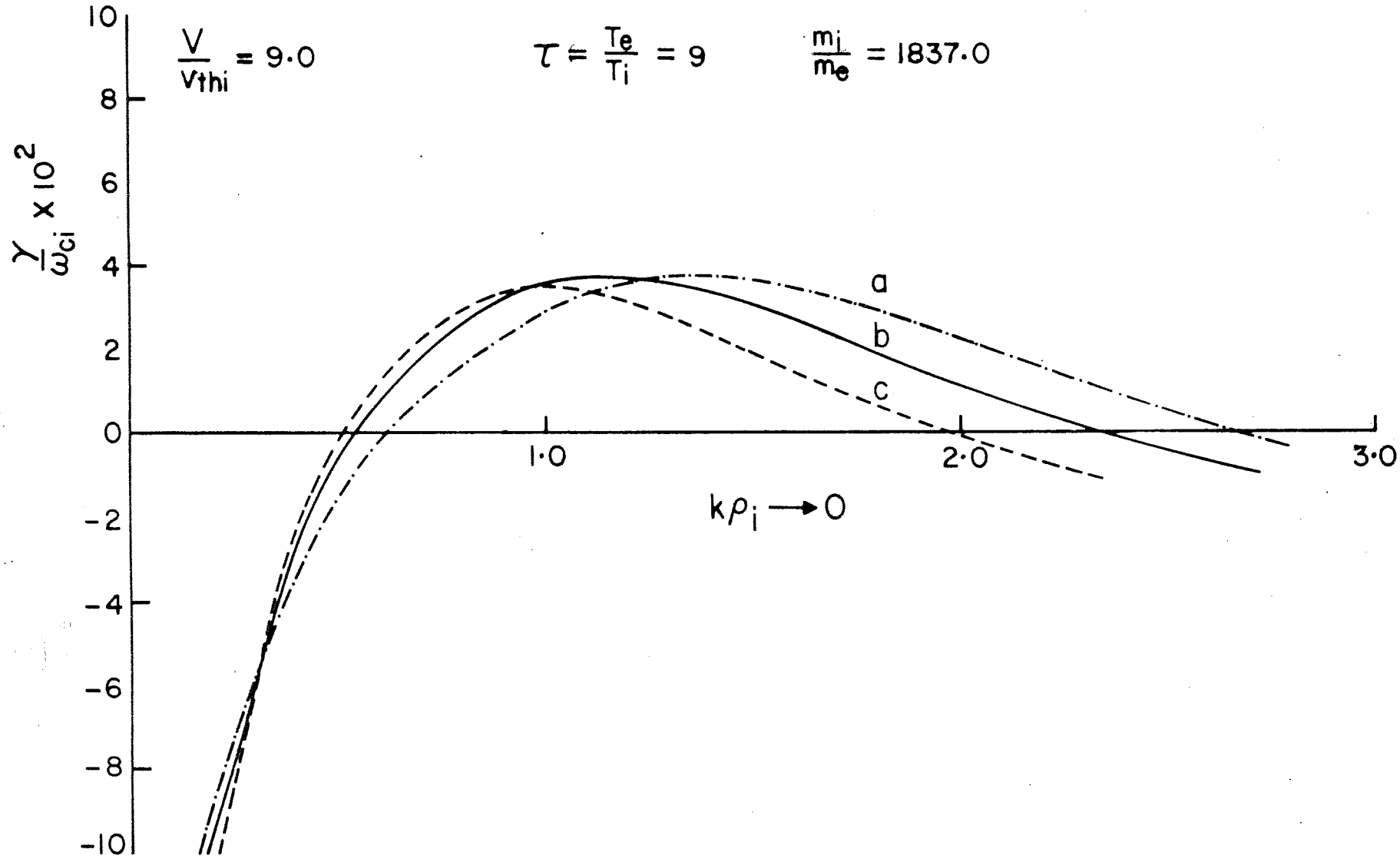
$\frac{V}{V_{thi}} = 9.0$
$\tau = \frac{T_e}{T_i} = 9$
$\frac{m_i}{m_e} = 1837.0$
$\frac{\gamma}{\omega_{ci}} \times 10^2$
10
8
6
4
2
0
-2
-4
-6
-8
-10
1·0
2·0
3·0
$k\rho_i \rightarrow 0$
a
b
c

FIG. 4.3

Chapter 5

Resistive firehose instability of a beam with a Bennett profile

5.1 Introduction

When a charged particle beam propagates in a resistive plasma channel it is susceptible to various forms of macro-instabilities. If the background plasma or gas has a finite resistivity the beam can encounter instabilities like the resistive sausage mode (m=0), resistive firehose mode (m=1) or the resistive filamentation (m=2) mode, etc. Out of these the most significant one is the resistive firehose mode with azimuthal mode number m=1 and has the fastest growth rate. As the free energy source for the instability is derived from the directed kinetic energy of the beam, this mode imposes severe limitations on beam transport [1]. In this chapter we investigate this instability in the Vlasov-Maxwell framework for a beam with a Bennett current profile, propagating in a background plasma with conductivity $\sigma(r)$. It has been shown theoretically [2] and in experiments [3] that when an energetic charged particle beam propagates in a gaseous

medium it undergoes a series of small angle scatterings by the medium and attains an isothermal equilibrium of the Bennett type in the plane perpendicular to the direction of propagation. Collisional ionisation of the gaseous medium by the beam particles gives rise to a plasma of high conductivity. Firehose instability results as a consequence of the interaction of the beam with the resistive plasma. When the beam is subjected to a small transverse displacement in the background plasma it gives rise to an eddy current which acts as a restoring force. This eddy current however decays in the resistive diffusion time τ_θ. Therefore, for time scales which are long compared to the diffusion time, the restoring force vanishes and the initial displacement of the beam tends to amplify, thus giving rise to unstable growth. Since the instability is driven by the directed kinetic energy of the beam, it grows at the expense of the beam, and thus results in rapid loss of the beam energy. The growth rate of the instability varies inversely as the resistive diffusion time and also depends sensitively on the equilibrium profiles of current and conductivity.

The firehose instability has been studied quite extensively by several workers. One of the earliest theoretical investigations of the hose mode was carried out by Rosenbluth [4]. He obtained a dispersion relation for the firehose instability of a neutralised relativistic electron beam in a resistive plasma channel using the relativistic Vlasov equation in the limit $\bar{\omega} << \omega_b$, $\bar{\omega}$ being

the frequency of the mode in the beam frame and ω_β the betatron frequency of the particles in the self-field of the beam. Employing a phenomenological approach, Yadavalli [5] has obtained a simplified dispersion relation for the hose instability of a uniform beam in the presence of a constant conductivity plasma channel assuming a rigid beam displacement in the limit $\omega << \omega_\beta$. Lee and Pearlstein [6] investigated the stability of a relativistic electron beam propagating in a pre-ionised channel of high conductitvity and showed that the beam could assume a hollow current profile as a result of the induced plasma currents. Weinberg [7] obtained the dispersion relation for the hose instability of relativistic electron beams propagating in resistive plasma channels in the limit $|\omega - kV| \lesssim \omega_{pe}$ assuming equilibrium particle orbits to be circular helices. An extensive analysis of the firehose mode was carried out by Lee [1] using a detailed kinetic description for the motion of the beam particles in the plane transverse to the direction of propagation, assuming an equilibrium Bennett profile. The analysis is based first on a 'rigid beam model' where all particles in a given thin segment of the beam suffer the same displacement and the beam is displaced more or less rigidly off the axis without any internal distortions. An approximate dispersion relation is obtained using this model in the low and high frequency limits by making appropriate perturbation expansions. However, this model assumed a single betatron frequency for all the particles, which is not true in the

case of the Bennett profile. The anharmonic pinch force, which gives rise to a radial dependence of the betatron frequency, would in principle lead to a phase-mixing between the particle orbits at various radial positions. It was suggested by Lee[1] that this could have a damping effect on the hose motion. He proposed a 'distributed mass model' to incorporate the effect of phase-mixing in a semi-quantitative manner. In this model, each segment of the beam is considered as made up of many rigid disks having the same profile as the undisturbed beam current but with different masses and executing simple harmonic motion in the r-ϕ plane. The distribution of masses is chosen according to the properties of the Bennett profile and their frequency ranges between 0 and $\omega_{\beta m}$, the betatron frequency corresponding to the particles localised near the axis. Using this model he obtained the growth rate of the hose mode and showed that the phase-mixing had a stabilizing influence on the mode. Subsequently, Uhm and Lampe [8] proposed a model for the resistive hose instability of a neutralised relativistic electron beam in the presence of an applied axial magnetic field. Using the Vlasov-Maxwell theory they obtained a general integro-differential equation for the eigenmodes. This was converted to an ordinary differential equation using a model in which the class of beam electrons with a given transverse energy displaces as a rigid segment. Later on, Sharp et al [9] proposed a refined version of this model by considering the beam as a superposition of rigid, independently moving

components with different radii, and obtained the eigenvalues and eigenfunctions for the hose dispersion relation. Lampe et al [10] have studied the hose instability of a beam moving in a weakly ionised medium. The conductivity of the channel which arises as a result of the ionisation of the medium by the beam is treated as a function of both position and time. They show that this leads to a convective nature of the instability. All these models have one common feature. They all adopt an averaging scheme to approximate the perturbed beam response in the plasma. In reality the beam particle orbits in the self field are quite intricate and the particles moving in these orbits encounter large local variations in the field quantities , leading to strong correlations between the different radial segments of the beam. Also the averaging scheme excludes wave-particle resonances that may give rise to Landau damping etc. In order to take account of these effects a more realistic model is required which would retain the details of the particle motion and at the same time yield a more quantitative account of the correlations between the different radial locations. This problem is analyzed in the present chapter by using a non-local theory described earlier in chapter 2. The present analysis has been carried out for non-relativistic electron and ion beams which are counterstreaming in the axial direction inside a cylindrical channel with a background plasma of finite conductivity $\sigma(r)$. We assume both the beams to have finite thermal spreads and obtain a matrix dispersion

relation in the next section. In the low-frequency limit we find that the dispersion relation can be reduced to a simple scalar form, which is solved both numerically as well as analytically in section 5.3. These results are compared with the predictions of earlier models in section 5.4.

5.2 Basic assumptions and the dispersion relation

We consider a self-pinched non-relativistic beam consisting of electrons and ions that are counterstreaming along the z-direction of an infinitely long cylinder embedded in a partially ionised gas. Each of the beams is characterised by an equilibrium drift velocity V_{zj} and a finite thermal spread represented by temperature T_j. At equilibrium these electron and ion beams are assumed to have a rigid-drift distribution of the form:

$$f_{oj} = C_1 \exp -\left(\frac{H_{oj} - P_{zj} V_j}{T_j}\right) \qquad (5.1)$$

In chapter 2 we have discussed in detail the equilibria represented by such a distribution. In the present case we assume a Bennett equilibrium for the beam. This choice is motivated by the knowledge that an energetic beam of charged particles passing through a gaseous medium evolves to the Bennett equilibrium as a result of multiple scatterings by the gas particles. As the beam propagates through the background gas a region of high conductivity is created mainly by the collisional ionisation of the gas molecules by the beam particles. The conductivity which depends on the plasma electron density is therefore assumed to have a Bennett profile. Usually this conductivity is very high so that the charge neutralisation time $\frac{1}{4\pi\sigma}$ is small

compared to the time scales of the problem. Therefore charge neutrality can be assumed and the displacement current can be neglected. For the hose instability which appears at nearly zero frequency the transverse motion of the particles are effectively decoupled from the axial motion. Under these conditions the fields can be described by a single component of the vector potential A_{1z}. The perturbed fields $\bar{E}_1$ and $\bar{B}_1$ can then be written as

$$\bar{B}_1 = \nabla \times \bar{A}_1 \hat{z} \tag{5.2}$$

$$\bar{E}_{1z} = -\frac{1}{c}\frac{\partial A_{1z}}{\partial t}\hat{z} \tag{5.3}$$

The plasma conductivity is assumed to have a Bennett profile and is given by:

$$\sigma(r) = \frac{\sigma_0}{\left(1+\frac{1}{4}k^2 r^2\right)^2} \tag{5.4}$$

σ_0 being the conductivity on the axis. To describe the resistive firehose instability, we use the linearized Vlasov-Maxwell equations as before:

$$\frac{\partial f_{1j}}{\partial t} + \bar{V}\cdot\frac{\partial f_{1j}}{\partial \bar{x}} + \frac{q_j}{m_j}\left(\frac{\bar{V}\times\bar{B}_0}{c}\right)\cdot\frac{\partial f_{1j}}{\partial \bar{v}} = -\frac{q_j}{m_j}\frac{\partial f_{0j}}{\partial \bar{v}}\left(\bar{E}_1 + \frac{\bar{V}\times\bar{B}_1}{c}\right) \tag{5.5}$$

The plasma is assumed to be collisional to the extent that it can be represented by a scalar conductivity, and its response is described by a scalar Ohm's law:

$$\bar{J}_1 = \sigma \bar{E}_1 \tag{5.6}$$

The perturbed magnetic field which is given by the linearised Ampere's equation with an additional source term arising from the background plasma response can be written as

$$\nabla \times \bar{B}_1 = \nabla \times (\nabla \times \bar{A}_1) = \frac{4\pi}{c}\left(\bar{J}_{b1} + \bar{J}_{p1}\right) \tag{5.7}$$

Using the Coulomb gauge $\left(\nabla . \bar{A}_1 = 0\right)$ this becomes,

$$-\nabla^2 A_{1z} = \frac{4\pi}{c}\left(J_{b1z} + J_{p1z}\right) \tag{5.8}$$

where J_{b1z} and J_{p1z} are the perturbed beam and plasma currents respectivly , and are given by

$$J_{b1z} = \sum_j q_j \int f_{1j}\, v_z\, d^3v \tag{5.9}$$

$$J_{p1z} = \sigma E_{1z} = -\frac{\sigma}{c}\frac{\partial A_{1z}}{\partial t} \tag{5.10}$$

Substituting in (5.8) from (5.9) and (5.10) we obtain

$$-\nabla^2 A_{1z} + \frac{4\pi\sigma}{c^2}\frac{\partial A_{1z}}{\partial t} = \frac{4\pi}{c}\sum_j q_j \int f_{1j}\, v_z\, d^3v \tag{5.11}$$

Using the normal mode approach and expressing A_{1z} in terms of the Fourier components, we have,

$$A_{1z}(r', \theta', z') = \sum_{k,m} A_{1z}(r')\, e^{i(kz' + m\theta' - \omega t')} \quad (5.12)$$

Substituting these in the above equations (5. 11) and expressing ∇^2 in cylindrical coordinates, we obtain,

$$\left[-\frac{1}{r}\frac{\partial}{\partial r}\left(r\frac{\partial}{\partial r}\right) + \frac{1}{r^2} + k^2 - \frac{4\pi i\sigma\omega}{c^2}\right] A_{1z} = \frac{4\pi}{c}\sum_j q_j \int f_{1j}\, V_z\, d^3v \quad (5.13)$$

This is an integro-differential equation for the resistive firehose mode. The perturbed distribution function f_{1j} in (5.13) is obtained by integrating equation (5. 5) over the unperturbed betatron orbits described in chapter 2. The derivation of the dispersion relation using the non-local approximation in this case follows along the same lines as given for the m=1 kink mode except that there is now an additional term coming from the beam plasma coupling. This additional term can be evaluated separately as follows:

We have from equation (5.13) the beam plasma coupling term given by

$$-\frac{4\pi i\sigma\omega}{c^2} A_{1z}$$

Following the non-local approximation the radial eigenfunction $A_{1z}(r')$ is expressed as a sum over a complete set of basis functions:

$$A_{1z}(r') = \sum_n \alpha_n \phi_n(r') \quad (5.14)$$

where ϕ_n's are the normalized basis functions. Substituting for A_{1z} and operating with $\int_0^{R_c} r\phi_n\, dr$ the beam plasma coupling

term in equation (5.13) becomes,

$$-\alpha_n \int_0^{R_c} \frac{4\pi i \sigma \omega}{c^2} \phi_{n'} \phi_n \, r \, dr$$

Substituting for $\sigma(r)$ from eq.(5.4) we have

$$-\sum_n \alpha_n \frac{4\pi i \sigma_0 \omega}{c^2} \int_0^{R_c} \frac{r \, dr \, \phi_{n'} \phi_n}{\left(1+\frac{1}{4}k^2 r^2\right)^2} = -\sum_n \alpha_n \frac{4\pi i \sigma_0 \omega}{c^2} A_{n'n}$$

where $A_{n'n}$ is the radial integral given by

$$\int_0^{R_c} \frac{r \, dr \, \phi_{n'} \phi_n}{\left(1+\frac{1}{4}k^2 r^2\right)^2}$$

Taking the beam radius a=2 Ln where Ln is the scale-length of the Bennett profile and defining the diffusion time $\tau_B = \frac{\pi \sigma_0 a^2}{2c^2}$ the beam plasma coupling term becomes

$$-\frac{2i\omega\tau_B}{L_n^2} A_{n'n} \qquad (5.15)$$

The non-local dispersion relation for the resistive firehose mode is thus obtained by adding this term in the matrix $D^{(4)}_{n'n}$ obtained earlier and setting the determinant of the resulting matrix to zero. The corresponding dispersion relation is then given by

$$\mathrm{Det}\left[D_{n'n}\right] = \mathrm{Det}\left[\left(k^2+\lambda_n^2\right)\delta_{n'n} - \frac{2i\omega\tau_B}{L_n^2} A_{n'n} - \sum_j \frac{\omega - kV_j}{\sqrt{2}kV_{thj}} \frac{1}{\lambda_{Dj}^2(\omega)}\right.$$

$$\left[\sum_{\alpha=0}^{\infty} \left\{\left(\frac{\omega-(1+2\alpha)\omega_{pj}}{ck}\right)^2 Z\left(\frac{\omega - kV_j - (1+2\alpha)\omega_{pj}}{\sqrt{2}kV_{thj}}\right) + \right.\right.$$

$$\left(\frac{\omega+(1+2\alpha)\omega_{\beta j}}{ck}\right)^2 \mathcal{Z}\left(\frac{\omega-kV_j+(1+2\alpha)\omega_{\beta j}}{\sqrt{2}\,k\,V_{th_j}}\right)\Bigg\}\Bigg] \; P^{(\alpha)}_{n'n} \qquad (5.16)$$

This is the most general dispersion relation for the eigenvalues of the resistive hose mode. The first term represents the radial correlations between the different modes and the geometrical effects arising from the finite boundary. The second term represents the coupling of the beam with the plasma motion through the resistivity of the latter. This has a destabilising effect on the mode. The third term contains the wave-particle resonances. These localised wave-particle resonances are expressed in terms of the plasma dispersion functions. From the arguments of the dispersion function, it is apparent that in the beam frame, the mode can be in resonance with odd harmonics of the corresponding betatron frequencies. The coefficient matrices $P^{(\alpha)}_{n'n}$ represent the strength of these resonances. The fundamental resonance corresponding to $\alpha = 0$ or $\omega - kV_j \approx \omega_{\beta j}$ is the strongest resonance. The successive terms in the α - summation represent the successive odd harmonics and their strength decreases as α is increased. The non-local nature of the perturbations is manifested in the infinite order of the matrix.

5.3 Numerical solution of the Non-local dispersion relation

The dispersion relation represented by equation (5.16) is an infinite order transcendental equation and is difficult to solve exactly. In practice, it is sufficient to retain a finite number of terms in the basis function expansion and thereby truncate the infinite matrix after a finite size.

We have solved the matrix dispersion relation and obtained the eigenvalues corresponding to the resistive firehose instability by taking a matrix of order 20 X 20. The matrix method based on the subroutine package EISPACK described in chapter 3 was used for the computation. This instability corresponds to the low-frequency regime and, therefore, it is sufficient to consider the fundamental mode, i.e., $\alpha = 0$, term in the wave-particle interactions. The matrix in this case can be written as

$$D_{m'm} \simeq (k^2+\lambda_m^2)\delta_{m'm} - \frac{2i\omega\tau_\beta}{l_m^2} A_{m'm} - \sum_j \frac{\omega-kV_j}{\sqrt{2}kV_{thj}} \frac{P^{(0)}_{m'm}}{\lambda^2_{De}(0)} \Bigg[\left(\frac{\omega-\omega_{pj}}{ck}\right)^2 Z\left(\frac{\omega-kV_j-\omega_{pj}}{\sqrt{2}kV_{thj}}\right) + \left(\frac{\omega+\omega_{pj}}{ck}\right)^2 Z\left(\frac{\omega-kV_j+\omega_{pj}}{\sqrt{2}kV_{thj}}\right) \Bigg] \qquad (5.17)$$

The solutions of this matrix are plotted for typical values of the beam plasma parameters. Figure (5.1) (solid curve) shows a plot of the real frequency and growth rate

versus wavenumber.

However, eq. (5.16) is a very inconvenient form for numerical calculations as it involves calculation of a large matrix determinant for every iteration in ω. For the m=1 modes it has been shown in chapter 3 that the matrix can be reduced to a very simple form which is easier to handle numerically and also analytically in some limiting cases. The matrix $A_{n'n}$ is related to $P_{n'n}$ as follows:
We have (from chapter 3)

$$A_{n'm} = \sum_{\alpha=0}^{\infty} 2\, P_{n'm}^{(\alpha)}$$

Substituting in (5.16) we have,

$$D_{n'm} = (k^2+\lambda_m^2)\,\delta_{n'm} - \frac{4i\omega\tau_\beta}{L_m^2}\sum_\alpha P_{n'm}^{(\alpha)} \; - \sum_j \frac{(\omega - kV_j)}{\sqrt{2}kV_{thj}\,\lambda_{Dj}^2(0)} \cdot$$

$$\sum_{\alpha=0}^{\infty} P_{n'm}^{(\alpha)} \left[\left(\frac{\omega-(1+2\alpha)\omega_{\beta j}}{ck}\right)^2 Z\left(\frac{\omega-kV_j-(1+2\alpha)\omega_{\beta j}}{\sqrt{2}kV_{thj}}\right) + \left(\frac{\omega+(1+2\alpha)\omega_{\beta j}}{ck}\right)^2 Z\left(\frac{\omega-kV_j+(1+2\alpha)\omega_{\beta j}}{\sqrt{2}kV_{thj}}\right)\right]$$

For low-frequency modes we need to keep the $\alpha = 0$ term only so that we have

$$D_{n'm} = (k^2+\lambda_m^2)\,\delta_{n'm} - \frac{4i\omega\tau_\beta}{L_m^2}\, P_{n'm}^{(0)} \; - \sum_j \frac{\omega - kV_j}{\sqrt{2}kV_{thj}\,\lambda_{Dj}^2(0)} \cdot$$

$$\left[\left(\frac{\omega-\omega_{\beta j}}{ck}\right)^2 Z\left(\frac{\omega-kV_j-\omega_{\beta j}}{\sqrt{2}kV_{thj}}\right) + \left(\frac{\omega+\omega_{\beta j}}{ck}\right)^2 Z\left(\frac{\omega-kV_j+\omega_{\beta j}}{\sqrt{2}kV_{thj}}\right)\right] P_{n'm}^{(0)} \quad (5.18)$$

The matrix D can therefore be written as

$$[D] = [K + f(\omega)\, P] \quad (5.19)$$

where

$$K = \left[(k^2 + \lambda_m^2)\ \lambda_{De}^2\ \delta_{m'm} \right]$$

and

$$f(\omega) = -\frac{2i\omega\tau_\beta}{L_m^2} - \frac{\omega + kV}{\sqrt{2}kV_{the}} \left\{ \left(\frac{\omega - \omega_{pe}}{ck}\right)^2 Z\left(\frac{\omega + kV - \omega_{pe}}{\sqrt{2}kV_{the}}\right) + \left(\frac{\omega + \omega_{pe}}{ck}\right)^2 \cdot Z\left(\frac{\omega + kV + \omega_{pe}}{\sqrt{2}kV_{the}}\right) \right\} - \frac{\omega\tau - kV}{\sqrt{2}kV_{thi}} \left\{ \left(\frac{\omega - \omega_{pi}}{ck}\right)^2 Z\left(\frac{\omega - \frac{kV}{\tau} - \omega_{pi}}{\sqrt{2}kV_{thi}}\right) + \left(\frac{\omega + \omega_{pi}}{ck}\right)^2 \cdot Z\left(\frac{\omega - kV/\tau + \omega_{pi}}{\sqrt{2}kV_{thi}}\right) \right\}$$

Operating on the right-hand side with $[P].[P^{-1}]$ and assuming the matrix [P] to be non-singular, we have,

$$[D] = P.P^{-1}\left[K + f(\omega) P\right]$$

$$= [P].\left[P^{-1}.K + f(\omega)\,\hat{I}\right]$$

Therefore,

$$|D| = |P| \cdot \left| P^{-1}.K + f(\omega)\,\hat{I} \right|$$

$$\therefore |D| = 0$$

$$\Rightarrow$$

$$\left| P^{-1}.K + f(\omega)\,\hat{I} \right| = 0 \qquad (5.20)$$

Equation (5.20) can be compared with the characteristic equation of the matrix $P^{-1}K$, namely,

$$\left| P^{-1}.K - \mu_i\,\hat{I} \right| = 0 \qquad (5.21)$$

Comparing the above two equations we find

$$f(\omega) + \mu_i = 0. \tag{5.22}$$

This equation gives the dispersion relation in a more compact form. The eigenvalues μ_i of the matrix $P^{-1}K$ are functions of the wavenumber. In the following section we discuss the numerical solutions and analytical approximations of the reduced dispersion relation (5.22).

5.4 Numerical Results and Discussion

We have carried out an extensive numerical investigation of the dispersion relation (5.22) in various parameter regimes. A plot of the temporal growth rate and real frequency against axial wavenumber k for a typical value of the equilibrium electron drift and the resistive diffusion time is shown in Figure (5.1) by the dashed curve.

For comparison the solution of the full matrix dispersion relations is also plotted in the same graph and is shown by the solid curve. It turns out that the two values are in good agreement thus justifying our approximation. Therefore, we will consider the reduced dispersion relation only in all our subsequent discussions.

Figure (5.2) shows the growth rate and the frequency of the hose mode for a fixed value of ζ_β but different values of the electron drift velocity. The electron to ion temperature ratio is chosen such that the ion drift remains constant and is small compared to the electrons so that majority of the current is carried by the electrons only. It is found that for each of the values of V there is a certain range of unstable values of k. For a given value of k the growth rate increases with the increase in V.The range of unstable wavenumbers decreases with the increase in the electron drift. For very small wavenumbers and very

large wavenumbers the mode is found to be stable. At intermediate values of k, the mode is unstable. At any given k the growth or the stability is determined by a balance between two competing processes. One is the destabilizing force due to the resistivity of the plasma represented by the $\omega\tau_\beta$ term and the other is the stabilising force due to the electron Landau damping. For very small values of the wavenumbers the destabilizing term $\omega\tau_\beta$ is small and hence the mode is stable. As k is increased this destabilizing force increases as well as the Landau damping term, until a value of k is reached where the Landau damping takes over and is the dominant mechanism.

The increase in growth rate for a given k with V is attributed to the fact that V determines the directed energy of the electron beam which supplies the free energy source for the instability. As V is increased the beam energy increases and more free energy is available to feed the instability thereby leading to larger growth rate.

Figure (5. 3) shows a plot of growth rate and real frequency as a function of wavenumber for fixed V but different values of τ_β. As τ_β is increased the diffusion time increases. This implies that the magnetic field persists for a longer duration and as this exerts a restoring force on the beam the growth of the instability is suppressed. These physical mechanisms become more apparent when we consider the analytic expansions of the various terms in the dispersion relation in asymptotic limits. In the limit of small k we have the following

inequalities:

$$\frac{\omega + kV \mp \omega_{pe}}{\sqrt{2}\,kV_{the}} >> 1 \quad ; \quad \frac{\omega - kV/\tau \mp \omega_{pi}}{\sqrt{2}\,kV_{thi}} >> 1$$

Taking large-argument expansions for the Z-functions and writing $\omega \sim \omega_n + i\gamma$ where $\omega_n << \gamma$ we have

$$f(\omega) + \mu_i = -\frac{4i\omega\tau_\beta}{L_n^2}\lambda_D^2 - \frac{\omega+kV}{\sqrt{2}\,kV_{the}}\left[\left(\frac{\omega-\omega_{pe}}{ck}\right)^2 Z\left(\frac{\omega+kV-\omega_{pe}}{\sqrt{2}kV_{the}}\right)\right.$$

$$\left. + \left(\frac{\omega+\omega_{pe}}{ck}\right)^2 Z\left(\frac{\omega+kV+\omega_{pe}}{\sqrt{2}\,kV_{the}}\right)\right] - \frac{\omega\tau - kV}{\sqrt{2}kV_{thi}}\left[\left(\frac{\omega-\omega_{pi}}{ck}\right)^2 Z\left(\frac{\omega-kV/\tau-\omega_{pi}}{\sqrt{2}\,kV_{thi}}\right)\right.$$

$$\left. + \left(\frac{\omega+\omega_{pi}}{ck}\right)^2 Z\left(\frac{\omega-kV/\tau+\omega_{pi}}{\sqrt{2}kV_{thi}}\right)\right] + \mu_i = 0$$

Substituting for the Z-functions and writing $\omega \simeq i\gamma$ we obtain:

$$4\gamma\tau_\beta\frac{\lambda_D^2}{L_n^2} + \frac{\omega+kV}{\sqrt{2}kV_{the}}\left[\frac{\omega_{pe}^2}{c^2k^2}\left\{\frac{\sqrt{2}kV_{the}}{\omega+kV-\omega_{pe}} + \frac{(\sqrt{2}kV_{the})^3}{2(\omega+kV-\omega_{pe})^3}\right.\right.$$

$$\left.\left. + \frac{\sqrt{2}kV_{the}}{\omega+kV+\omega_{pe}} + \frac{(\sqrt{2}kV_{the})^3}{2(\omega+kV+\omega_{pe})^3}\right\}\right] + \frac{\omega\tau-kV}{\sqrt{2}kV_{thi}}\left[\frac{\omega_{pi}^2}{c^2k^2}\left\{\frac{\sqrt{2}kV_{thi}}{\omega-kV/\tau-\omega_{pi}}\right.\right.$$

$$\left.\left. + \frac{1}{2}\frac{(\sqrt{2}kV_{thi})^3}{(\omega-kV/\tau-\omega_{pi})^3} + \frac{\sqrt{2}kV_{thi}}{(\omega-kV/\tau+\omega_{pi})} + \frac{(\sqrt{2}kV_{thi})^3}{2(\omega-kV/\tau+\omega_{pi})^3}\right\}\right]$$

$$+ \mu_i = 0$$

$$\Rightarrow 4\gamma\tau_B\frac{\lambda_D^2}{L_n^2} + 2\omega_{pe}^2\frac{V^2}{c^2}\frac{1}{k^2V^2-\omega_{pe}^2} + \frac{V_{the}^2}{c^2}\omega_{pe}^2k^2V^2\frac{(k^2V^2+3\omega_{pe}^2)}{(k^2V^2-\omega_{pe}^2)^3}$$

$$+\mu_i = 0$$

$$\Rightarrow \gamma\tau_B = 1 + \frac{k^2V^2}{\omega_{pe}^2} +$$

$$k^2V_{the}^2\left(3 + \frac{10k^2V^2}{\omega_{pe}^2} + \frac{3k^4V^4}{\omega_{pe}^4}\right) - \frac{\mu_i}{4}\frac{L_n^2}{\lambda_{De}^2} \qquad (5.23)$$

Figures (5.4a and 5.4b) show the plot of the analytical solution versus the numerical solution for a fixed value of τ_B and the drift velocity V. For very small values of k the two results are in good agreement. However for large k more terms have to be retained in the Z-function expansion and this makes the analytical solution difficult.

The inverse dependence of the growth rate is obvious from the analytic limit obtained above for a given k and V. Figure(5. 5) shows a plot of the growth time as a function of τ_B for different k's and for a fixed V. However the threshold k for instability cannot be obtained from the above analytic expression because μ_i is a function of k and its exact functional dependence is not known.

In figure(5. 2) it is shown that the peak growth rate decreases with V and the cut-off k for damping increases with reduction in V.This result can be better understood by plotting the growth rate against k/k_β where k_β is the betatron wavenumber and determines the scale length of the

oscillation in the axial direction. Figure(5.6) shows a plot of the growth rate versus k/k_β for different values of V. As V is increased the ratio V/V_{the} also increases and therefore requires a larger value of k for the Landau damping to be effective. Hence the upper cut-off in k shifts to the right. In this region of cut-off we can make a rough estimate of the growth rate or damping by an approximate analytic limit. In this limit we have $|\omega_r + kV| \simeq \omega_{pe}$. The damping therefore comes from the electron Z-function term. Putting $\omega = \omega_r + i\tau$ and setting $\tau = 0$ we obtain

$$-\frac{\omega_{pe}^2}{c^2k^2}\frac{(\omega_r+kV)}{\sqrt{2}kV_{the}}\sqrt{\pi}\exp-\left(\frac{\omega_r+kV-\omega_{pe}}{\sqrt{2}kV_{the}}\right)^2 - 4\pi\omega_r\tau_\beta + \mu_1 = 0$$

or taking the imaginary part we have

$$\frac{\omega_{pe}^2}{k^2V^2}\frac{(\omega_r+kV)}{kV_{the}}\sqrt{\frac{\pi}{2}}\exp-\left(\frac{\omega_r+kV-\omega_{pe}}{\sqrt{2}kV_{the}}\right)^2 + 2\omega_r\tau_\beta = 0$$

$$\Rightarrow$$

$$\omega_r \simeq -\frac{\omega_{pe}^2}{k^2V^2\cdot kV_{the}}\sqrt{\frac{\pi}{2}}\exp-\left(\frac{kV-\omega_{pe}}{\sqrt{2}kV_{the}}\right)^2 \Big/ 2\tau_\beta + \sqrt{\frac{\pi}{2}}\frac{\omega_{pe}^2}{} \qquad (5.24)$$

Experimental work on the firehose instability of a relativistic beam traversing through a background gas has been carried out by several workers [3,11,12]. Lauer et al

have observed the disruption of a relativistic electron beam in a neutral gas and shown it to be due to the firehose instability [12]. These experiments usually involve high energy pulsed beams that are injected into the gas at a fixed point and tickled with a fixed frequency. The subsequent development of the perturbation is studied in space rather than time. The instability therefore depends on whether Imk$_r$>0. In the experiment the spatial growth of the instability was studied as a function of frequency and they found an upper cut-off in frequency. This was explained in terms of the 'distributed mass model' of Lee, according to which the damping of the perturbation was an effect related to the phase mixing between the particle orbits at various radial locations. Phase mixing in case of betatron orbits arises as a result of the radial dependence of the betatron frequency. A perturbation with a given phase can match with the phase of the betatron oscillation at one radial coordinate at a particular instant of time. As the perturbation moves outwards in the course of its propagation it will go out of phase with the particles at another radial point. Therefore the net result may lead to a damping of the wave or perturbation. Lee's model takes into account the phase mixing effect in a semi-quantitative way by treating the betatron frequency as a function of the radial coordinate. However the process of averaging the motion of the particles in the transverse plane ignores the non-local effects arising from the inhomogeneities in the density profiles. It also does not

account for the Landau damping which is a wave particle effect. Our model on the other hand accounts for the non-local effects as well as wave-particle resonances by means of expansion of radial amplitudes over a complete set of basis functions and the integration over the betatron orbits. However these orbits are obtained under the assumption of a linear magnetic field (the $K^2r^2/4$ term in the denominator of B being neglected) ,and thus exclude the phase mixing effect arising from the radial dependence of the betatron frequency. In some sense therefore our theory is complementary to that of Lee and others where this effect is considered,but wave-particle resonances have been ignored.

We have solved Lee's dispersion relation obtained from the 'distributed mass model' for real k in the complex ωplane. Figure(5. 4c) shows a plot of this solution against our numerical solution (5.4b). It is seen that for both the models the growth rates are of the same order of magnitude. The other mode characteristics like the range of unstable wavenumbers, the wavelength corresponding to maximum growth as well as the upper cutoff in k for instability are comparable for the parameters considered.This shows that the non-local and wave-particle effects are as important as the phase mixing in determining the stability of the mode. Our calculation also predicts a lower cutoff in k which is not predicted by the phase mixing models.

References

1. Lee,E.P., Phys. Fluids 21, 1327 (1978).

2. Lee,E.P., Phys. Fluids 19, 60 (1976).

3. Briggs, R. J. , Hester, R. E., Lauer,E.J., Lee,E.P. & Spoerlin,R.L.,Phys. Fluids 19, 1007 (1976).

4. Rosenbluth,M.N., Phys. Fluids 3, 932 (1960).

5. Yadavalli,S.V., Zeit. Fur Physik 196, 255 (1966).

6. Lee, E. P. & Pearlstein, L. D., Phys. Fluids 16, 904 (1973).

7. Weinberg, S. , J. Math. Phys. 5, 1371 (1964); 8, 614 (1967).

8. Uhm,H.S. & Lampe,M., 23, 1574 (1980).

9. Sharp, W.M., Lampe,M. & Uhm,H.S., Phys. Fluids 25, 1456 (1982).

10. Lampe, M., Sharp,W.M., Hubbard,R.F., Lee,E.P. & Briggs, R.J.,27, 2921 (1984).

11. Moses, K.G., Bauer,R.W. & Winter,S.D., Phys. Fluids 16, 436 (1973).

12. Lauer, E.J., Briggs,R.J., Fessenden,T.J., Hester,R.E. &

Lee,E.P., Phys. Fluids 21, 1344 (1978).

Figure captions for chapter 5

Fig. (5. 1) Plot of ω_n and γ vs. k. a)Solid curve (matrix solution) b)Dashed curve (reduced form).

Fig. (5.2) Plot of γ vs. k for fixed τ_β and different V's.

Fig. (5. 3) Plot of ω_n and γ vs. k for fixed V and different τ_β's.

Fig. (5. 4) Plot of γ vs. k for fixed V and τ_β. a) analytical solution. b) Numerical solution of the reduced dispersion relation. c) Lee's solution(distributed mass model).

Fig. (5.5) Plot of $1/\gamma$ vs. τ_β for fixed k and V.

Fig. (5.6) Plot of $\gamma\tau_\beta$ vs. k/k_β for different V's.

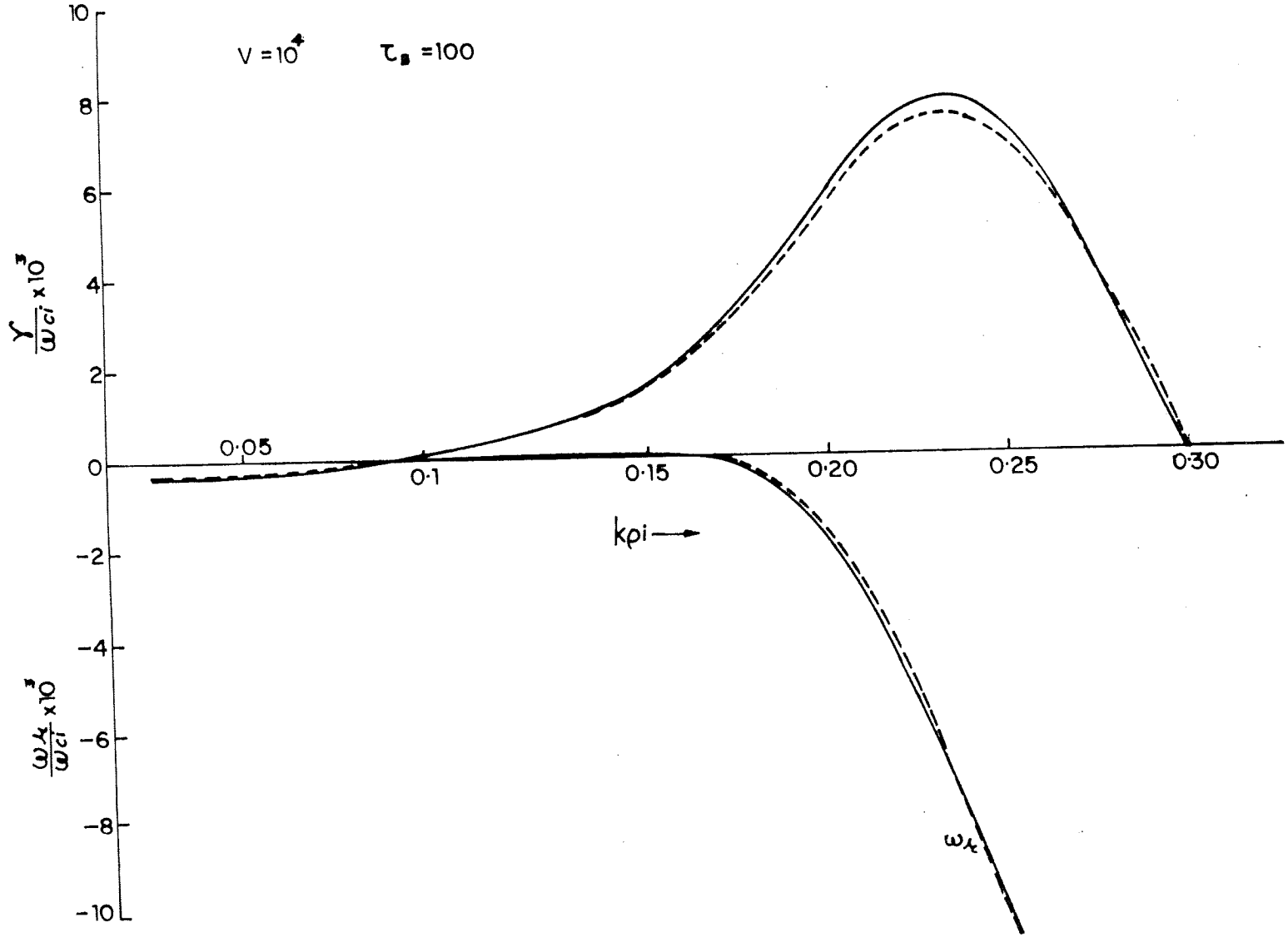
V = 10⁴
τ_e = 100
10
8
6
4
2
0
-2
-4
-6
-8
-10
γ/ω_ci x10³
ω_r/ω_ci x10³
0·05
0·1
0·15
0·20
0·25
0·30
kρi
ω_r

FIG. 5.1

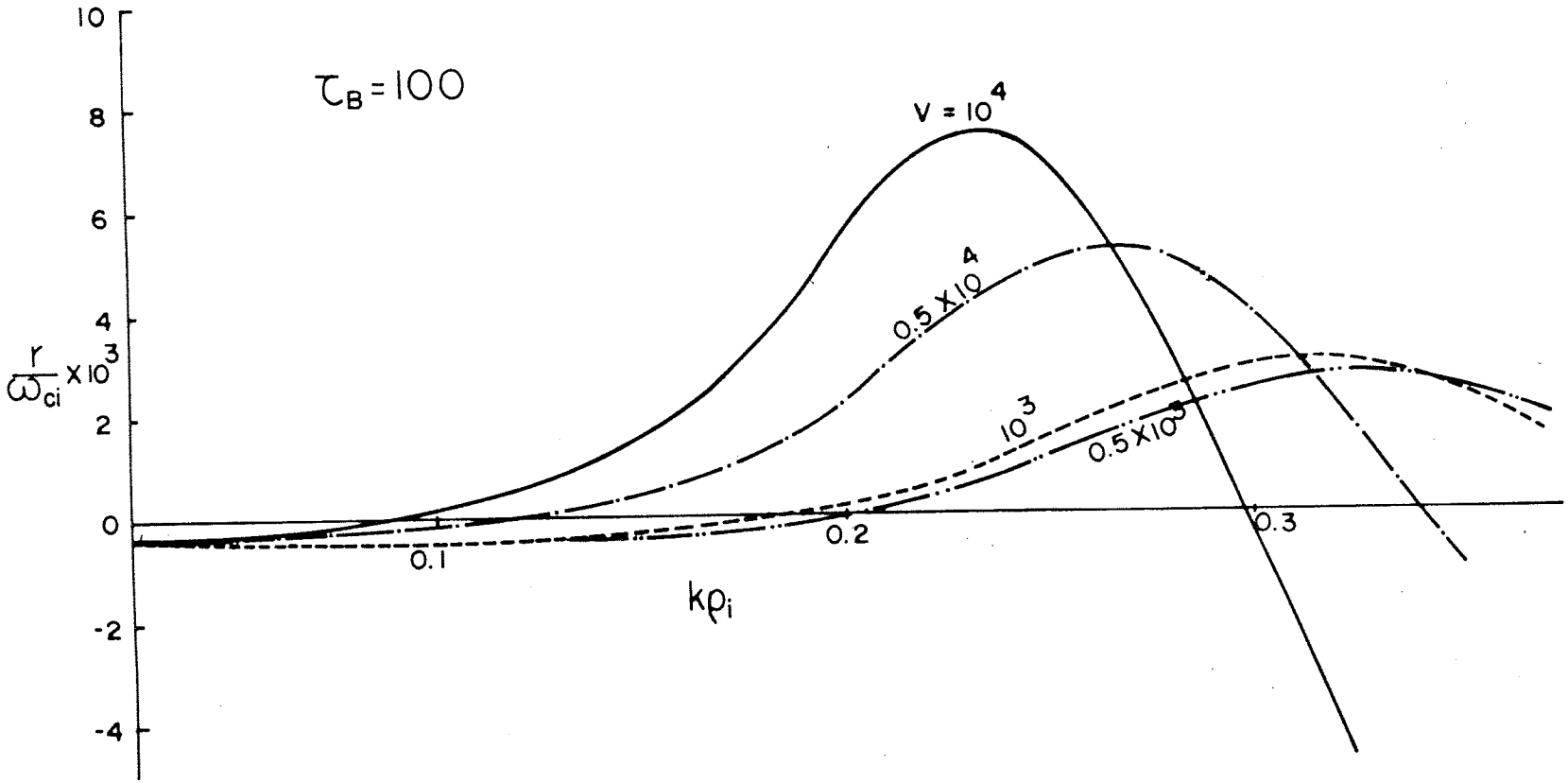
$\tau_B = 100$
$V = 10^4$
0.5×10^4
10^3
0.5×10^3
$\frac{\gamma}{\omega_{ci}} \times 10^3$
$k\rho_i$
10
8
6
4
2
0
-2
-4
0.1
0.2
0.3

FIG. 5.2

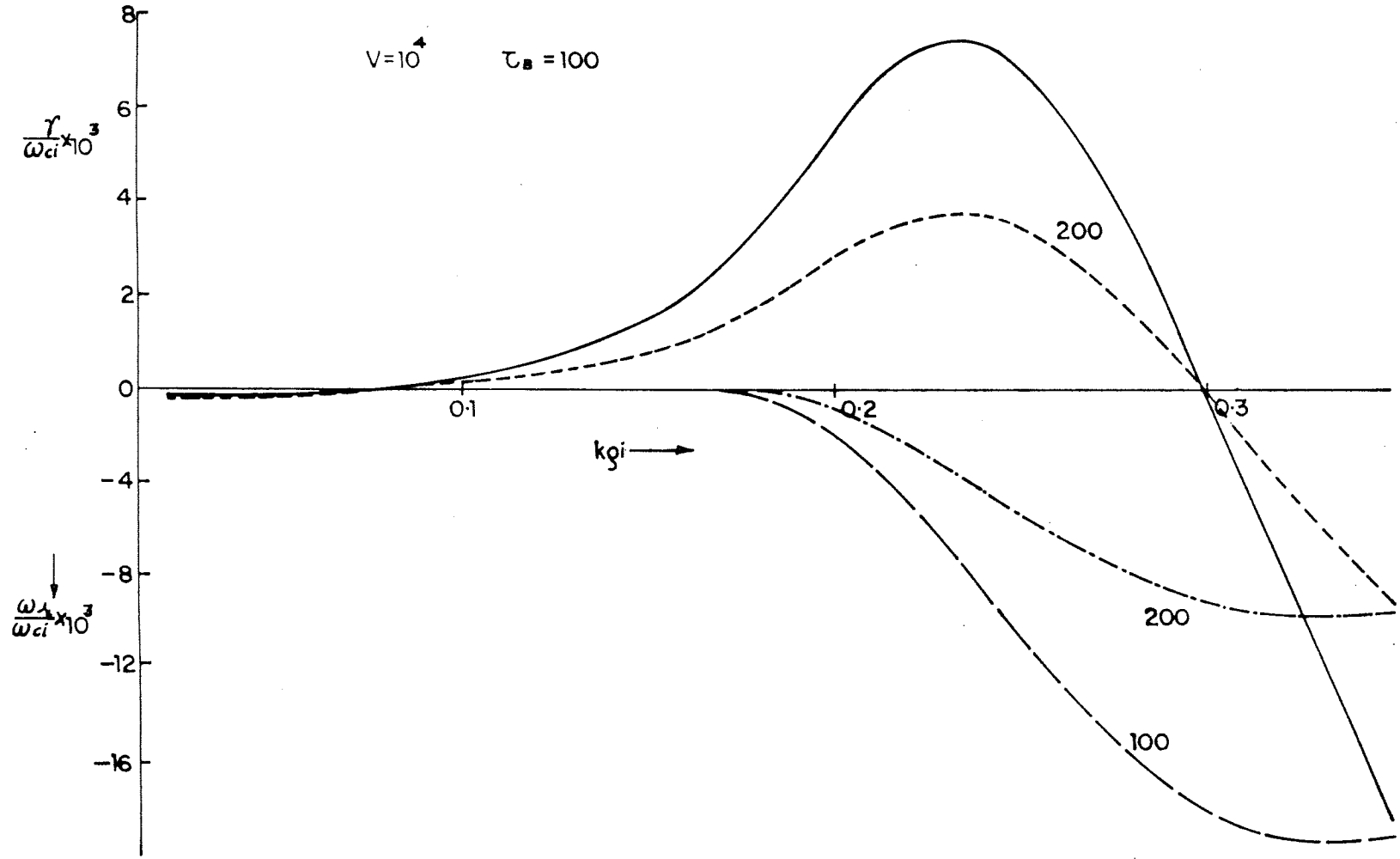
V=10^4
τe = 100
γ/ωci x10^3
ωr/ωci x10^3
8
6
4
2
0
-4
-8
-12
-16
0·1
0·2
0·3
kρi
200
200
100

FIG. 5.3

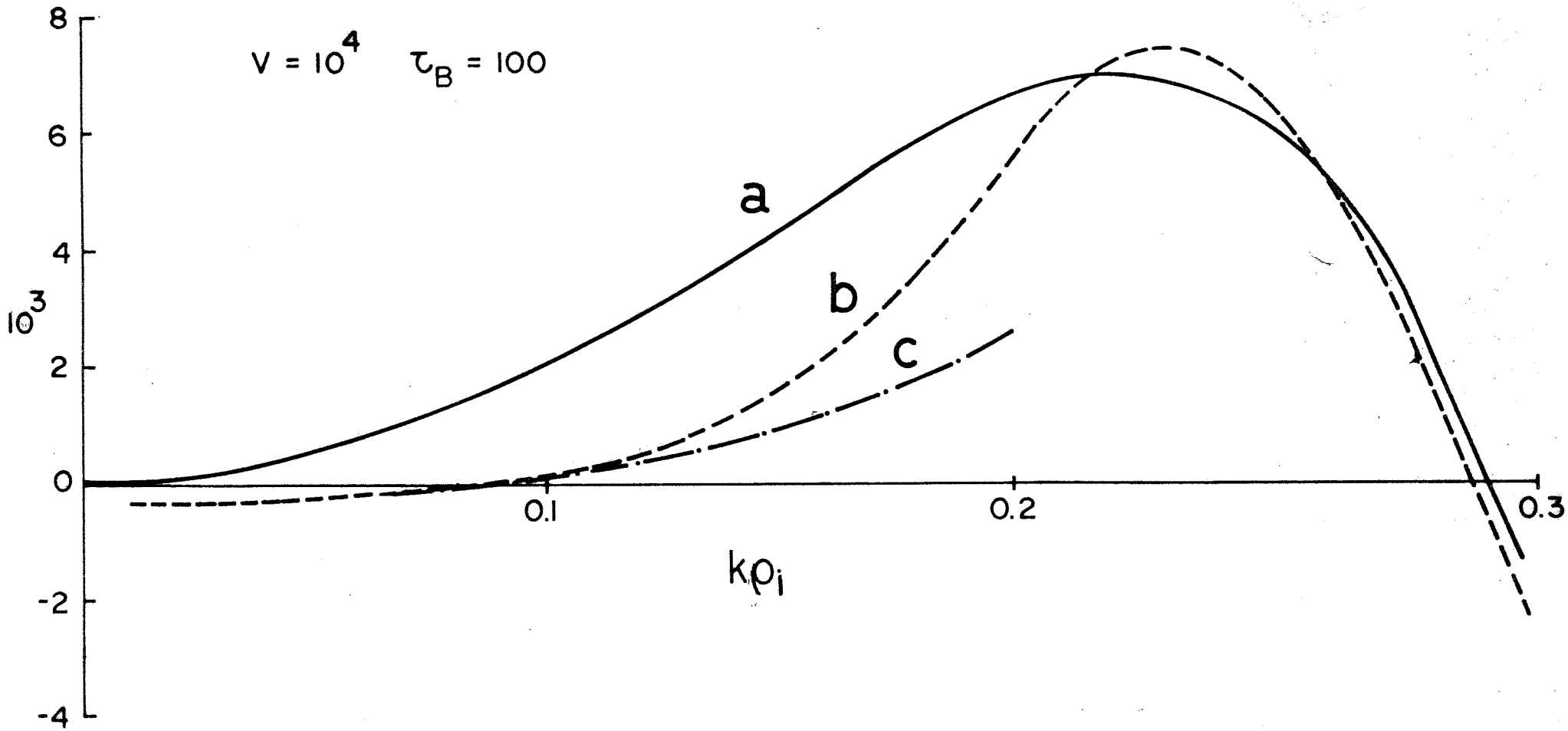

FIG. 5.4

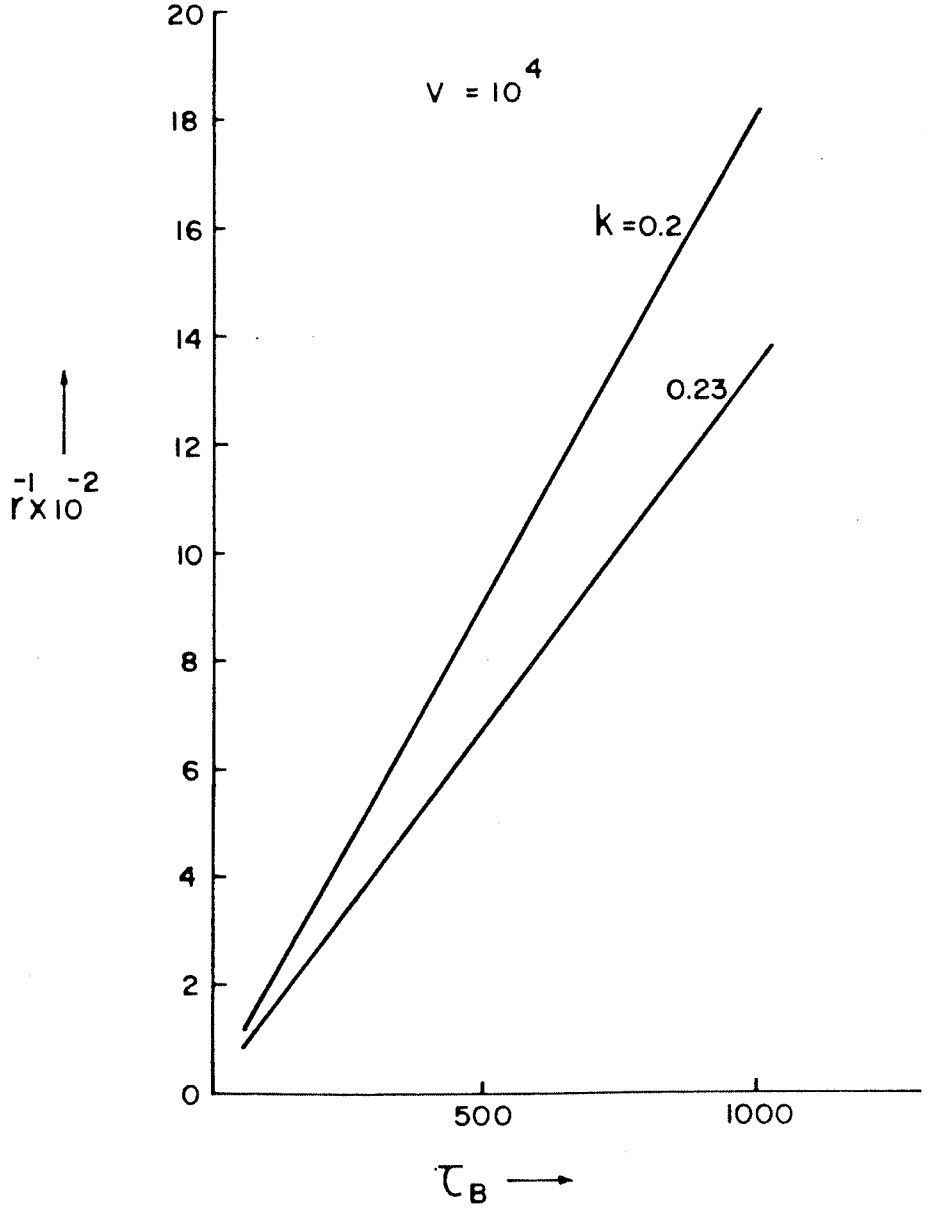

FIG. 5.5

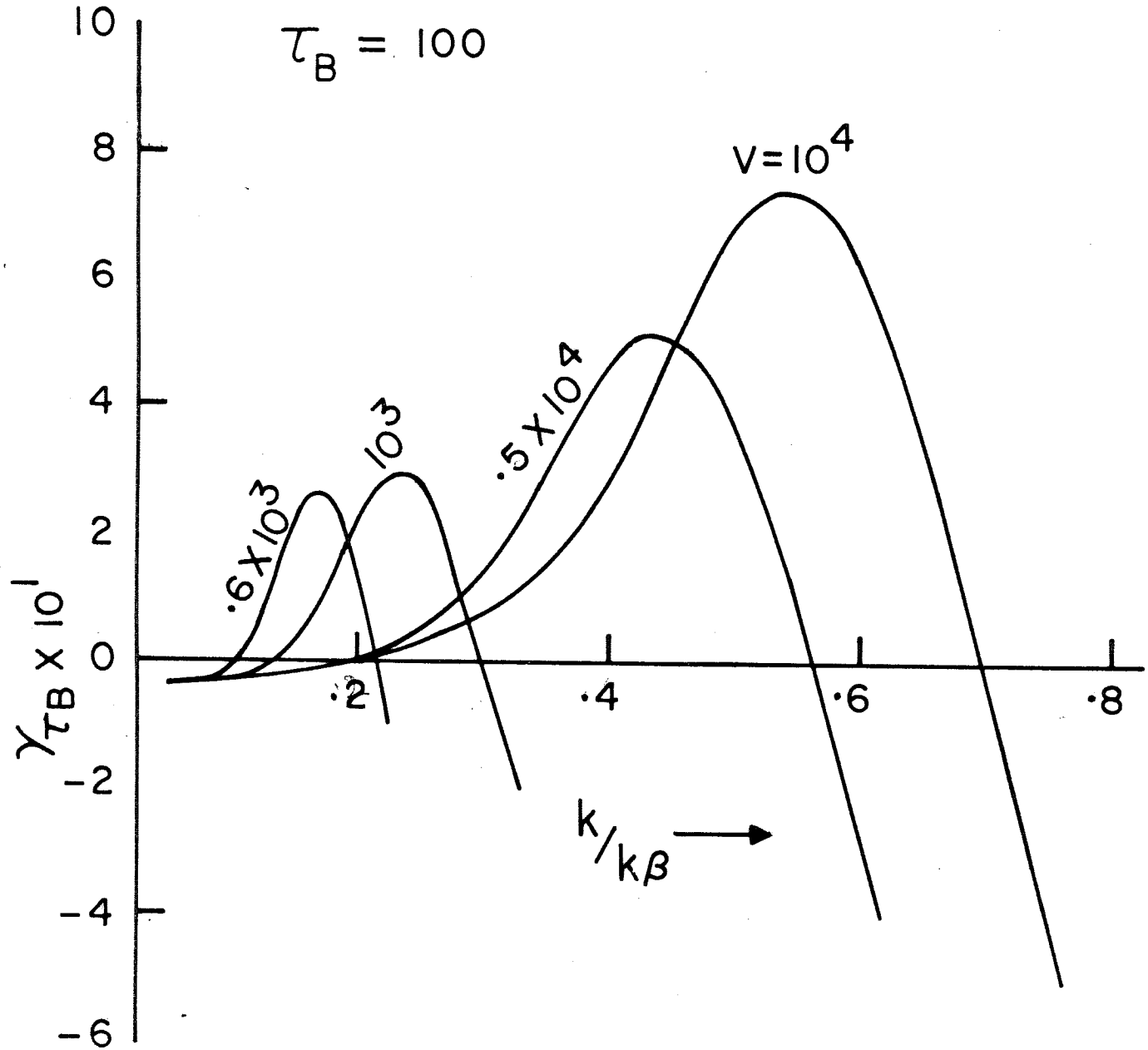
$\tau_B = 100$
$V=10^4$
$.5\times10^4$
10^3
$.6\times10^3$
$\gamma_{\tau_B} \times 10^1$
k/k_β
10
8
6
4
2
0
-2
-4
-6
.2
.4
.6
.8

FIG. 5.6

Chapter 6

Summary

6.1 Results and conclusions

In this thesis,we have carried out a detailed study of the Bennett equilibrium with regard to its linear stability using a kinetic and non-local theory. By expanding the radial amplitudes of the perturbations over a complete set of basis functions a matrix dispersion relation is obtained. The non-local effects arising from the spatial inhomogeneities in the system are reflected in the elements of the dispersion matrix.

The non-local dispersion relation obtained for an electromagnetic perturbation of the Bennett equilibrium in Chapter 2 is a general result and is applied in various limiting cases to study the instabilities in different experimental configurations where the Bennett profile provides a close representation of the plasma equilibrium. One such experimental configuration is the pure Z-pinch with $B_z = 0$. In recent experiments conducted on the Z-pinch in the FLR regime, several new features have been observed which cannot be explained using the earlier fluid treatments[1]. For example, the observed growth rates of the global MHD modes are found to be much less than those

predicted by the fluid theory. This was attributed to the particle effects which are not incorporated in the fluid theories. Moreover, in the proposed Z-pinch reactors the particle orbit size is of the same order as the plasma dimension and hence the kinetic effects are expected to be quite important [2]. One of the most important global MHD modes is the m = 1 current-driven kink mode. We have investigated the kinetic effects on this mode using our kinetic formulation in the pure electromagnetic limit, putting $\phi_1 = 0$ and solved for the growth rate spectrum. We have also reduced the matrix dispersion relation to a simpler form by using certain analytic relations between the coefficients. This reduced form is easier to solve numerically and yields approximate analytic solutions in certain limits. It is found that this mode is unstable for small k and the growth rate is linear in k. As the wavenumber is increased beyond a certain value the mode is stabilized, due to the kinetic damping effects. The maximum growth rate as well as the corresponding wavenumber increase with the increase in the electron drift velocity. The range of unstable wavenumbers also increases with increase in the velocity. The fluid treatments of this mode are all based on simplified current models. In order to have a more realistic estimate of the MHD growth rate we have computed these growth rates for the Bennett profile numerically, by integrating the eigenmode equations. It is found that the growth rates for the Bennett profile are much less than those obtained for the other profiles from

approximate solutions of the MHD equations [3]. The corresponding eigenfunction is found to be peaked on the axis of the plasma and falls off rapidly at large distances. This peak is sharper for large wavenumbers as discussed in Chapter 3.

Various experiments also report the observations of microinstabilities in the pinch, in the later stages of compression [4, 5]. These could possibly give rise to turbulence, enhanced resistivity and thereby cause heating and expansion of the pinch. These effects are believed to be dominant for low atomic number and low line density regimes which are relevant to the Dense Z-pinch reactor [6]. This has been discussed by several workers [7,8] and some of the important modes which have been suggested are the Buneman, the ion-acoustic and the lower-hybrid-drift instabilities. We have studied this aspect by looking at the electrostatic limit of our dispersion relation in Chapter 4 [9]. In this limit we have found that the matrix dispersion relation can again be reduced to a simple form which admits analytic solutions in certain limits. This reduced dispersion relation has been solved numerically as well. The numerical solution reveals a mode in the ion-acoustic range and its characteristics are similar to the ion-acoustic instability in a two-component plasma with a relative drift. This mode is driven by the electron drift velocity. There is a threshold velocity $V > 6V_{thi}$ below which the mode is stable at all wavelengths. As the electron drift increases beyond this value there is a

finite range of k for which the mode is unstable. At very small and very large values of k the mode is stable. The range of unstable k increases with increase in the electron drift. At large k, the real part of the frequency is close to $-kC_s$, C_s being the ion acoustic speed, but at small k the betatron motion causes a shift in the real frequency, this shift being proportional to the betatron frequency of ions. At small k the betatron motion has a stabilizing effect on the mode and increases the threshold for instability. These results are applicable to some of the Z-pinch and plasma focus experiments. Some of these experiments have reported the observation of density fluctuations [4] and it is suggested that these could be attributed to ion-acoustic turbulence. However, the electron drifts for these experiments are found to be well below that required by our theory. Therefore, these reported fluctuations cannot be due to ion-acoustic turbulence.

In Chapter 5, we have applied the kinetic formulation to study the resistive firehose instability of a beam propagating in a resistive plasma channel. This instability results from a resistive phase lag between the magnetic field and the plasma. This instability has been studied quite extensively [10-12] in the past using simplified beam models. These models have usually ignored two important physical effects. Due to the anharmonic nature of the pinch force, the particles have a spread in betatron frequencies, which causes a phase mixing between the particle orbits. Also, the particle orbits are quite intricate and lead to

localized wave-particle resonances. Some of the recent models [13-16] have accounted for the phase mixing effect in an approximate way but ignored the wave-particle resonances by averaging over the beam motion in the transverse plane. We have considered the localised wave-particle resonances by using the Vlasov theory and considering the betatron orbits of the particles to do the orbit integrations. However, in obtaining these orbits we have approximated the magnetic field to be linear as this is true for a majority of the particles that are located near the axis. This assumption leads to a constant betatron frequency for all the particles of a given species and thereby excludes the phase mixing effects. This is one of the limitations of the present analysis. However, even with the inclusion of wave-particle resonances alone, our model predicts damping effects which are of the same order as those predicted by the phase mixing models. It is found that the mode is stable for very small and very large wavenumbers and the growth rate varies inversely as the resistive diffusion time, as expected. We have compared the growth rates obtained from our model with those of the 'distributed mass model' of Lee [13]. It is found that the mode characteristics like the range of unstable wavenumbers, the wavelength corresponding to maximum growth as well as the upper cutoff for the instability are comparable in the parameter regime considered.

6.2 Limitations and future extensions of the present work

Our present theoretical model which takes into account the kinetic and non-local effects on the stability of the Bennett equilibrium, is useful in understanding the role of inhomogeneities and wave-particle resonances in plasma stability. This may be extended to the case of other inhomogeneous equilibria, where the effects due to the spatial inhomogeneities being of the same order as the size of the particle orbits are of interest. The non-local effects arising from the large spatial inhomogeneities lead to a coupling between the different Fourier components of the system, and are represented by the elements of the dispersion matrix.

However there are certain limitations and approximations in our model, which we would now like to discuss. In obtaining the trajectories of the particles in the equilibrium field we have taken the magnetic field to be linear in r neglecting the $K^2r^2/4$ term in the expression for self-field. This leads to a constant betatron frequency for all the particles. However, in the actual field there are generally two types of particle orbits for a given species. In the region of small r the orbits are the betatron orbits while beyond a certain radius they are Larmor orbits. The actual transition point between the two kinds of orbits is a function of the initial conditions. It

is therefore desirable to have a more realistic model that will be able to incorporate two types of orbits for a given species. It is difficult to do this in the framework of our model. However, it is possible to extend this work in a straightforward manner to the case when different species have different types of orbits. The stability analysis for the case when the particles have Larmor orbits has also been developed [17].

The assumption $K^2r^2/4 << 1$ in the magnetic field also eliminates an important effect from our model, namely, the phase mixing between the particle orbits. Inclusion of this term would lead to a radial dependence of the betatron frequency and, thereby, cause phase mixing - an effect which could be significant in determining the stability of low m modes [13-15]. However, the orbit integrals in this case cannot be done analytically, and numerical techniques, though cumbersome have to be resorted to. This could be an interesting extension of the present work.

In the analysis we have assumed a pure Z-pinch configuration having only an azimuthal magnetic field. These results, are therefore applicable only to those Z-pinch experiments which do not have any external fields. The addition of an external field configuration would not affect the equilibrium but will lead to different kinds of particle trajectories. The theory can be extended to such cases as well.

The present work is carried out for a radially bounded

the corresponding radial wavefunction is expressed as a sum over a discrete set of basis functions. If the plasma is unbounded or if the external boundary is removed to infinity the eigenvalues form a continuum and the radial wavefunction may be expressed as an integral over this continuum [18]. The dispersion relation in this case becomes an integral equation and may be solved approximately using variational techniques. This would be an interesting limit of the present theory, and more amenable to analytic solution.

Within the above mentioned constraints, the present theory is still quite useful in understanding the linear stability of Z-pinch-like configurations, particularly, in domains where the fluid theory is not applicable and provides a theoretical basis for the interpretation of experimental observations, as well as a more realistic comparison with the measured growth rates.

References

1. Struve, K. W. , Ph. D. Thesis, Lawrence Livermore Laboratory (1980)

2. Haines,M.G., J. Phys. D : Appl. Phys. 11, 1709 (1979).

3. Nycander, J. & Wahlberg, C. , Nucl. Fusion 24, 1357 (1984).

4. Bernard, A. , Garconnet,J.P., Jolas,A., LeBreton,J.P. & DeMascureau , J. , in Plasma Physics and Controlled Nuclear Fusion, IAEA, II, 159 (1979).

5. Haines, M. G. , Phil. Trans. Roy. Soc. London A300, 649 (1981).

6. Hartman, C. W. , Carlson, G., Hoffman,M., Werner,R. & Cheng,D.Y.,Nuclear Fusion 17, 909 (1977).

7. Liewer,P.C. & Krall,N.A., Phys. Fluids 16, 1953 (1973).

8. Vikhrev, V.V. & Korzhavin,V.M., Sov. J. Plasma Phys. 4, 411 (1978).

9. Krishnamurthi, U., Sen,A., Sharma,A.S. & Sundaram,A.K., Nucl. Fusion 25, 1953 (1985).

10. Rosenbluth,M.N., Phys. Fluids 3, 931 (1960).

11. Yadavalli,S.V., Zeit. fur Physik 196, 255 (1966).

12. Weinberg,S., J. Math. Phys. 8, 614 (1967).

13. Lee,E.P., Phys. Fluids 21, 1327 (1978).

14. Uhm,H.S. & Lampe,M., Phys. Fluids 23, 1574 (1980).

15. Sharp, W.M., Lampe,M. & Uhm,H.S., Phys. Fluids 25, 1456 (1982).

16. Lampe, M., Sharp,W.M., Hubbard,R.F., Lee,E.P. & Briggs, R.J., Phys. Fluids 27, 2921 (1984).

17. Sharma,A.S., Atomkernenerg. Kerntech. 44, 201 (1984).

18. Davidson,R.C., Phys. Fluids 19, 1189 (1976).